



**NATIONAL AND KAPODISTRIAN UNIVERSITY OF ATHENS**

**SCHOOL OF SCIENCES**

**DEPARTMENT OF CHEMISTRY**

**DOCTORAL THESIS**

**Development of non-target screening workflows for the  
identification of biotransformation products of emerging  
pollutants in wastewater by mass spectrometric techniques**

**PSOMA AIKATERINI**

**MSc CHEMIST**

**ATHENS 2018**









**ΕΘΝΙΚΟ ΚΑΙ ΚΑΠΟΔΙΣΤΡΙΑΚΟ ΠΑΝΕΠΙΣΤΗΜΙΟ ΑΘΗΝΩΝ**

**ΣΧΟΛΗ ΘΕΤΙΚΩΝ ΕΠΙΣΤΗΜΩΝ**

**ΤΜΗΜΑ ΧΗΜΕΙΑΣ**

**ΔΙΔΑΚΤΟΡΙΚΗ ΔΙΑΤΡΙΒΗ**

**Ανάπτυξη μεθόδων μη στοχευμένης σάρωσης για την ανίχνευση  
προϊόντων βιομετατροπής αναδυόμενων ρύπων σε υγρά  
απόβλητα με τεχνικές φασματομετρίας μαζών**

**ΨΩΜΑ ΑΙΚΑΤΕΡΙΝΗ**

**MSc ΧΗΜΙΚΟΣ**

**ΑΘΗΝΑ 2018**



## **DOCTORAL THESIS**

# **Development of non-target screening workflows for the identification of biotransformation products of emerging pollutants in wastewater by mass spectrometric techniques**

**PSOMA AIKATERINI**

**Registration Number: 001224**

### **Supervising Professor:**

Dr. Nikolaos S Thomaidis, Associate Professor

### **Three – member consultative committee:**

Dr. Antony C. Calokerinos, Professor, Chemistry Department, N.K.U.A.

Dr. Euaggelos Gikas, Assistant Professor, Pharmacy Department, N.K.U.A.

Dr. Nikolaos S. Thomaidis, Professor, Chemistry Department, N.K.U.A.

### **Seven-member examination committee:**

Dr. Antony C. Calokerinos, Professor, Chemistry Department, N.K.U.A.

Dr. Evangelos Gikas, Assistant Professor, Pharmacy Department, N.K.U.A.

Dr. Emmanuel Dasenakis, Professor, Chemistry Department, N.K.U.A.

Dr. Anastasios Economou, Professor, Chemistry Department, N.K.U.A.

Dr. Eirini Panteri, Associate Professor, Pharmacy Department, N.K.U.A.

Dr. Athanasios Stasinakis, Associate Professor, Department of

Environment, University of the Aegean

Dr. Nikolaos S. Thomaidis, Professor, Chemistry Department, N.K.U.A.

**Defending Date: 02/07/2018**





## **ΔΙΔΑΚΤΟΡΙΚΗ ΔΙΑΤΡΙΒΗ**

# **Ανάπτυξη μεθόδων μη στοχευμένης σάρωσης για την ανίχνευση προϊόντων βιομετατροπής αναδυόμενων ρύπων σε υγρά απόβλητα με τεχνικές φασματομετρίας μαζών**

**ΨΩΜΑ ΑΙΚΑΤΕΡΙΝΗ**

**Αριθμός μητρώου: 001224**

### **Επιβλέπων καθηγητής:**

Δρ. Νικόλαος Θωμαΐδης, Καθηγητής, Τμήμα Χημείας, Ε.Κ.Π.Α.

### **Τριμελής συμβουλευτική επιτροπή:**

Δρ. Αντώνιος Καλοκαιρινός, Καθηγητής, Τμήμα Χημείας, Ε.Κ.Π.Α.

Δρ. Ευάγγελος Γκίκας, Επίκουρος Καθηγητής, Τμήμα Φαρμακευτικής, Ε.Κ.Π.Α.

Δρ. Νικόλαος Θωμαΐδης, Καθηγητής, Τμήμα Χημείας, Ε.Κ.Π.Α.

### **Επταμελής εξεταστική επιτροπή:**

Δρ. Αντώνιος Καλοκαιρινός, Καθηγητής, Τμήμα Χημείας, Ε.Κ.Π.Α.

Δρ. Ευάγγελος Γκίκας, Επίκουρος Καθηγητής, Τμήμα Φαρμακευτικής, Ε.Κ.Π.Α.

Δρ. Εμμανουήλ Δασενάκης, Καθηγητής, Τμήμα Χημείας, Ε.Κ.Π.Α.

Δρ. Αναστάσιος Οικονόμου, Καθηγητής, Τμήμα Χημείας, Ε.Κ.Π.Α.

Δρ. Ειρήνη Παντερή, Αναπληρώτρια Καθηγήτρια, Τμήμα Φαρμακευτικής, Ε.Κ.Π.Α.

Δρ. Αθανάσιος Στασινάκης, Αναπληρωτής Καθηγητής, Τμήμα Περιβάλλοντος, Πανεπιστήμιο Αιγαίου.

**Ημερομηνία εξέτασης: 02/07/2018**

## ABSTRACT

The omnipresence of emerging pollutants in several environmental compartments has been highlighted over the last decades due to incomplete removal in wastewater treatment plants (WWTPs). Secondary or biological treatment applied in WWTPs is the main transformation process for the elimination of the organic loading that finally discharged to the aquatic environment through urban sewer systems. The main objectives of this doctoral thesis was the identification of transformation products (TPs) of emerging pollutants by applying suspect and non-target screening strategies based on liquid chromatography quadrupole-time-of-flight mass spectrometry (LC-QTOF-MS).

Initially, an introduction is presented on the issue of emerging pollutants and their transformation products produced during secondary sewage treatment. Specific analytical approaches based on high-resolution mass spectrometric analysis, are then presented for the identification of EPs and their TPs.

The experimental section consists of three parts: (i) Development of an integrated workflow for the identification of biotransformation products where citalopram was used as a case study (Chapter 3), (ii) Identification of biotransformation products of several emerging pollutants from different chemical classes including pharmaceuticals, new psychotropic drugs and industrial chemicals (Chapter 4) and (iii) Environmental fate of selected pharmaceuticals under nitrifying and denitrifying conditions: comparison of aerobic, anaerobic degradation and formation of biotransformation products (Chapter 5 ).

It is our strong belief that these studies will constitute a step forward in environmental analysis by identifying new TPs of emerging pollutants as well as will provide useful data to the WWTPs authorities and policy makers and raise awareness about the future measures that should be adopted in order to minimize release of emerging pollutants and their transformation products, and minimize the environmental risk.

**SUBJECT AREA:** Analytical Chemistry

**KEYWORDS:** Emerging pollutants, Biotransformation, LC-QTOF-MS, Transformation products, Non-target screening, HILIC

## ΠΕΡΙΛΗΨΗ

Η απανταχού παρουσία των αναδυόμενων ρύπων σε πολλά περιβαλλοντικά τμήματα έχει επισημανθεί τις τελευταίες δεκαετίες λόγω της ατελούς απομάκρυνσης τους στις εγκαταστάσεις επεξεργασίας λυμάτων. Η δευτερογενής ή βιολογική επεξεργασία που εφαρμόζεται στις εγκαταστάσεις επεξεργασίας λυμάτων είναι η κύρια διαδικασία μετασχηματισμού για την απομάκρυνση του οργανικού φορτίου που τελικά απορρίπτεται στο υδάτινο περιβάλλον μέσω των αστικών αποχετευτικών συστημάτων. Οι κύριοι στόχοι αυτής της εργασίας ήταν η ταυτοποίηση προϊόντων μετασχηματισμού (ΠΜ) αναδυόμενων ρύπων με τη χρήση στρατηγικών ύποπτης και μη-στοχευμένης σάρωσης που βασίζονται στην τεχνική της υγρής χρωματογραφία συζευγμένης με φασματομετρία μάζας τετραπόλου-χρόνου-πτήσης (LC-QTOF-MS).

Αρχικά παρουσιάζεται μια εισαγωγή στο ζήτημα των αναδυόμενων ρύπων και των προϊόντων μετασχηματισμού τους που παράγονται κατά τη δευτεροβάθμια επεξεργασία λυμάτων. Στη συνέχεια, παρουσιάζονται ειδικές αναλυτικές προσεγγίσεις με βάση τη χρήση φασματομετρίας μάζας υψηλής διακριτικής ικανότητας για την ταυτοποίηση των αναδυόμενων ρύπων και των προϊόντων μετατροπής τους.

Το πειραματικό κομμάτι αποτελείται από τρία μέρη: (i) Ανάπτυξη ενός ολοκληρωμένου διαγράμματος ροής εργασίας για την ταυτοποίηση προϊόντων βιομετατροπής όπου η ένωση σιταλοπράμη χρησιμοποιήθηκε ως περίπτωση εργασίας (Κεφάλαιο 3), (ii) Ανίχνευση προϊόντων βιομετατροπής αρκετών αναδυόμενων από διαφορετικές χημικές τάξεις συμπεριλαμβανομένου των φαρμακευτικών ενώσεων, των νέων ψυχοτρόπων ενώσεων και των βιομηχανικών χημικών (κεφάλαιο 4) και (iii) Περιβαλλοντική τύχη επιλεγμένων φαρμάκων υπό συνθήκες νίτρωσης και απονιτροποίησης: σύγκριση αερόβιας, αναερόβιας αποικοδόμησης και σχηματισμού προϊόντων βιομετατροπής (κεφάλαιο 5).

Πιστεύουμε ότι αυτές οι μελέτες θα αποτελέσουν ένα βήμα προόδου στην περιβαλλοντική ανάλυση προσδιορίζοντας νέα προϊόντα μετατροπής

αναδυόμενων ρύπων καθώς και θα παράσχουν χρήσιμα στοιχεία στις αρχές των κέντρων επεξεργασίας λυμάτων και τους υπεύθυνους για τη χάραξη πολιτικής και θα ευαισθητοποιήσουν σχετικά με μελλοντικά μέτρα που πρέπει να υιοθετηθούν προκειμένου να ελαχιστοποιηθεί η απελευθέρωση αναδυόμενων ρύπων και προϊόντων μετασχηματισμού τους και ο περιβαλλοντικός κίνδυνος.

**ΘΕΜΑΤΙΚΗ ΠΕΡΙΟΧΗ:** Αναλυτική Χημεία

**ΛΕΞΕΙΣ ΚΛΕΙΔΙΑ:** Αναδυόμενοι Ρύποι, Βιομετατροπή, LC-MS, LC-QTOF-MS, Προϊόντα μετασχηματισμού, μη στοχευμένη σάρωση, HILIC

## ACKNOWLEDGEMENTS

First and foremost, I would like to express my sincere gratitude to my supervisor Prof. Nikolaos Thomaidis for the continuous support of my Ph.D study and related research, for his patience, motivation, knowledge and for giving me the opportunity to carry out my research project as a member of TrAMS group.

Besides my supervisor, I would like to thank the rest of my three-member consultative committee: Prof. Antonios Calokairinos and Assoc. Prof. Evangelos Gikas, for their insightful comments and encouragement, as well as the seven-member examination committee for their cooperation throughout this doctoral thesis and their valuable comments.

I am also hugely appreciative to Dr. Kathrin Fenner from Swiss Federal Institute of Aquatic Science and Technology (EAWAG) for her guidance, assistance and remarkable comments when revising my manuscripts derived from this study.

I would like also to thank Dr. A. Stasinakis and his team, from University of Aegean for their collaboration during the experimental part of Chapter 4.3 and Chapter 5.

Special mention goes to my colleagues in TREMEPOL project Pablo Gago-Ferrero and Reza Alizadeh for introducing me to the new terms of non-target screening, *in silico* fragmentation tools and QSRR prediction models, I had to face with.

I am thankful to each and every “TrAMSer” I met in the lab during all these years and that contributed to create a friendly and creative environment and especially my lab mates Anna Bletsou, Maristina Nika, Giorgos Koulis and Dimitris Damalas for the stimulating discussions, for their encouragement on the conferences and for the sleepless nights we were working together before deadlines, and for all the fun we have had in the last five years.

I would also like to thank Dr. Juliet Kinyua (University of Antwerp), Dr. Katerina Mazioti (University of Aegean), Dr. Olga Arvaniti (University of

Aegean), M.Sc. Eleni Georgantzi (University of Athens) and M.Sc. Sofia Attiti (University of Athens) for our collaboration during this research.

Words are powerless to express my gratitude to my “scientific” friends, who became more close friends during all these five years, Vassiliki Beretsou and Nikolaos Rousis for their support and infinite talks when difficulties arose and always gave me strength to carry on, even miles away.

Last but not the least; I would like to thank my husband, Christos, my parents Kostas and Anna and my sister Niki, for supporting me spiritually throughout writing this doctoral thesis and in my life in general.

# CONTENTS

<b>CONTENTS .....</b>	<b>17</b>
<b>LIST OF FIGURES .....</b>	<b>21</b>
<b>LIST OF TABLES .....</b>	<b>23</b>
<b>PREFACE .....</b>	<b>24</b>
<b>CHAPTER 1. Emerging pollutants: Occurrence, fate and transformation during conventional wastewater treatment processes ..</b>	<b>25</b>
1.1 Introduction .....	25
1.2 Emerging pollutants (EPs) and their transformation products (TPs) ..	26
1.2.1 Emerging pollutants (EPs).....	26
1.2.2 Transformation Products (TPs) .....	27
1.3 Conventional wastewater treatment.....	29
1.3.1 Secondary biological treatment.....	30
1.4 Identification of TPs .....	32
1.4.1 Identification of TPs-Laboratory approaches.....	33
1.4.2 Identification of TPs-Analytical approaches.....	35
1.4.3 Identification approaches .....	39
1.4.4 Structure elucidation and identification confidence levels in HR-MS.....	43
<b>CHAPTER 2. Scope and Objectives.....</b>	<b>46</b>
2.1 The analytical problem.....	46
2.2 Research objectives and Scope .....	47
<b>CHAPTER 3. Citalopram as a case study for the development of an integrated workflow for the identification of biotransformation products.....</b>	<b>50</b>
3.1 Introduction .....	50



3.2	Materials and methods.....	52
3.2.1	Chemicals and reagents.....	52
3.2.2	Sampling .....	53
3.2.3	Biotransformation batch experiments .....	54
3.2.4	LC-HR-MS/MS analysis .....	55
3.2.5	Analysis of WWTP samples .....	57
3.2.6	Suspect and non-target screening for the identification of TPs ..	57
3.2.7	Retrospective suspect screening of CTR and its TPs .....	59
3.2.8	Environmental risk assessment.....	59
3.3	Results and discussion .....	60
3.3.1	Degradation of CTR in batch experiments with activated sludge	60
3.3.2	Identification of biotransformation products of CTR .....	60
3.3.2.1	CTR 343 ( $C_{20}H_{24}FN_2O_2^+$ ) .....	64
3.3.2.2	CTR 344 ( $C_{20}H_{23}FNO_3^+$ ) .....	64
3.3.2.3	CTR 311 ( $C_{19}H_{20}FN_2O^+$ ) .....	65
3.3.2.4	CTR 329 ( $C_{19}H_{22}FN_2O_2^+$ ) .....	65
3.3.2.5	CTR 330 ( $C_{19}H_{21}FNO_3^+$ ) .....	65
3.3.2.6	CTR 341 ( $C_{20}H_{22}FN_2O_2^+$ ) .....	69
3.3.2.7	CTR 359A and CTR 359B ( $C_{20}H_{24}FN_2O_3^+$ ) .....	69
3.3.2.8	CTR 360A and CTR 360B ( $C_{20}H_{23}FNO_4^+$ ) .....	70
3.3.2.10	CTR 357 ( $C_{20}H_{22}FN_2O_3^+$ ) .....	71
3.3.2.11	CTR 355 .....	71
3.3.2.12	CTR 339 .....	71
3.3.3	Proposed transformation pathway of CTR .....	71
3.3.4	Retrospective analysis of CTR and its TPs in real wastewater samples .....	75

3.3.5	Environmental risk assessment of CTR and its confirmed TPs..	76
3.4	Conclusions .....	77
<b>CHAPTER 4. Identification of biotransformation products of several emerging pollutants from different chemical classes .....</b>		
<b>79</b>		
4.1	Introduction .....	79
4.2	Identification of biotransformation products of pharmaceuticals .....	80
4.2.1	Introduction .....	80
4.2.2	Material and methods.....	82
4.2.3	Results and discussion.....	87
4.2.4	Conclusions.....	106
4.3	Identification of biotransformation products p-methoxy methylamphetamine (PMMA) and dihydromephedrone (DHM).....	108
4.3.1	Introduction .....	108
4.3.2	Material and methods.....	109
4.3.3	Results and discussion.....	110
4.3.4	Conclusions.....	117
4.4	Identification of biotransformation products of benzotriazoles and hydroxyl-benzothiazole in laboratory scale hybrid moving bed biofilm reactor (HMBBR) system .....	120
4.4.1	Introduction .....	120
4.4.2	Material and methods.....	121
4.4.3	Conclusions.....	124
<b>CHAPTER 5. Environmental fate of selected pharmaceuticals under nitrifying and denitrifying conditions: comparison of aerobic, anaerobic degradation and formation of biotransformation products .....</b>		
<b>130</b>		
5.1	Introduction .....	130
5.2	Materials and methods.....	131

5.2.1	Analytical standards and reagents .....	131
5.2.2	Biodegradation experiments.....	132
5.2.3	Analytical Method .....	133
5.2.4	Calculation and modelling equations.....	135
5.2.5	Suspect screening for the identification of TPs .....	135
5.3	Results and Discussion.....	135
5.3.1	Biodegradation experiments.....	135
5.3.2	By –products formation .....	139
5.4	Conclusions .....	146
<b>CHAPTER 6. Conclusions .....</b>		<b>147</b>
<b>ABBREVIATIONS AND ACRONYMS.....</b>		<b>150</b>
<b>REFERENCES .....</b>		<b>156</b>

## LIST OF FIGURES

<b>Fig.1. 1:</b> Graphical abstract of Chapter 1 ( <a href="https://www.thermofisher.com">https://www.thermofisher.com</a> , last access 11/05/2018).....	25
<b>Fig.1.2:</b> Simplified layout of the activated sludge process [2]. .....	30
<b>Fig.1.3:</b> Historical development of activated sludge process: (A) BOD removal; (B) phosphate precipitation and nitrification; (C) nitrification and denitrification; (D) enhanced biological P removal; (E) MBR; (F) MBBR [2]...	32
<b>Fig.1.4:</b> Schematic presentation of a Q-TOF instrument (Maxis Impact, Bruker). .....	39
<b>Fig.1.5:</b> Proposed identification confidence levels in HR-MS analysis [48]. ..	45
 <b>Fig.2. 1:</b> Graphical abstract of Chapter 2.....	46
 <b>Fig. 3.1:</b> Graphical abstract of Chapter 3.....	50
<b>Fig. 3.2:</b> Time profile of biotransformation products of CTR obtained by HILIC analysis.....	62
<b>Fig. 3.3:</b> Degradation of CTR in aerobic batch experiments.....	62
<b>Fig. 3.4:</b> Mass balance of CTR and its TPs.....	63
<b>Fig. 3.5:</b> Observed fragmentation patterns in selected MS/MS spectra of the formed TPs of CTR.....	73
<b>Fig. 3.6:</b> Proposed biotransformation pathway for CTR. Dotted arrows indicate that a single TP can be formed through different reactions from different precursors. ....	74
 <b>Fig.4.1:</b> Graphical abstract of chapter 4.2. ....	80
<b>Fig.4.2:</b> Developed workflow for suspect and non-target screening for the identification of TPs.....	89

<b>Fig.4.3:</b> Time courses of pharmaceuticals concentrations in activated sludge, blank, sorption, and abiotic controls for metformin, ranitidine, lidocaine and atorvastatin along with the respective formed transformation products are depicted in plots by peak area. ....	90
<b>Fig.4.4:</b> Proposed biotransformation pathway of ranitidine. Dotted arrows indicate proposed structures of the TPs while line arrows indicate confirmed TPs. ....	93
<b>Fig.4.5:</b> Proposed biodegradation pathway of ATR. The formation of TP ATR515 and ATR471 are driven by single and double $\beta$ -oxidation, respectively. The steps followed for $\beta$ -oxidation are the same with the catabolism of fatty acids in animal metabolism. ....	97
<b>Fig.4.6:</b> Graphical abstract of Chapter 4.3.....	108
<b>Fig.4.7:</b> (a) The degradation of PMMA in four reactors; (b) Formation of PMMA TPs in the biotic reactor over a 7-day incubation period. ....	111
<b>Fig.4.8:</b> Proposed (bio)transformation pathway for PMMA. Dotted arrows indicate the possible reactions that can lead to the formation of a single TP. ....	113
<b>Fig.4.9:</b> (a) The degradation of DHM in the four reactors; (b) Formation of DHM TPs in the biotic reactor over a 7-day incubation period. ....	114
<b>Fig.4.10:</b> Proposed (bio)transformation pathway for DHM. Dotted arrows indicate the possible reactions that can lead to the formation of a single TP. ....	116
<b>Fig.4.11:</b> Graphical abstract of chapter 4.4. ....	120
<b>Fig.5.1:</b> Time profiles of CTR, RAN and LDC under aerobic, anoxic and anaerobic conditions, respectively. ....	138
<b>Fig.5. 2:</b> Time profiles of TRA, TOP, MTF and EPH under aerobic, anoxic and anaerobic conditions, respectively. ....	139

## LIST OF TABLES

<b>Table 3.1:</b> Identified transformation products (TPs) of citalopram (CTR) during biodegradation batch experiments. ....	66
<b>Table 4.1:</b> Overview on the experimental set up was performed to investigate both the degradation kinetics and the biotransformation of the selected compounds. ....	84
<b>Table 4.2:</b> Identified transformation products (TPs) of the selected pharmaceuticals during biodegradation batch experiments. ....	99
<b>Table 4.3:</b> Biotransformation products (TPs) identified for PMMA and DHM over a 7-day incubation in the activated sludge reactor. ....	118
<b>Table 4.4:</b> Biotransformation products (TPs) identified for BTR, 4TTR, 5TTR, XTR, CBTR and OHBTH, over a 24-hour incubation in BC1. ....	125
<b>Table 5.1:</b> Experimental conditions used in the different biodegradation batch experiments (A to L).....	134
<b>Table 5.2:</b> Estimated dissipation times and pseudo- first order rate constants under different redox conditions for the study analytes.....	140

## PREFACE

The experimental part of this doctoral thesis was performed in two laboratories.

The first experimental part (Chapter 3) as well as the part 1 (Chapter 4.1) and part 2 (Chapter 4.2) of the second study were carried out at the Laboratory of Analytical Chemistry, Department of Chemistry of the National and Kapodistrian University of Athens, Greece, under the supervision of Dr. Nikolaos Thomaidis. The experimental parts of Chapter 4.3 and entirely Chapter 5 were performed at the Laboratory of Water and Air Quality, Department of Environment, University of the Aegean, Mytilene, Greece under the supervision of Dr. Athanasios Stasinakis and in collaboration with Dr. Nikolaos Thomaidis.

An extended Electronic Electronic Supplementary Material of **85** pages, consisting of **15** Sections (including **46** Figures and **17** Tables) is also available along with this doctoral thesis.

All the experimental parts of this doctoral thesis (Chapters 3 to 5) have been co-financed by the European Union and Greek national funds through the Operational Program "Education and Lifelong Learning" of the National Strategic Reference Framework (NSRF) – ARISTEIA 624 (TREMEPOL project). (<http://tremepol.chem.uoa.gr/>)



# CHAPTER 1.

## Emerging pollutants: Occurrence, fate and transformation during conventional wastewater treatment processes

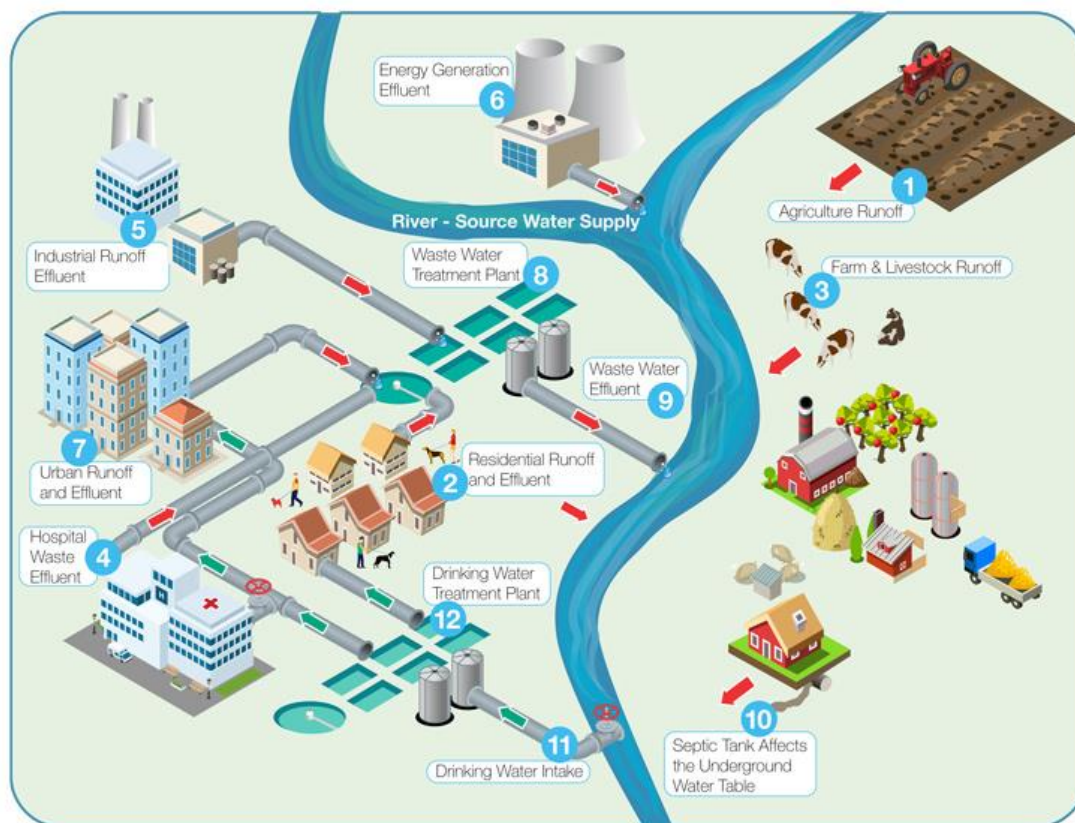


**Fig.1. 1:** Graphical abstract of Chapter 1 (<https://www.thermofisher.com>, last access 11/05/2018).

### 1.1 Introduction

Chemical pollution poses an increasing threat to our environment, amplified by population growth and climate change. Thousands of chemicals, including pesticides, biocides, pharmaceuticals, industrial chemicals, and chemicals from consumer products are present in our wastewater and water from other sources, such as agricultural runoff or storm water, as well as in the terrestrial environment [1]. Continuous contamination of the environment with diverse groups of chemical compounds and their adverse effects on both ecosystem and human health is one of the most relevant environmental issues of today. According to European Inventory of Existing Commercial Chemical



Substances (EINECS), in European Union (EU), there are more than 100,000 registered chemicals of which 70,000 are in daily use [2].

Moreover, since analytic techniques continue to improve, the number and frequency of detections of still unregulated, emerging pollutants are increasing. Although many of those compounds are present at low concentrations in the environment, their effects on ecosystems are still unknown, especially because they occur in complex chemical mixtures. Some of those compounds are continuously introduced into the environment; therefore, regardless of their persistence in given conditions, they are permanently present (pseudo-persistent), which might lead to unexpected chronic effects of affected species [2].

Compounding this issue, chemicals are also transformed in the environment, and while some of the resulting transformation products (TPs) are known to be more abundant in the aquatic environment than their parent compounds the majority of TPs present most likely have not even been identified yet. Thus, humans and aquatic ecosystems are exposed to a highly variable and unknown cocktail of chemicals. Although individual chemicals are typically present at low concentrations, they can interact with each other resulting in additive or potentially even synergistic mixture effects. The formation and environmental presence of TPs thus adds further complexity to chemical risk assessment [1].

## **1.2 Emerging pollutants (EPs) and their transformation products (TPs)**

### **1.2.1 Emerging pollutants (EPs)**

The term ““emerging pollutants or emerging contaminants or contaminants contaminant of emerging concern” is being used to identify chemicals and other substances that have no regulatory standard, have been recently “discovered” in natural streams (often because of improved analytical chemistry detection levels), and potentially cause deleterious effects in aquatic life at environmentally relevant concentrations. They are pollutants not currently included in routine monitoring programs and may be candidates for

future regulation depending on their (eco)toxicity, potential health effects, public perception, and frequency of occurrence in environmental media. EPs are not necessarily new chemicals. They include pollutants that have often been present in the environment, but whose presence and significance are only now being evaluated [3].

EPs include several types of chemicals and their metabolites/transformation products such as:

- Persistent organic pollutants (POPs) such as polybrominated diphenyl ethers (PBDEs; used in flame retardants, furniture foam, plastics, etc.) and other global organic contaminants such as perfluorinated organic acids
- Pharmaceuticals and personal care products (PPCPs), including a wide suite of human prescribed drugs (e.g., antidepressants, blood pressure), over-the-counter medications (e.g., ibuprofen), bactericides (e.g., triclosan), sunscreens, synthetic musks;
- Veterinary medicines such as antimicrobials, antibiotics, anti-fungals, growth promoters and hormones;
- Endocrine-disrupting chemicals (EDCs), including synthetic estrogens (e.g., 17 $\alpha$ -ethynylestradiol, which also is a PCPP) and androgens (e.g., trenbolone, a veterinary drug), naturally occurring estrogens (e.g., 17 $\beta$ -estradiol, testosterone), as well as many others (e.g., organochlorine pesticides, alkylphenols) capable of modulating normal hormonal functions and steroidal synductoral thesis in aquatic organisms;
- Nanomaterials such as carbon nanotubes or nano-scale particulate titanium dioxide, of which little is known about either their environmental fate or effects [3].

### **1.2.2 Transformation Products (TPs)**

Once released into the environment, EPs are subject to both biotic and abiotic transformation processes that are responsible for their transformation and/or elimination, according to their persistence, transport, and ultimate destination. Various transformations can take place, producing compounds that, to some extent, differ in their environmental behavior and ecotoxicological profile from

the parent compound. Formation of TPs occurs mainly through oxidation, hydroxylation, hydrolysis, conjugation, cleavage, dealkylation, methylation and demethylation. The EPs and their TPs can move vertically through the soil profile to groundwater and away from the source site with mobile groundwater. They also have the potential to reach surface water, when they travel laterally either as surface runoff or through subsoil tile drains, entering streams, major rivers, reservoirs, and ultimately estuaries and oceans [4].

Since there is a gap on the information on the occurrence and toxicity of TPs in the environment, we are unable to evaluate their significance in risk assessment [5, 6]. Standardized toxicity tests can provide quantitative information on the toxicity of the TP, compared to its parent compound, but these studies are limited [7-9]. In general, transformation products are less toxic and more polar than the parent compounds. However, in some cases, they may be more persistent or exhibit higher toxicity or be present at much higher concentrations [10].

Although there is legislation regulating chemicals like pesticides, veterinary drugs, POPs and others, few is mentioned for their TPs. Concerns over the TPs of pesticides in plants have been expressed since 1991 (European Directive 91/414/EEC), while the term “metabolite” appears in Regulation (EC) 1107/2009 concerning the plant protection products and in Directives 2001/82/EC and 98/8/EC, concerning the veterinary medical and biocidal products, respectively. European Medicines Agency (EMA, 2006) referred also to the need for assessment of potential environmental risks of human medicinal products. However, in all these documents, there is no clarification on the determination, limits and toxicological effects of metabolites or TPs. In Organisation for Economic Co-operation and Development (OECD) guidelines, concerning the “Aerobic and Anaerobic Transformation in Aquatic Sediment Systems”, adopted in 2002, it is claimed that TPs detected at  $\geq 10\%$  of the applied radioactivity should be identified. Meanwhile, the EU Regulation 1907/2006 (REACH) requires the identification of major transformation and degradation products for the registration of the substance. In the Regulation (EC) 850/2004 on POPs, a reference to their transformation processes also exists.

Transformation products occurring in the environment can be classified into two main categories: TPs formed by biotic or abiotic processes. The biotransformation products include human, animal and microbial metabolites in engineered and natural systems. The abiotic TPs are the outcome of abiotic processes such as hydrolysis, photolytic and photocatalytic degradation in the natural environment as well as water treatment processes, like chlorination, ozonation and advanced oxidation processes.

### **1.3 Conventional wastewater treatment**

Domestic wastewaters are generally subjected to a treatment sequence including preliminary treatments, a primary gravity settling, secondary biological treatment (by activated sludge, fixed-film reactors, lagoon systems, and/or sedimentation) [11] and finally tertiary steps, including advanced oxidation processes (AOPs) for disinfection and removal of micropollutants (chlorination, chloramination, ozonation, and advanced oxidation by UV/H<sub>2</sub>O<sub>2</sub> treatment) [1].

Modern sewage treatment plants (STPs) can effectively accomplish carbon and nitrogen removal, as well as microbial pollution. The reported overall removal rates of EPs in full-scale STPs vary strongly and they clearly show that their elimination is often incomplete. As a consequence, a significant fraction is discharged with the final effluent into the aquatic environment or sorbed onto the primary and secondary sludge, whose deposition on land can be another significant pathway of releasing these substances in the environment [12].

#### **➤ Primary treatment**

Primary treatment comprises the removal of suspended solids and fat using sedimentation and flotation units. Therefore, although some degradation can also occur, sorption is the main mechanism involved in the removal of micropollutants during primary treatment, and consequently, only those substances with higher sorption properties are expected to be eliminated [12].

#### **➤ Biological treatment**

The widest biological treatment technology used in large urban areas is conventional activated sludge (CAS), operating at hydrolytic retention time (HRT) of 4–14 h. Most CAS plants operate exclusively under aerobic conditions, although many installations are being upgraded in order to include also anoxic zones for nutrient removal due to more restrictive legislation. More recently, membrane technology has been incorporated to biological treatment in order to substitute secondary settlers. The biomass developed in such systems is characterized by higher sludge retention times (SRT) and smaller floc size, which might influence the removal efficiency of micropollutants [12].

### 1.3.1 Secondary biological treatment

For the secondary step, activated sludge treatment is the process that most extensively employed all over the world for processing both urban wastewaters from small and large communities and industrial effluents. Activated sludge treatment consists mainly of flocculating microorganisms held in suspension and contact with wastewater in a mixed aerated tank. The CAS system consists of a biological reactor (where activated sludge may develop and grow) followed by a secondary clarifier: The simplest diagram of this process is that shown in **Fig.1.2**, and subsequent configurations developed over the years are shown in **Fig.1.3**.

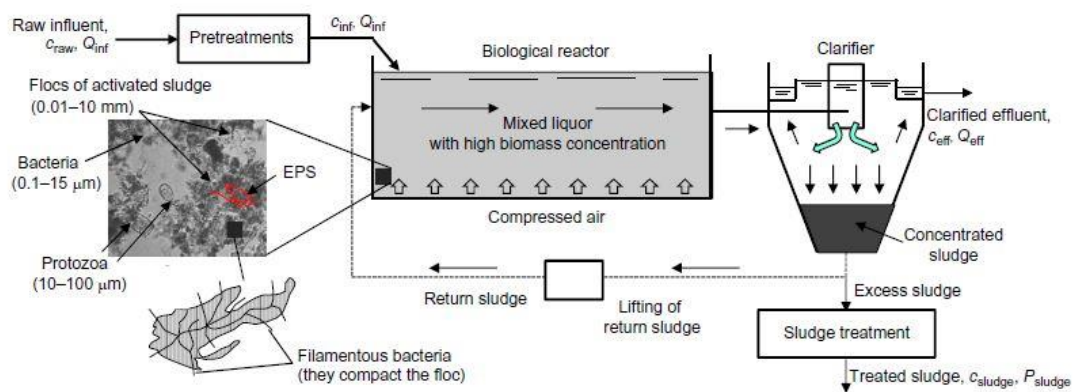


**Fig.1.2:** Simplified layout of the activated sludge process [2].

The biological reactor may consist of one (**Fig.1.2 and Fig.1.3A**) or more compartments (**Fig.1.3B-F**). Multiple compartments provide different operational conditions, namely, aerobic, anoxic, and anaerobic, and enable C, N, and P removal. Adsorption, absorption, flocculation, oxidation–reduction

reactions, and sedimentation are the main physical and biochemical processes occurring within the activated sludge process. Biochemical reactions (anabolic, catabolic, and co-metabolic reactions) take place within the biological reactor and bring about the degradation of the organic compounds in the influent wastewater. The reactions are performed by the microorganisms suspended in the liquid, namely, bacteria, protozoa, rotifers, and fungi, which together form the biomass, which develops and grows as these reactions take place. Organic compounds subject to biodegradation include not only lipids, proteins, and carbohydrates, which occur at the order of  $\text{mg L}^{-1}$ , but also micropollutants (i.e., PPCPs), occurring at concentrations of  $\text{ng L}^{-1}$  or  $\text{mg L}^{-1}$ .

After enough time for the appropriate biochemical reactions, the mixed liquor is transferred to a settling tank (secondary clarifier) to allow gravity separation of the suspended solids (in form of floc particles) from the treated effluent. Some of the settled solids are returned to the biological reactor in order to maintain the desired biomass concentration inside (about  $3\text{--}4 \text{ g L}^{-1}$ ). The remainder is considered waste (the so-called excess sludge) and is subjected to thickening, by removing a portion of the liquid fraction in order to increase its solid content. Through the processes of stabilization, dewatering, drying, and combustion, both the water and organic fractions are considerably reduced, and the processed solids (treated or digested sludge) are suitable for reuse or disposal.

Over the years, different configurations of the activated sludge process were developed to promote nitrification, denitrification, and phosphorus removal. More recent evolutions in CAS include membrane bioreactors (MBRs) (**Fig.1.3E**) and moving bed biological reactors (MBBRs) (**Fig.1.3F**). MBRs were developed with the primary aim not only to improve effluent quality but also to upgrade existing wastewater treatment plants (WWTPs) by replacing the previous secondary settler with a membrane compartment able to better separate the solid from the liquid phase. MBBRs were designed to enhance biological processes by promoting the growth of both suspended and attached biomass, thereby increasing the biomass concentration in the aeration tank. One of the main advantages of the two new configurations is that they are

able to treat a higher pollutant load in the “original” reactor volume. Although these two treatments are becoming more diffuse, CAS is still by far the most common in operation (and most studied) [16].

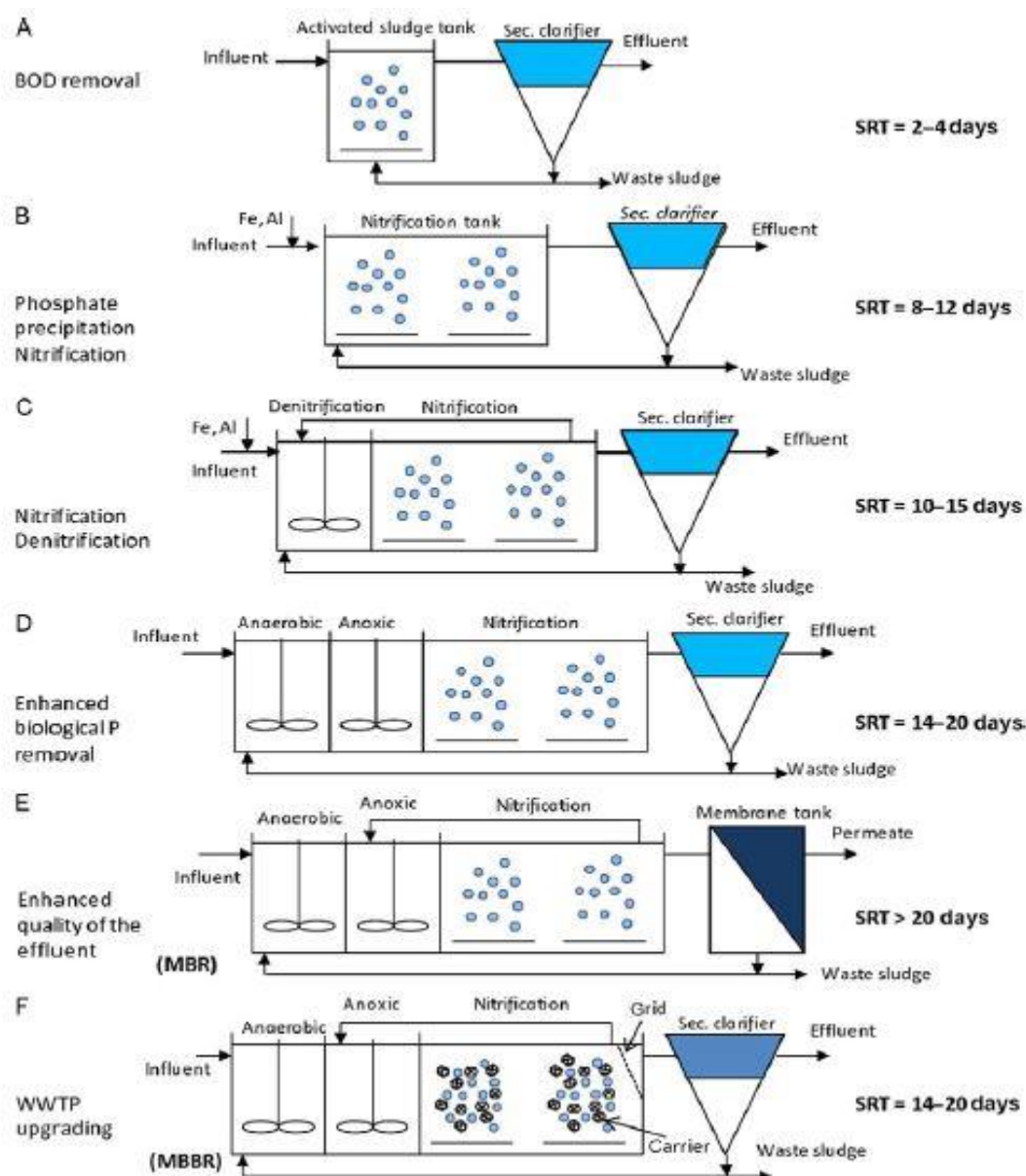


**Fig.1.3:** Historical development of activated sludge process: (A) BOD removal; (B) phosphate precipitation and nitrification; (C) nitrification and denitrification; (D) enhanced biological P removal; (E) MBR; (F) MBBR [2].

## 1.4 Identification of TPs

Identification of TPs of EPs is a challenging task and represents a higher grade of difficulty than the analysis of target pollutants, consequence of the unknown nature of these compounds, and the absence of analytical standards

to confirm their identity. Analytical difficulties are mainly derived from the vast number of intermediates generated, their different physicochemical properties, the complexity and diversity of the matrices and the broad range of concentrations at which these TPs are produced. Additional problems arise from the formation of isomer compounds, difficult to differentiate, and the occurrence of co-elution of compounds with related structures. Therefore, identification of TPs requires the use of advanced analytical instrumentation and appropriate analysis strategies providing high selectivity, high sensitivity and, in particular, high capability for structure elucidation [13, 14].

#### **1.4.1 Identification of TPs-Laboratory approaches**

There are two different approaches to identify TPs: laboratory studies and environmental screening. These approaches are complementary and mutually enriching rather than the opposite of each other. Commonly, laboratory studies offer the advantage of simulating transformation processes under well-defined conditions with appropriate control that facilitates the establishment of differences in the samples that contain the compounds. However, the detection of at least a few of these compounds in the environment is the next necessary step [15].

The laboratory studies are focused on the different types of degradation mechanisms, biotic and abiotic, at relatively high concentrations of the parent EPs [13]. Samples can be provided directly from a WWTP [16] or a pilot-scale WWTP [17] or from natural waters [18].

Biodegradability is mostly evaluated in activated sludge batch experiments under different operational conditions: aerobic, anaerobic and anoxic [16, 19-25]. For aerobic treatment, the sludge is aerated and mixed to suspend the microorganisms whereas N<sub>2</sub> stripping is applied at the beginning of the batch and after each sampling to establish anaerobic and anoxic conditions [21]. Temperature, pH, dissolved oxygen content, and content of total suspended solids are monitored and adjusted to allow direct comparison with environmental conditions [21-23, 25]. Spiked and non-spiked samples for background subtraction caused by natural sludge matrices, run in parallel, as do spiked autoclaved diluted sludge or autoclaved groundwater and ultrapure



water in order to correct for abiotic transformation processes [19, 20]. Samples are collected periodically so that the reaction kinetics of the analytes can be determined sufficiently [22, 24].

Better simulation of the conditions in the full-scale system can be achieved by using alternative water treatment technologies such as MBRs. These MBRs are commonly fed with synthetic wastewater and inoculated with activated sludge from the full-scale WWTP [26].

Batch experiments have also been performed to establish biodegradation in soil [27] and water/river sediments [28, 29], where microorganisms play an important role in degradation.

The simulation of abiotic degradation occurs concurrently with engineered processes, such as oxidation reactions with chlorine, chlorine dioxide, or ozone and transformations by ultraviolet light [15]. There have also been a number of studies with laboratory-scale reactors reported in literature [30-34]. Biotic and abiotic degradations occur together to transform EPs during the biological wastewater treatment [15].

When preliminary studies in batch experiments are completed, verification of the results should then be carried out using real environmental samples [13]. Those studies that correlate the identified TPs from batch experiments with detection in real matrices demonstrated that at least some of them are present in wastewaters and surface waters [16, 19, 21, 22, 31-33], pointing out the interest in small-scale simulation to increase knowledge of TPs [15].

To this end, there is a need for developing sensitive and selective analytical methods including the TPs expected to be present at low concentrations in the environment. Extraction procedures able to isolate and preconcentrate the analytes are extremely important, and conventional solid-phase extraction (SPE) is commonly used in the case of water. These procedures which sometimes also used in laboratory studies are not sophisticated, but are generic and robust since the physicochemical properties of the TPs are sometimes unknown [15]. To achieve sufficient enrichment for this broad range of compounds, Kern et al. used simultaneously four different SPE sorbents in one manually filled cartridge (weak anion, weak cation-exchange

material, and nonpolar and hydrophilic-lipophilic interaction sorbents) [18]. Environmental screening studies of TPs are scarcer and some of them have focused on effluent wastewaters [35-37], while others have been performed in surface and natural waters [18, 38] or water sediments [39].

#### **1.4.2 Identification of TPs-Analytical approaches**

Both liquid (LC) and gas (GC) chromatography is used for the determination of EPs, depending on the polarity, volatility and thermal stability of the concerning compounds. Due to the polarity of most pharmaceuticals, either liquid chromatography-mass spectrometry (LC-MS), or gas chromatography-mass spectrometry (GC-MS) combined with derivatization processes, is normally used for their determination [6, 17].

##### **1.4.2.1 Gas Chromatography (GC) - Mass Spectrometry**

Gas chromatography coupled to mass spectrometry (GC-MS) is the technique most commonly employed today for the analysis of volatile organic pollutants in environmental samples. The very high number of applications is the result of the efficiency of gas chromatography separation and the good qualitative information and high sensitivity provided by mass spectrometry.

The MS fragmentation pattern can often provide unambiguous component identification by comparison with library spectra. Huge electron ionization mass spectral libraries are commercially available, such as NIST Library, which contains 250,000 spectra and the Wiley Library with 720,000 spectra with the new combined version including approximately 950,000 spectra (<http://www.sisweb.com/software/ms/wiley.htm>). The identification process is based on search algorithms that compare the obtained spectra with those of a library, which are generally implemented in the GC-MS instrument.

Mixtures to be analyzed are injected into an inert gas stream and swept into a tube packed with a solid support coated with a resolving liquid phase. The compounds most commonly analyzed by GC-MS include alkanes, polycyclic

aromatic hydrocarbons (PAHs), pesticides, polychlorinated biphenyls (PCBs), as well as endocrine disrupting chemicals [40].

#### **1.4.2.2 Liquid Chromatography - High Resolution Mass Spectrometry (LC-HRMS)**

LC-MS techniques provide a universal approach applicable to the widest number of emerging pollutants and this is the reason why they have today become the technique of choice in the field of environmental analysis. Conventional LC–MS interfaces involve soft ionization techniques that produce little fragmentation but provide information on the molecule. The fragmentation of the analyte required for the structural elucidation is most commonly produced by collision-induced dissociation, which can be done in a specialized collision cell or in the intermediate-pressure part of the mass spectrometer (so- called in-source collision-induced dissociation). The fragmentation pattern of the molecule helps, after the application of long and complicated processes and the use of a number of additional confirmatory analyses, to establish the structure of unknown TPs [15].

#### **1.4.2.3 High Resolution Mass Spectrometry**

LC-MS employing accurate mass measurements has been proven as a successful technique for quantitative analysis of target compounds and rapid qualitative analysis of “unknown” environmental mixtures. Due to the high complexity of some environmental samples (i.e., wastewater, sludge samples, and soil samples), high-resolution techniques with additional structural information on fragment ions are needed and this has made these techniques become more and more popular. These techniques provide a high degree of confidence for identification of target analytes and aid in the structural elucidation of degradation products and unknown compounds, which are also usually present in environmental samples [2] .

Mass analyzers commonly employed are, time-of-flight (TOF), ion-trap (IT), Orbitrap and hybrid [e.g., quadrupole time-of-flight (Q-TOF), quadrupole-linear ion trap (Q-LIT), linear ion trap-Orbitrap or quadrupole-Orbitrap [13]

##### **1.4.2.3.1 Time of Flight (TOF) MS**

The basic principle of a Q-TOF instrument is outlined in **Fig. 1.4**.

TOF resolution is directly related to the length of the flight path. As a consequence modern high resolution instruments share the characteristics of flight paths with a combined length of several meters. The introduction of a reflectron doubles the flight path and regulates the kinetic energy, resulting in higher resolution. Since resolution is related to the length of flight time, TOF provides the highest resolution for relatively high  $m/z$  ion masses. Orbitrap instruments produce the highest resolution for low  $m/z$  ions, which is opposite to the typical TOF performance. Of course, the price to be paid for high resolution is the number of acquired data points per time unit. Mass-resolving power in TOFMS is limited and increasing the mass-resolving power in Orbitrap-MS requires a reduced acquisition speed. Moreover in TOF instruments, the ratio of mass-to-peak width (at FWHM) is relatively constant over the entire mass range in contrast with Orbitrap analyzers.

The importance of sufficient mass resolution is that accurate and precise mass ( $m/z$ ) measurements become possible. Mass-measurement uncertainty in terms of mass accuracy (i.e. average mass error) and mass precision (i.e. standard deviation on the mass error) is based on calculating the relative (ppm) or absolute (mDa) difference between the measured accurate mass and the calculated exact mass of an analyte. Both mass accuracy and precision are essential for proper measurements of accurate mass, and pinpointing different causes of mass-measurement uncertainty can lead to improvement [41].

Hybrid tandem mass instruments, such as the Q-TOF, provide relevant structural information by obtaining product ion full spectra at accurate mass. QTOF MS/MS experiments are an excellent way of confirming potential positives, and are highly useful for elucidating the structures of unknown compounds. There are 2 main MS/MS, also reported in the literature, depending on the nature of the analysis. For target analysis, data-independent acquisition (IDA) is the most preferred one. This approach, termed  $MS^E$  (Waters) or bbCID (broad band Collision Induced Dissociation) (Brukers), involves simultaneous acquisition of accurate mass data at low and high collision energy. By applying low energy (LE) in the collision cell, no

fragmentation is taking place and the information obtained is actually is full scan MS spectrum. At high collision energy (HE), fragmentation of the ions takes place and MS/MS spectra are acquired. With IDA, both molecular and fragment ion are obtained in a single acquisition without the need of pre-selection of the analytes.

On the other hand, for suspect and non-target analysis, data-dependent acquisition (DDA) is more favorable, since information over specific ions can be collected. In this case, two possibilities are available. Either, 2 injections are made, one as a survey and the next with pre-selected ions, or the determination of the candidates of interest for MS/MS information is based on predefined selection criteria. So, there is a first scan, which is processed “on-the-fly” to determine the ions that will be fragmented in a second (data-dependent) scan. The major advantage of this approach is the collection of structural information in just one injection [42].

One of the drawbacks of TOF analyzers is the possibility of the detector saturation which usually implies loss of mass accuracy. Temperature changes are responsible for small thermal expansion or contraction of the flight tube length. This is why it is very important to perform mass calibration. There are three levels of mass calibration, external, internal and lock mass calibration. External and internal calibration must include at least the mass range of interest and can be performed with the same calibrant mixture. Lock mass calibration provides an automated way of applying the linear correction calibration to each spectrum in the analysis and it requires the presence of a continuous signal.

## Schematic Hardware Overview

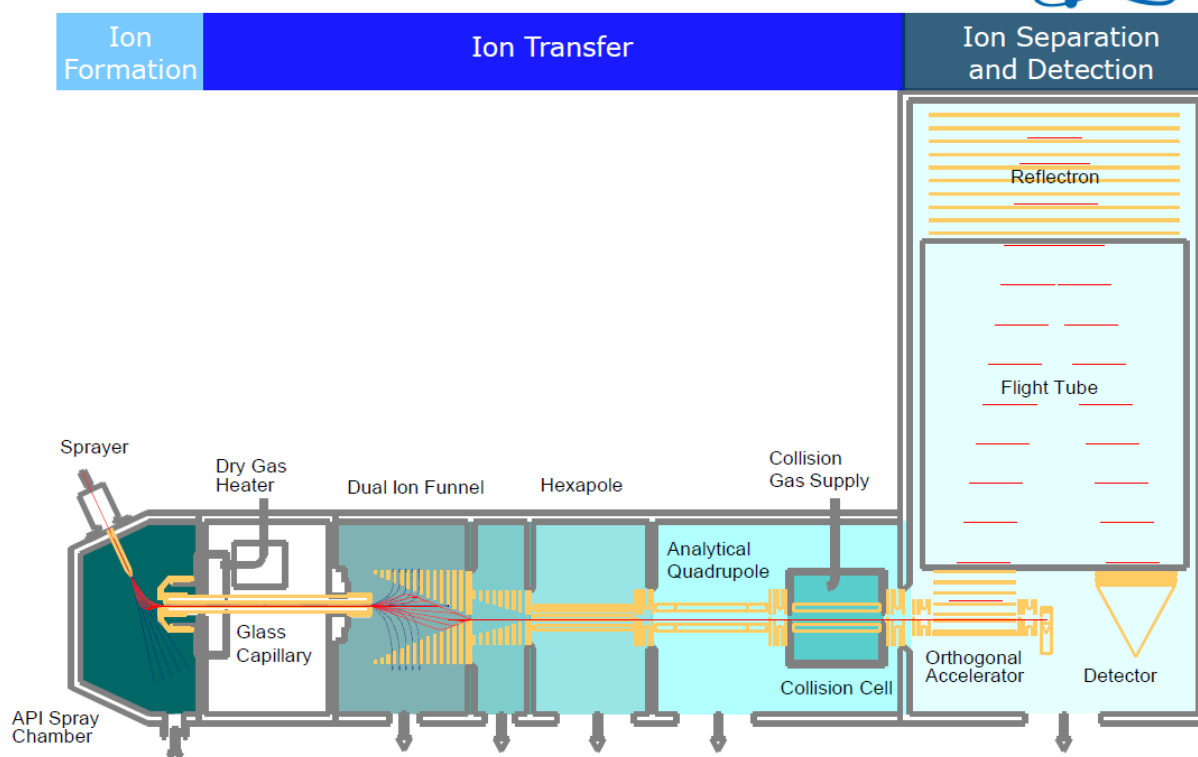


**Fig.1.4:** Schematic presentation of a Q-TOF instrument (Maxis Impact, Bruker).

### 1.4.3 Identification approaches

The challenge in identifying TPs in environmental samples is a lack of knowledge on how compounds will transform, making in situ studies aimed at quantifying and assessing the risk of TPs rarely possible. Larger sets of biotransformation data for organic micropollutants would not only be useful for assessing the potential for exposure to these TPs, but also in the development of structure-based biodegradation prediction tools designed to predict TPs formed in specific environmental compartments. As such, methods are needed that can increase the efficiency and throughput of biotransformation assays. The application of a variety of post-acquisition data processing techniques that are uniquely afforded by high-resolution mass spectrometers have particular value in the identification of microbial TPs in batch systems [17].

#### **1.4.3.1 Target screening**

The first approach guarantees the undoubted confirmation of a TP, and it could be performed with low resolution tandem MS systems or with full scan-based methods with HRMS instrumentation is target screening [43]. In target screening, EPs and TPs are already known and standards are available, so that they can be included within a defined MS method and be monitored in routine analysis [13].

The identification and quantification of micropollutants at low concentrations requires both a high sensitivity and selectivity against complex matrix backgrounds. For a large range of compounds, selected reaction monitoring (SRM) of precursor-product ion transitions by using triple quadrupole (QqQ) or QIT instruments fulfills these prerequisites. A range of studies have shown, however, that monitoring only one transition might result in false positive identifications for individual compounds and thus at least two transitions are required [44].

HRMS target analysis offers promising solutions to the limitations of SRM analysis. Virtually all compounds present in a sample can be determined simultaneously with HRMS instruments operating in full-scan mode, making no preselection of compounds and associated SRM transitions necessary. Additionally, hybrid instruments offer the possibility of data-dependent (also termed information-dependent) MS/MS acquisition, i.e., an MS/MS analysis is triggered if a compound from a target ion list is detected in the full scan. This additionally allows for full-scan product ion spectra recording within the same run for 500 compounds or more [44].

#### **1.4.3.2 Suspect screening**

In contrast to target analysis, the suspects screening approach does not rely on reference standards for quantification and confirmation. These reference standards are currently not available for a large number of potential environmental contaminants, in particular transformation products [44].

However, specific information for compounds that are expected to be in the samples (the “suspects”) should be available for tentative identification. Suspect screening is limited by the creation of databases as large as

possible, with retention times and accurate HR mass spectra of both molecular and fragment ions related to TPs [43]. As a minimum requirement, molecular formula allows for the calculation of an exact  $m/z$  of the expected ion, which is in turn extracted from the high resolution full-scan chromatogram. For electrospray ionization (ESI), this task benefits from the fact that predominantly  $[M+H]^+$  and  $[M-H]^-$  ions are formed, except for some compounds which exclusively show adduct formation. In the case of positive findings, further confirmatory steps based solely on structure-derived information can be employed [44].

For the compilation of such databases potential environmental contaminants and their TPs can be retrieved from literature as well as by using computational (*in silico*) prediction tools.

Several tools are currently available to predict microbial transformation pathways of xenobiotics and the structures of likely TPs. These tools include METAOR, PathPred, CATABOL, and the EAWAG Pathway Prediction System (EAWAG-PPS). Each of these tools contains sets of transformation rules that predict likely microbial transformations based on compound substructure recognition. Transformation rules in the latter two systems are based on data contained in the EAWAG Biocatalysis/Biodegradation Database (EAWAG-BBD), which is a manually maintained collection of literature-reported, microbially mediated metabolic pathways and enzyme-catalyzed reactions. However, most data aggregated within the EAWAG-BBD have been generated in pure culture systems within which the compound of concern serves as the sole carbon source. As a result, transformations observed may not be representative of the transformation pathways occurring in the environment. In environmental systems such as WWTPs, mixed bacterial consortia transform chemicals present in trace concentrations relative to high carbon fluxes of easily degradable material. Therefore the product spectrum is expected to be determined by the microbial diversity of the system and the available pool of enzymes. Additionally, enzymes from fungus species relevant to WWTPs have been shown to catalyze unique biotransformation reactions. It therefore remains unknown how well predictive systems such as



EAWAG-PPS or CATABOL are suited to predict microbial transformations of xenobiotics under environmentally relevant conditions [45].

“Suspects” can be screened, as previously mentioned, by using the exact mass of their expected ions, calculated from the molecular formula. Additional evidence such as isotope pattern match is usually employed for further confirmation. For example, element information such as the presence of Cl, Br, or S has been successfully used to restrict possible molecular formulas due to their distinct isotope signal at [M+2] and characteristic mass defect compared with natural compounds [43]. Moreover, the large number of suspects required an efficient filtering approach, comprising rather straightforward and obvious criteria such as absence in analytical blanks and the match of the observed isotope pattern with the theoretically predicted ones for the molecular formula of the suspect [44].

Another data-processing method based on peak detection, time-trend filtration and structure assignment can be used for the identification of key TPs in terms of persistence over the time of the experiment. Peak peaking and processing of the chromatograms can be carried out by open-source software (e.g., MZmine, enviMass). After blank subtraction, a meaningful time trend is acquired and the remaining candidate peaks are compared with a list from EAWAG-BBD PPS or literature for tentative identification [19].

#### **1.4.3.3 Non-target screening**

In contrast to suspect screening, non-target (unknown) screening in a strict sense starts without any *a priori* information on the compounds to be detected. Many studies in the literature thus fall in between these two categories, as in systems with well-controlled boundary conditions such as transformation experiments, the number of chemically meaningful structures which can be assigned to an unknown peak detected is limited to structures showing a close relationship with the parent compound and an adequate control sample or time series is available. For this type of experiment, an identification by HRMS(/MS) alone can often be considered as definitive.

The non-target workflow focused on the following key features: (i) an automated peak detection by exact mass filtering from the chromatographic

run; (ii) an assignment of an elemental formula to the exact mass of interest; and (iii) a database search of plausible structures for the determined elemental formula. For an automated compound detection several software packages using different peak detection algorithms are available and usually offered by the MS manufacturer.

Searching in large compound databases (e.g., Pubchem) for possible structures of an elemental formula normally results in numerous hits which need to be ranked further by MS/MS data. The search for unknowns in MS/MS or in-source fragment ion libraries is limited to the recorded spectra of reference standards, which is not sufficient for a real unknown screening and suffers from limited comparability among instruments. Therefore an *in silico* strategy for determining unknown chemical structures by matching measured with computational fragmentation spectra of compounds queried from chemical databases seems to be a valuable tool [44].

Open-source and commercial software option for non-target screening, such as MZmine, XCMS, enviMass, Bruker Metabolite Tools and Profile Analysis, Waters MassLynx and MetaboLynx, Thermo Scientific MetWorks and SIEVE, and Agilent MassHunter providing rapid, accurate and efficient data mining are necessary for post-acquisition data-processing [13].

#### **1.4.4 Structure elucidation and identification confidence levels in HR-MS**

High mass accuracy coupled with high isotopic abundance accuracy is fundamental to elicit a reliable molecular formula generated by the software incorporated in the HR-MS instruments. The acceptable deviation of the experimental  $m/z$  from its corresponding theoretical of parent ions is usually defined at 5 ppm. This limit guarantees the correct prediction of their molecular formula. Higher errors, generally below 10 ppm, are acceptable in the workflow regarding their characteristic fragment ions. In spite of the fact that the accurate extrapolation of the elemental composition of a TP is essential, it is not sufficient to lead in a correct structure proposal.

A process which is very helpful in structure investigation is the observation of the presence or absence of similar characteristic ions in the fragmentation

pattern between the parent compounds and its TPs. In addition, information from experimental MS/MS spectra can be compared with *in silico* mass spectral fragmentation tools (e.g. MetFrag, MetFusion, Mass Frontier, MOLGEN-MS and ACD/MS Fragmenter) or with mass spectra in libraries (e.g. MassBank and MetLin) [46]. On the other hand, the use of mass spectral libraries is restricted for LC/MS-MS data because they do not have a great amount of available data and mass spectra of different instruments are not so comparable [47].

Consequently, the HR-MS based identifications of TPs differ among studies and compounds because it is not always possible to synthesize each compound and confirm it. In order to make easier the communication of identification confidence of TPs, Schymanski et al. proposed a level system which is described below (**Fig. 1.5**) [48].

- **Level 1:** Confirmed structure is the perfect situation where the candidate structure is confirmed by the measurement of a reference standard with MS, MS/MS and retention time matching.
- **Level 2:** Probable structure refers to a proposal for an exact structure based on different evidence.
- **Level 2a:** Library which includes indisputable matching between literature or library spectrum data and experimental.
- **Level 2b:** Diagnostic which refers in the case of no other structure fits in experimental data, but no standard or literature information is available.
- **Level 3:** Tentative candidate(s) is the situation where there is evidence for possible structure(s) but the experimental information is insufficient to the exact proposal.
- **Level 4:** Unequivocal molecular formula describes the case of an unambiguous formula which is assigned by the spectral information but there is no sufficient evidence to propose possible structures.
- **Level 5:** Exact mass (m/z) is detected in the sample but no experimental information exists in order to propose even a formula.

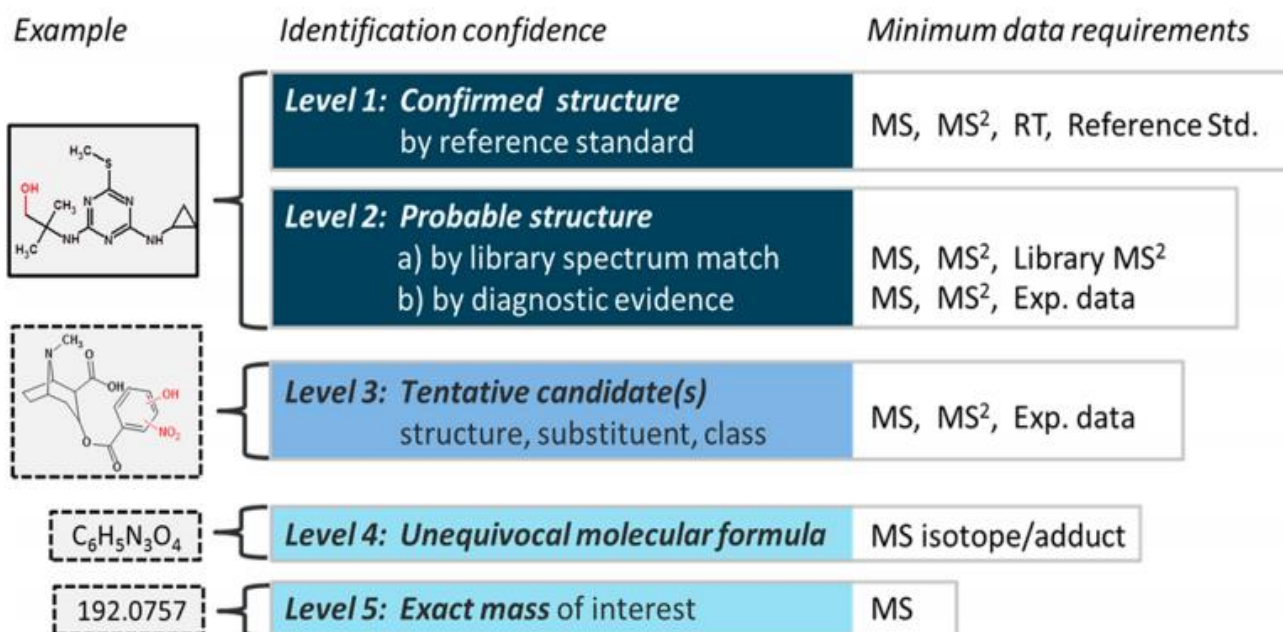


**Fig.1.5:** Proposed identification confidence levels in HR-MS analysis [48].

## CHAPTER 2. Scope and Objectives

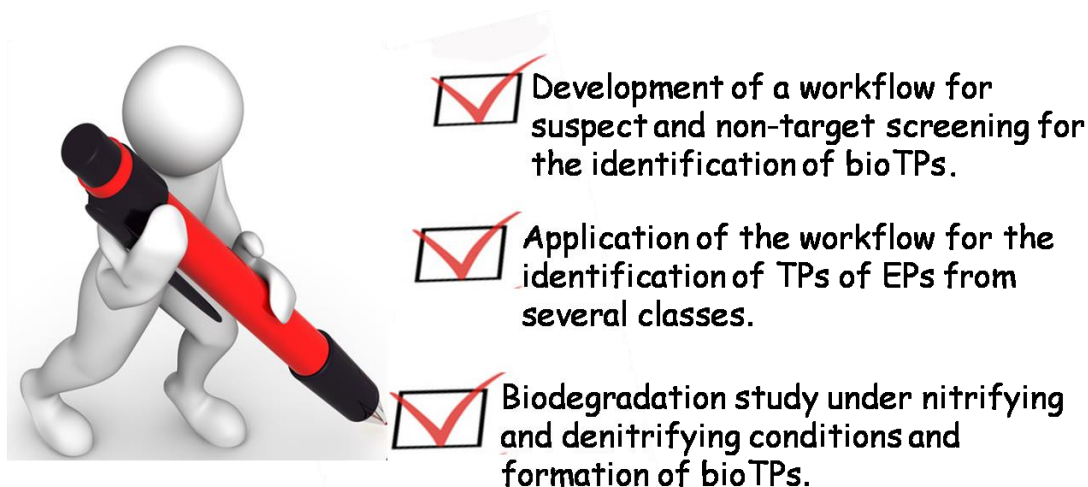


**Fig.2. 1:** Graphical abstract of Chapter 2.

### 2.1 The analytical problem

The chemical pollutants that are regulated under international and EU legislation represent a very small fraction of the universe of chemicals that occur in the environment as a result of human activities. Thus a great number of emerging pollutants, including PPCPs, drugs of abuse and industrial chemicals as well as their transformation products are present in domestic, agricultural and industrial wastewaters and end up to WWTPs. As conventional municipal sewage treatment facilities were never designed to remove these anthropogenic chemicals with structures and mechanisms of biological action that are foreign to biological degradative/transformation systems, many of these micropollutants occur zero or partial removal during conventional processes that are applied in WWTPs, and thus are detected many environmental compartments.

Once released into the environment, EPs are subject to both biotic and abiotic processes that contribute to their transformation and/or elimination. Depending on the compartment in which synthetic chemicals are present in the environment (e.g., surface water) or in the “technosphere” (e.g., WWTPs), different transformations can take place, producing products that, to some

extent, differ in their environmental behavior and ecotoxicological profile compared to the parent compound [1]. Some TPs may be more persistent than their corresponding parent compounds [49] or exhibit greater toxicity [50]. In general, transformation products are mostly unknown and probably more polar than the parent compounds. Since there is a gap in the information on the occurrence and the toxicity of TPs in the environment, we are unable to evaluate their significance in risk assessment.

There is therefore a clear need to reveal the qualitative and quantitative occurrence of TPs in the environment, but this is only possible with continual development of instrumental analysis. With respect to obtaining a holistic view of risk, high-resolution (HR) hybrid mass spectrometers have been proved highly resolved and accurate. Complementarily with improved sophisticated software, HRMS has enabled more reliable, selective target analysis of highly polar compounds, and screening for unknown pollutants.

However, it is still challenging to profile TPs in environment samples, since they are formed through many possible reactions, automatic workflows for the identification are not readily available, so manual data inspection is necessary, though time consuming, and, finally, there are no standards available.

Having said all that above, the study of EPs removal during secondary treatment processes, the identification of their TPs and finally their toxicity assessment has become a significant trend in Environmental Chemistry studies.

## **2.2 Research objectives and Scope**

The study aimed to contribute as high quality research in Environmental Analysis, by filling a gap in the current perspective on the (bio) transformation products of EPs. More specifically, the main objectives of the current research were the identification of metabolites and (bio)transformation products of various classes of EPs which enter the wastewater treatment plant by influents, are formed during secondary treatment and discharged in the aquatic environment.

The experimental part of this doctoral thesis is consisted of three individual studies.

In the first study (**Chapter 3**), an integrated workflow was developed for the identification of TPs. As a case study, selective serotonin reuptake inhibitor (SSRI) drug citalopram was used and batch reactors with activated sludge were designated to investigate its behaviour and the formation of TPs during activated sludge treatment. Both suspect and non-target approaches were applied. To address the completeness of the developed workflow for the detection of additional more polar TPs, hydrophilic interaction liquid chromatography (HILIC) was also evaluated. Extra tools to enhance the identification confidence, such as in-house developed quantitative structure-retention relationship (QSRR) prediction models, were also used. The environmental relevance of the results was assessed by performing retrospective analysis real influent and effluent wastewater samples from the WWTP of Athens. Finally, an environmental risk assessment study was performed by using the predictive ecological structure activity relationships (ECOSAR) model to assess the potential threat for aquatic organisms.

The application of the workflow, fully or partially, for the identification of TPs in several classes of EPs was the objective of the second study (**Chapter 4**). Biodegradation batch experiments were set up to investigate the biotransformation of selected pharmaceuticals and new psychoactive substances (NPs), while lab-scale hybrid moving bed biological reactors (HMBBRs) were set up to investigate the removal of benzotriazoles and hydroxyl benzothiazole from domestic wastewater and the formation of TPs. The occurrence of the pharmaceuticals' TPs was estimated in real influent (IWW) and (EWW) samples, for four consecutive years, through retrospective analysis. The origin of the TPs was assessed by comparing the formation ratios in the IWW and EWW with those in urine reported in literature. Risk assessment was also performed to assess the potential threat for aquatic organisms with two different toxicity models.

Finally, in the third study (**Chapter 5**), the biodegradation of seven pharmaceuticals in activated sludge process and sludge anaerobic digestion were investigated. The effect of aerobic and anoxic conditions on

biotransformation kinetics was assessed in activated sludge experiments. The extent of biotransformation was compared between the target analytes under nitrifying and denitrifying conditions as well as the number and the origin of the formed TPs.

The originality of this doctoral thesis relies on the development of an integrated non-target screening workflow supported by novel strategies for the completeness of the method as well as for the enhancement of the identification confidence. To the author's knowledge, this is the first time HILIC is used complementarily with RPLC to investigate the potential identification of additional, more polar TPs. QSRR prediction models are also proposed, for the first time, as supporting tools in the identification of TPs of emerging pollutants. The environmental relevance of the developed workflow is summarized on the detection of the identified TPs not only on purpose sampling campaigns but in IWW and EWW samples from previous years through semi-quantitative retrospective analysis. Moreover, the detected TPs that showed environmental relevant concentrations were assessed for potential ecotoxicological treat that may pose to the aquatic organisms by different toxicity prediction models. The selected compounds tested were among the most prescribed and consumed pharmaceuticals in Greece. BTRs and OHBTH are worldwide industrial and domestic chemicals that have arisen environmental concerns due to their elevated concentrations in several environmental compartments and their partial elimination from the conventional wastewater treatment plants. Herein, the biotransformation of BTRs and OHBTH was studied in a lab-scale hybrid moving bed biological reactor (HMBBR). Finally, the comparative study of aerobic, anoxic and anaerobic conditions highlights the significance of the different redox conditions on the removal and biotransformation of emerging pollutants. Also, to the author's knowledge, this is a first attempt for comparing the removal rates, biotransformation and sorption losses as well as the formation of biotransformation products of emerging pollutants that may occur in the presence of free or bounded oxygen or under total absence of oxygen.



## CHAPTER 3.

### Citalopram as a case study for the development of an integrated workflow for the identification of biotransformation products

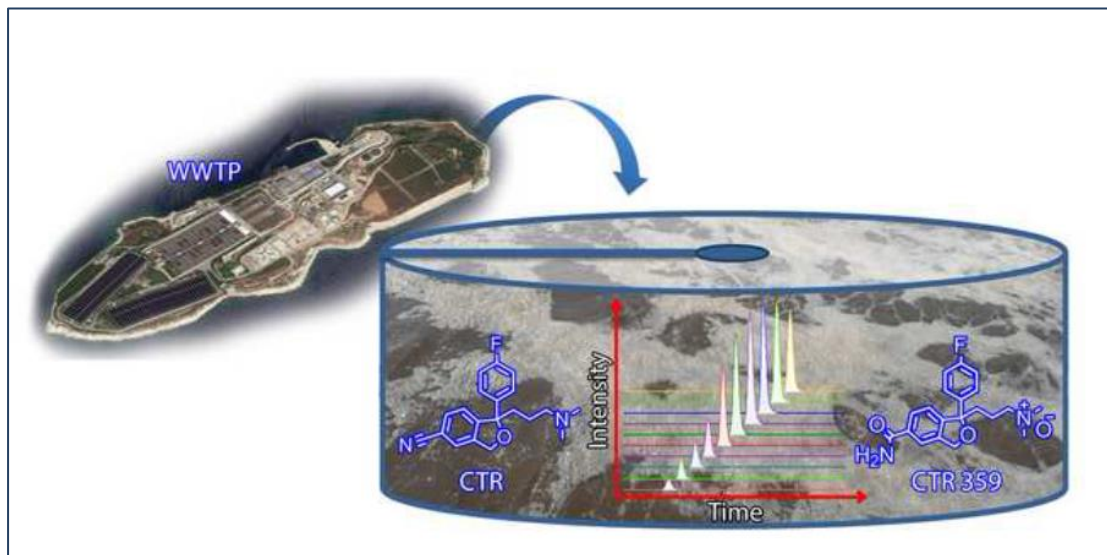


**Fig. 3.1:** Graphical abstract of Chapter 3.

#### 3.1 Introduction

Citalopram (CTR), a selective serotonin re-uptake inhibitor (SSRI), is a compound of interest due to its worldwide high consumption for the treatment of depression. Following oral ingestion, it undergoes hepatic metabolism in order to form more hydrophilic excretable compounds. The phase I human metabolites of CTR include N-desmethylCTR, N-didesmethylCTR, CTR-N-oxide, and a CTR propionic acid derivative [51, 52]. Several studies carried out in different countries reported the presence of CTR in different environmental matrices, including influent wastewaters (IWW), effluent wastewaters (EWW), sewage sludge, surface waters and biota [52, 53]. A literature review of worldwide levels in different environmental compartments (**Table S3.1**, Section S3.1) reveals CTR's global ambiguous distribution. However, fewer studies (**Table S3.2**, Section S3.1) have focused on the presence of CTR's metabolites in environmental samples: N-desmethylCTR has been detected in IWW, EWW, sewage sludge [54], surface waters [55]

and biota [56], while N-didesmethyl CTR was only detected in one study in IWW and EWW samples[57].

In contrast to the large number of studies evaluating the occurrence of CTR, the studies dealing with its fate and transformation processes in the environment or during wastewater treatment are scarce. For CTR, biodegradation is considered to be the most important removal mechanism during wastewater treatment while the contribution of sorption and volatilization seems to be insignificant [58, 59]. The compound was moderately biodegraded under both aerobic and anoxic conditions with an approximate elimination rate of 60% and 40%, respectively, in the studies carried out by Suarez et al. [60, 61]. Moreover, CTR was found to be hydrolytically stable at pH 5, 7 and 9, whereas photodegradation at pH 9 resulted in the formation of two photoproducts: N-desmethylCTR and CTR-N-oxide, both tentatively identified by LC-MS/MS [62]. Another study, dealing with its fate during water treatment with O<sub>3</sub> and ClO<sub>2</sub> oxidation, reported N-desmethylCTR, CTR-N-oxide and three other TPs (3-oxo-CTR, a hydroxylated dimethylamino-side chain derivative and a defluorinated derivative of CTR) [34].

Apart from the presence and the fate of CTR and its TPs in the environment, another aspect to assess is their toxicity by determining possible effects that can be expected at relevant concentrations. CTR has been found to present low acute and chronic toxicity so far, being considered the least toxic among the SSRIs, but also the one least tested for ecotoxicological effects [53, 63].

Therefore, the detection and identification of biotransformation TPs is a necessary but challenging task, which requires the use of modern high resolution mass spectrometric (HR-MS) systems and appropriate analytical strategies [13, 15, 64]. In this regard, hydrophilic interaction liquid chromatography (HILIC) is becoming an attractive alternative (or complement) to the commonly used reversed phase liquid chromatography (RPLC), due to its ability to separate hydrophilic compounds which are poorly retained on RPLC columns [65]. The use of reliable quantitative structure-retention relationships (QSRR) prediction models is also a very useful tool for the identification of suspect and unknown compounds [66].

The present study aims to contribute to the existing knowledge on fate and transformation of CTR during the biological treatment process. For this purpose, biodegradation batch experiments under aerobic conditions were carried out to investigate its behaviour and the formation of TPs during activated sludge treatment. The identification of the formed TPs was based on an integrated LC-HRMS-based workflow, using both suspect and non-target approaches. Analysis was performed by both RPLC and HILIC to investigate their complementarity for the detection of additional compounds. In-house developed QSRR prediction models were also used to support identification. The presence of the identified TPs in the batch experiments was investigated in real wastewater samples from the WWTP of Athens through retrospective analysis. Finally, an environmental risk assessment study was performed by using the predictive ECOSAR model to assess the potential threat for aquatic organisms.

## **3.2 Materials and methods**

### **3.2.1 Chemicals and reagents**

All pharmaceutical standards were of high-purity grade (>95%). CTR was purchased from LGC Promochem (Molsheim, France) and 3-oxo-CTR (CTR Related Compound C) was provided by US Pharmacopoeia (Twinbrook Parkway, Rockville, MD, USA). N-DesmethylCTR, CTR amide and CTR carboxylic acid were obtained by Jubilant Life Sciences Ltd (Shanghai, China).

Methanol (MeOH) and acetonitrile (ACN) of LC-MS grade were purchased from Merck (Darmstadt, Germany), whereas 2-propanol and ethyl acetate of LC-MS grade was from Fisher Scientific (Geel, Belgium). Sodium hydroxide monohydrate for trace analysis  $\geq 99.9995\%$ , ammonium formate  $\geq 99.0\%$ , ammonium acetate and formic acid 99% were purchased from Fluka (Buchs, Switzerland). Distilled water was provided by a Milli-Q purification apparatus (Millipore Direct-Q UV, Bedford, MA, USA).

The biotransformation batch experiments were performed in amber Schott glass bottles from ISOLAB (Wertheim, Germany). Regarding the

consumables for the sample preparation of influent and effluent WWTP samples, the empty solid phase extraction polypropylene tubes (6 mL), as well as the cartridge sorbent materials Septra ZT (Strata-X), Septra ZT-WCX (Strata-X-CW) and ZT-WAX (Strata-X-AW) were obtained from Phenomenex (Torrance, USA). The Isolute ENV+ sorbent material and the frits (20  $\mu\text{m}$ , 6 mL) were from Biotage (Ystrad Mynach, UK). Glass fiber filters (GFF, pore size 0.7  $\mu\text{m}$ , diameter 47 mm) used in wastewater filtration and disposable GFF syringe filters (pore size 1.0  $\mu\text{m}$ , diameter 25 mm) were obtained from Whatman (Maidstone, UK). Regenerated cellulose syringe filters (RC, pore size 0.2  $\mu\text{m}$ , diameter 15mm) were purchased from Phenomenex (Torrance, CA, USA).

Stock standard solutions of individual compounds (1000  $\mu\text{g mL}^{-1}$ ) were prepared in MeOH and stored at  $-20\text{ }^{\circ}\text{C}$  in amber glass bottles to prevent photodegradation.

### **3.2.2 Sampling**

Activated sludge and EWW were sampled from the WWTP of Athens (Greece) for the biotransformation batch experiments. Moreover, 24-hour composite flow-proportional samples of IWW and EWW, collected in March of 2014 and 2015 during eight consecutive days for each year, were used for the retrospective analysis of CTR TPs.

The WWTP of Athens is designed with primary sedimentation, activated sludge process with biological nitrogen (nitrification, denitrification) and phosphorus removal and secondary sedimentation. The hydraulic retention time in bioreactors was 9 hours, the sludge retention time was 7 days and the estimated sewage flow for the collected samples was 750,000  $\text{m}^3 \text{ day}^{-1}$ . The residential population connected to the WWTP was 3,700,000. The WWTP is designed to serve a population equivalent of 5,200,000 and thus is by far the largest in Greece and one of the largest in the world.

Activated sludge, IWW and EWW were collected in pre-cleaned high-density polyethylene (HDPE) bottles. Biotransformation experiments commenced within 24 hours after sampling. Wastewater samples were filtered through sterile glass fiber filters (GFFs) of pore size 0.7  $\mu\text{m}$  immediately upon arrival

at the laboratory, then stored in the dark at 4 °C until analysis within the next 24 hours.

### **3.2.3 Biotransformation batch experiments**

Biotransformation of CTR was investigated within a 6-day batch experiment. The biodegradation test system was prepared in 500 mL amber glass bottles with 200 mL of appropriate content.

Activated sludge was sampled in order to seed the biotic reactor. Total suspended solids (TSS) concentration was measured using Standard Method 2540B [67]. Additionally, two different control experiments were carried out. A batch reactor with EWW was run as hydrolysis and volatilization control (abiotic reactor) and another batch reactor with sterilized sludge (autoclaved at 121 °C for 24 hours) diluted with EWW was set up to examine the sorption losses (sorption reactor) [68]. All bioreactors were spiked with 400 µL of CTR standard stock solution to obtain a final concentration of 2 mg L<sup>-1</sup>. A non-spiked blank reactor seeded with activated sludge was always run in parallel to check for potential cross-contamination between sampling and to subtract the background caused by the natural sludge matrices in post-acquisition data treatment.

Each bioreactor was loosely covered with a perforated cap to allow oxygen diffusion, but avoiding contamination and evaporation, and placed on a magnetic stirrer to further simulate the conventional activated sludge system. Initial pH was in the range 7.4-8.4 and the bottles were at controlled temperature (20 °C) under dark conditions.

Samples were taken immediately after spiking, 1, 2, 4, 6, 8 and 10 hours later and after 1, 2, 3, 4, 5 and 6 days. 1 mL was sampled from each reactor, filtered first through a 1.0 µm disposable GF syringe filter and then through a 0.2 µm regenerated cellulose (RC) syringe filter and divided in two aliquots. In RPLC mode, the extracts were diluted with methanol (MeOH) to achieve an in-vial composition of 50:50 MeOH:H<sub>2</sub>O. For HILIC analysis, the filtrates were dried under a gentle stream of nitrogen and reconstituted in ACN:H<sub>2</sub>O (95:5) prior to analysis.

### 3.2.4 LC-HR-MS/MS analysis

Analysis was carried out using a UHPLC-QTOF-MS system, equipped with a UHPLC apparatus (Dionex UltiMate 3000 RSLC, Thermo Fisher Scientific, Dreieich, Germany), consisting of a solvent rack degasser, auto-sampler, a binary pump with solvent selection valve and a column oven coupled to the QTOF-MS mass analyzer (Maxis Impact, Bruker Daltonics, Bremen, Germany). The QTOF-MS system was equipped with an electrospray ionization (ESI) source, operating in positive and negative ionization mode.

In RPLC mode, an Acclaim RSLC C18 column (2.1 × 100 mm, 2.2 µm) from Thermo Fisher Scientific (Dreieich, Germany), preceded by an ACQUITY UPLC BEH C18 1.7 µm, VanGuard Pre-Column from Waters (Dublin, Ireland), and thermostated at 30 °C, was used. For positive ionization mode, the aqueous phase consisted of H<sub>2</sub>O:MeOH 90:10 with 5 mM ammonium formate and 0.01% formic acid and the organic phase was MeOH with 5 mM ammonium formate and 0.01% formic acid. For negative ionization mode, the aqueous phase consisted of H<sub>2</sub>O:MeOH 90:10 with 5 mM ammonium acetate and the organic phase was MeOH with 5 mM ammonium acetate. The adopted elution gradient for both ionization modes in RP mode started with 1% of organic phase (flow rate 0.2 mL min<sup>-1</sup>) for one minute, increasing to 39 % by 3 min (flow rate 0.2 mL min<sup>-1</sup>), and then to 99.9 % (flow rate 0.4 mL min<sup>-1</sup>) in the following 11 min. These almost pure organic conditions were kept constant for 2 min (flow rate 0.48 mL min<sup>-1</sup>) and then initial conditions were restored within 0.1 min, kept for 3 min and then the flow rate decreased to 0.2 mL min<sup>-1</sup> for the last minute. The injection volume was set to 5 µL.

In HILIC, an Acquity UHPLC BEH Amide column (2.1 × 100 mm, 1.7 µm) from Waters (Dublin, Ireland), preceded by a guard column of the same packaging material, Acquity UPLC BEH Amide 1.7 µm, VanGuard Pre-Column from Waters (Dublin, Ireland), and thermostated at 40 °C was used. For positive ionization, the aqueous phase consisted of H<sub>2</sub>O with 1 mM ammonium formate and 0.01% formic acid and the organic phase was ACN:H<sub>2</sub>O 95:5 with 1 mM ammonium formate and 0.01% formic acid. For negative ionization, the aqueous phase consisted of H<sub>2</sub>O with 10 mM ammonium formate and the organic phase was ACN:H<sub>2</sub>O 95:5 with 10 mM ammonium formate. The

adopted elution gradient, for both ionization modes, started with 100% of organic phase and kept stable for 2 minutes, decreasing to 5 % in 10 min, and kept constant for the following 5 min. The initial conditions were restored within 0.1 min and let to re-equilibrate for 8 min. The flow rate was 0.2 mL min<sup>-1</sup> and the injection volume was set to 5 µL.

When RPLC system was used, the operation parameters of ESI were the following: capillary voltage, 2500 V for positive and 3500 V for negative mode; end plate offset, 500 V; nebulizer pressure, 2 bar (N<sub>2</sub>); drying gas, 8 L min<sup>-1</sup> (N<sub>2</sub>); and drying temperature, 200 °C. In HILIC chromatographic separation, the corresponding MS parameters were: capillary voltage, 3500 V for positive and 2500 V for negative mode; end plate offset, 500 V; nebulizer pressure, 2 bar (N<sub>2</sub>); drying gas, 10 L min<sup>-1</sup> (N<sub>2</sub>); and drying temperature, 200 °C.

The samples from biotransformation experiments and the wastewater samples were first analyzed in full scan mode. The QTOF-MS system was operating in broadband collision-induced dissociation (bbCID, data-independent) acquisition mode and recorded spectra over the range m/z 50–1000 with a scan rate of 2 Hz. This mode provides MS and MS/MS spectra at the same time working at two different collision energies; at low collision energy (4 eV), MS spectra were acquired. At high collision energy (25 eV), no isolation is taking place at the quadrupole, and the ions from the preselected mass range are fragmented at the collision cell.

A second analysis was performed in AutoMS acquisition mode. Data-dependent MS/MS acquisition was conducted using an inclusion (preselected) mass list containing the exact masses of the precursor ion of the parent compound and plausible TPs with an intensity threshold of 1,000 counts. Spectra time was shortened to 0.25 seconds. The collision energy applied was set to predefined values, according to the mass and the charge state of every ion.

A QTOF-MS external calibration was daily performed with a sodium formate solution (10 mM sodium formate in a mixture of H<sub>2</sub>O:isopropanol (1:1)), using a calibrant injection at the beginning of each run. Fourteen cluster ions of the calibrant solution Na(NaCOOH)<sub>1-14</sub> in the range of 50-1000 Da were used for calibration. The instrument provided a typical resolving power of 36000–40000 during calibration.

Data treatment and evaluation were processed with DataAnalysis 4.1 and TargetAnalysis 1.3 (Bruker Daltonics, Bremen, Germany) [64, 69].

### 3.2.5 Analysis of WWTP samples

IWW and EWW samples were extracted using a slightly modified protocol from the one developed by Kern et al. [70]. Briefly; after filtration sample aliquots of 100 mL were adjusted to pH 6.5. SPE was conducted using four different SPE materials simultaneously in an in-house cartridge to achieve sufficient enrichment for a very broad range of compounds (200 mg Oasis HLB, 150 mg Isolute ENV+, 100 mg Strata-X-AW and 100 mg Strata-X-CW). The cartridges were preconditioned with MeOH and water and the water samples were loaded, then there was a drying step under vacuum. The elution was conducted with 4 mL of 50:50 MeOH:ethyl acetate containing 2% ammonia, followed by 2 mL of 50:50 MeOH:ethyl acetate containing 1.7% formic acid. Extracts were evaporated under a gentle nitrogen stream to a volume of 100  $\mu$ L and then reconstituted to 0.5 mL with a final proportion of 50:50 MeOH:H<sub>2</sub>O. Finally, the extracts were filtered through a 0.2  $\mu$ m RC syringe filter and were ready for injection in the RP chromatographic system. Analysis was carried out using the UHPLC-QTOF-MS system in RPLC mode.

### 3.2.6 Suspect and non-target screening for the identification of TPs

A two-step post-acquisition data processing approach was employed to detect and identify candidate TPs of CTR [64].

As a first step, a suspect database of plausible TPs was compiled by using two different *in silico* prediction tools: (1) the Eawag-Biocatalysis/Biodegradation Database Pathway Prediction System (Eawag-BBD/PPS,) (<http://eawag-bbd.ethz.ch/predict/>), an artificial intelligence system, which predicts microbial metabolic reactions based on biotransformation rules set in the Eawag-BBD and scientific literature. Eawag PPS was used with the “relative reasoning mode” switched off, and (2) the MetabolitePredict software (Metabolite Tools 2.0, Bruker Daltonics, Bremen, Germany), a rule-based expert system, which predicts metabolites from Phase I, II and Cytochrome P450 reactions. The prediction results from both



programs include the molecular formula as well as the structures of the generated TPs from two subsequent reactions in the metabolic pathway. Already known and reported metabolites from the literature were also added to the suspect database [51, 52].

Interval samples were screened in full scan, in both chromatographic systems and in both ionization modes, for the detection of suspect TPs from the database. The criteria used for the reduction of features in both chromatographic modes included a threshold in peak area ( $\geq 2,000$  for ESI(+)) and  $\geq 800$  for ESI(-)), a threshold in intensity counts ( $\geq 500$  for ESI(+)) and  $\geq 200$  for ESI(-)), a threshold in mass accuracy of  $\pm 5$  ppm on the monoisotopic peaks, the existence of a good isotopic pattern fit ( $\leq 100$  mSigma) and the chromatographic retention time plausibility in RPLC and HILIC, using in-house QSRR prediction models [71]. Additional criteria for the identification of the suspects were the existence of a meaningful time trend during the batch experiments, their absence (or presence at very low levels) in the zero-time samples, the blank and the control samples.

Samples were also screened for additional TPs not present in the suspect database, following a non-target approach. Background subtraction and peak picking were carried out using Metabolite Detect (Metabolite Tools 2.0, Bruker Daltonics, Bremen, Germany) in order to find TPs present in the biotic samples, but absent in the control samples, and that showed a meaningful time trend. Chromatograms of the biotic samples were compared with those of the control samples, using the following parameters in Metabolite Detect software: subtraction algorithm eXpose mode, delta time  $\leq 0.1$  min, delta mass  $\leq 0.05$  m/z and ratio 5.

Structure elucidation of both suspect and non-target TPs was based on the use of characteristic fragmentation (i.e., fragmentation pattern) during data-dependent MS/MS fragmentation events. The fragmentation pattern of the parent compound and TPs with available reference standards (N-desmethylCTR, CTR amide, CTR carboxylic acid, 3-oxo-CTR) was investigated and different diagnostic neutral losses as well as the absence of characteristic fragment ions were recorded. Subsequently, the MS/MS spectrum of each detected TP was examined for the presence or absence of these diagnostic neutral losses or the presence of new ones, generalizing the

previous “known” fragmentation pathways of CTR and its TPs in order to propose a new tentative structure.

The level of confidence for the identification of the detected compounds was determined according to Schymanski et al. [48], where level 1 corresponds to confirmed structures (reference standard is available), level 2 to probable structures with diagnostic evidence, level 3 to tentative candidate(s), level 4 to unequivocal molecular formulas, and level 5 to exact mass(es) of interest.

### **3.2.7 Retrospective suspect screening of CTR and its TPs**

A retrospective suspect screening was performed in order to evaluate the occurrence of the identified TPs in real wastewater samples. The criteria for the tentative identification (or confirmation, when standards were available) of these TPs were the mass accuracy of the precursor ion ( $\leq 5$  ppm), isotopic fit ( $m\text{Sigma} \leq 100$ ), identical chromatographic retention time ( $\pm 0.2$  min) and the presence of, at least, two qualifier ions in the MS/MS spectra.

### **3.2.8 Environmental risk assessment**

Acute toxicity data were estimated by using the predictive ECOSAR (US EPA) model for three different trophic levels (fish, *daphnia magna* and algae) to evaluate the potential risk of CTR and its TPs, individually, in the aquatic environment. The ECOSAR program predicts toxicity by assessing the structural similarity of a given compound with compounds whose toxicity to aquatic organisms has already been experimentally determined [72].

According to the Technical Guidance Document of the European Commission (European Commission, 2003), the risk quotient (RQ) was calculated as the maximum Measured Environmental Concentration (MEC) divided by the Predicted No Effect Concentration (PNEC), which was calculated as the  $EC_{50}$  or  $LC_{50}$  value divided by 1000 for the case of acute toxicity data. For CTR,  $EC_{50}$  values for *daphnia magna* and algae were obtained from the literature [63]. RQs greater than 1 were considered indicative of an ecotoxicological risk for the aquatic environment.

### 3.3 Results and discussion

#### 3.3.1 Degradation of CTR in batch experiments with activated sludge

Incomplete aerobic degradation of CTR was observed in the activated sludge system (biotic reactor) after 6 days (**Fig.3.3**). The concentration of CTR (spiked at  $2 \text{ mg L}^{-1}$  with a TSS concentration of  $3 \text{ g L}^{-1}$ ) was dissipated by approximately 70% during the first 3 days and then remained stable the next 3 days. An exponential decrease during the first 72 hours of the experiment was observed (**Fig.3.3**).

The control experiments with diluted autoclaved sludge (sorption reactor) showed that only a small fraction (13%) was lost due to sorption processes or reactions with sludge particles. These losses could also be explained by a partial reactivation of the autoclaved sludge as the sludge could be contaminated by active bacteria each time it was sampled [22]. The control reactor with EWW (abiotic reactor) showed negligible losses (3%) of CTR as it was still present at the initial concentration after 6 days. Thus, decreasing CTR's concentration in the active bioreactor can be clearly associated with biological activity (**Fig.3.3**).

The pH was measured in the active bioreactor of the CTR degradation experiment and increased slightly from 7.35 to 8.15 within the first 48 hours, and subsequently decreased continuously to pH 6.60 until CTR was removed 70%. The decrease in the pH was related to the protons produced during the nitrification, which was an ongoing process in the biotic reactor. This trend was not observed for the abiotic and sorption control reactors, which did not contain active biomass and had an average pH of  $8.5 \pm 0.3$  and  $8.4 \pm 0.3$ , respectively [23].

#### 3.3.2 Identification of biotransformation products of CTR

Parallel to the biodegradation of CTR under aerobic conditions, fourteen TPs were formed in the biotic reactor (**Fig.3.2**) and identified through the use of the suspect and non-target screening approaches described in Section 3.2.6. All TPs were detected in the ESI(+) mode. Analysis performed in ESI(-) mode did not reveal any additional TPs. Thirteen out of the fourteen TPs were detected in both RPLC and HILIC systems while the remaining one (CTR

360B) was only detectable by HILIC. Comparison between the peak areas of CTR and the sum of peak areas of the detected TPs (based on the assumption that CTR and its TPs have the same response factor between peak area and concentration) suggested that some TPs may remained undetected (**Fig.3.4**). However, to perform a complete mass balance, quantification of TPs with corresponding reference standards is required, which are currently unavailable for most of the TPs.

**Fig. 3.2** shows the formation/elimination profile (Peak area vs time, from HILIC analyses) for all the detected TPs. CTR 311, CTR 339A, CTR 339B, CTR 341, CTR 343 and CTR 344 were the major TPs and were formed during the first 6 hours of the experiment. The other compounds were detected at lower intensity and their abundance increased after the first 24 hours. CTR 341, CTR 359B and CTR 344 presented maximum peak intensities at 72, 96 and 120 hours, respectively, and then started to decrease. All the other TPs continued to increase over the time course of the experiments.

It should be mentioned that four TPs (CTR 311, CTR 339A, CTR 341 and CTR 343) were also formed in the control reactors at very low abundances (**Fig.S3.1**, Section S3.2), probably catalyzed by matrix components [19]. The formation of these compounds seem to be mainly a result of abiotic processes, but at a negligible rate, as the peak area of the formed TPs in control samples corresponded approximately to 5-10% of their peak area in biotic samples at 6 days.

The identification of the structure of the formed TPs was based on the comprehensive interpretation of the MS/MS spectra. Six important fragmentation patterns with diagnostic neutral losses were observed and are illustrated in **Fig. 3.5**. In all cases, the obtained spectra presented the neutral loss of a H<sub>2</sub>O molecule directly from the precursor ion. N-oxides followed a different pattern with a direct cleavage of the NH(CH<sub>3</sub>)<sub>2</sub>O group and a further elimination of H<sub>2</sub>O. Subsequently, different diagnostic neutral losses occurred: the loss of NHCO (amides), CO<sub>2</sub> (carboxylic acids), NH<sub>2</sub>CH<sub>3</sub> (N-desmethyls), CO (TPs with furan ring oxidized) and an additional H<sub>2</sub>O molecule (hydroxylated TPs). TP identification of the individual TPs is discussed later in this Section.

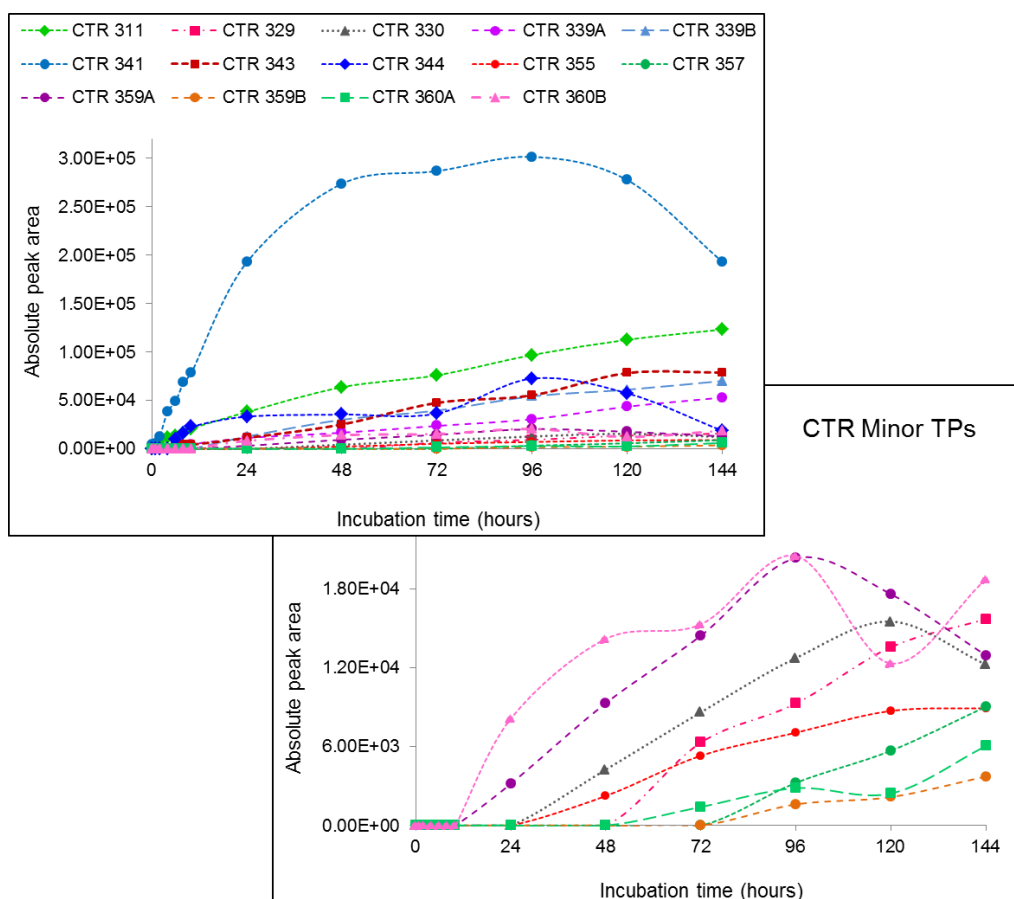


**Fig. 3.2:** Time profile of biotransformation products of CTR obtained by HILIC analysis.

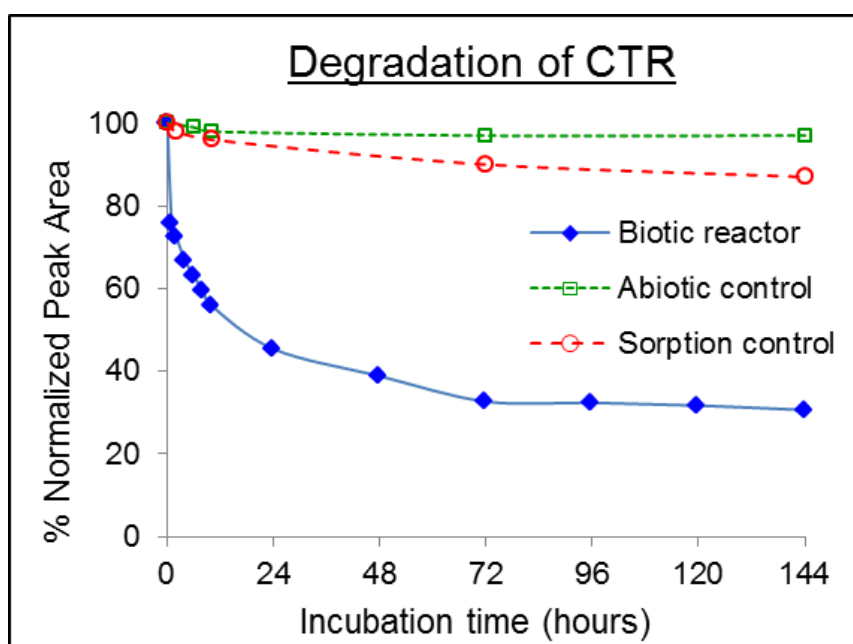


**Fig. 3.3:** Degradation of CTR in aerobic batch experiments.

Another important tool to support identification of TPs was the complementarity of RPLC and HILIC systems in order to obtain orthogonal confirmation, plus the detection of additional TPs. It is important to note that the identification of the CTR 360B was possible only in HILIC, since RPLC was not able to separate the isomers. Moreover, two in-house QSRR prediction models [71] were used as additional experimental evidence for the identification [48]. Predicted retention time for most TPs in both chromatographic systems were in agreement with the experimental ones (**Table S3.3**, Section S3.3). The N-oxide derivatives (CTR 341, CTR 355, CTR 359B and CTR 360A) were rejected only by the HILIC QSRR model, since they were outside of its applicability domain. However, the proposed structures were strongly supported by the observed fragmentation pattern.

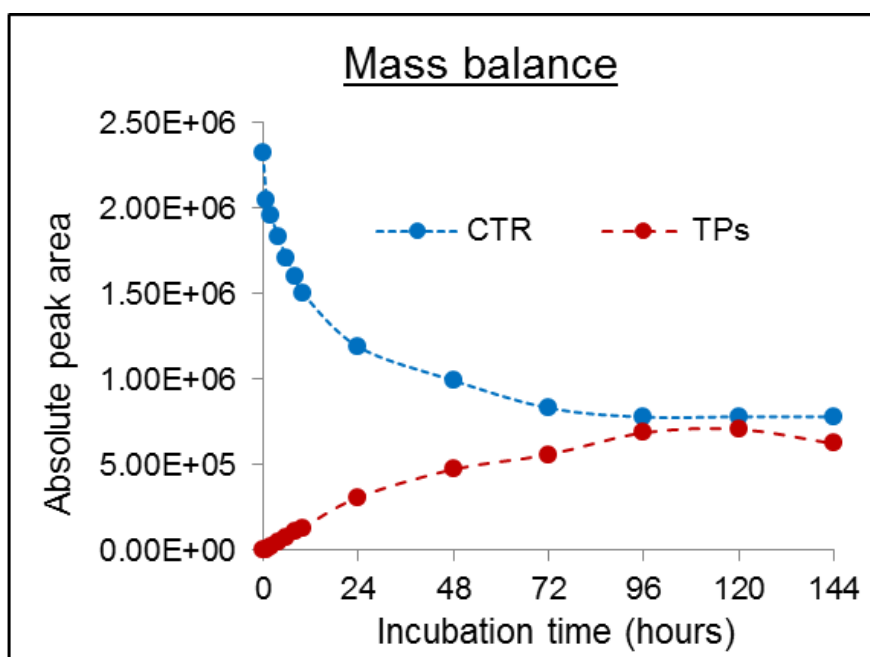


**Fig. 3.4:** Mass balance of CTR and its TPs.

**Table 3.1** summarizes the TPs with their corresponding theoretical mass of the precursor ions ( $[M+H]^+$ ) and molecular formula, the time trend, the time of first appearance, the time corresponding to the maximum intensity, the reached identification levels and the proposed structures. The elemental composition of CTR and its TPs along with their main product ions used for their identification, the measured  $m/z$ , the theoretical  $m/z$  and the mass error in ppm in both RPLC and HILIC systems are summarized in **Table S3.4**

(Section S3.4). The XICs in RPLC and HILIC of the detected TPs at all the incubation time points (time trend) are shown in **Fig. S3.2-S3.18** (Section S3.4). These figures also show the MS/MS spectra (obtained in RPLC and HILIC at the time point of maximum intensity) for each TP including the proposed structures for the fragments.

The obtained MS/MS spectrum of CTR along with its chromatograms in RPLC and HILIC are shown in **Fig. S3.2** (Section S3.4). It can be observed that the ions  $m/z$  307 ( $C_{20}H_{20}FN_2^+$ ) and 280 ( $C_{18}H_{15}FNO^+$ ) were formed by cleaving off a  $H_2O$  molecule and a dimethyl amino group ( $NH(CH_3)_2$ ). The major characteristic fragment with  $m/z$  262 ( $C_{18}H_{13}FN^+$ ) can be explained by the cleavage of either a  $NH(CH_3)_2$  unit from 307 or  $H_2O$  from 280. Further on, the fragment  $m/z$  262 was subjected to losses of a methyl ( $CH_3$ ) and an ethyl group ( $CH_2CH_2$ ), exhibiting ions with  $m/z$  247 ( $C_{17}H_{10}FN^+$ ) and 234 ( $C_{16}H_9FN^+$ ), respectively. Additional characteristic fragments of CTR were  $m/z$  109 ( $C_7H_6F^+$ ) and  $m/z$  58 ( $C_3H_8N^+$ ).

The structure assignment for the twelve TPs identified through suspect screening is presented below:

#### 3.3.2.1 CTR 343 ( $C_{20}H_{24}FN_2O_2^+$ )

This TP has an additional atom of oxygen and two extra atoms of hydrogen in comparison to the parent compound. The MS/MS spectra (**Fig. S3.3**, Section S3.4) showed diagnostic neutral losses of one  $H_2O$  molecule and a  $NH(CH_3)_2$  group, producing the fragment  $m/z$  280 ( $C_{18}H_{15}FNO^+$ ). A further loss of  $NHCO$  (indicating the presence of a primary amide moiety) formed the most abundant ion,  $m/z$  237 ( $C_{17}H_{14}F^+$ ), and a CTR amide structure was assigned. The identity of this compound was confirmed through the purchase of the corresponding standard, reaching identification level 1.

#### 3.3.2.2 CTR 344 ( $C_{20}H_{23}FNO_3^+$ )

The elemental composition of this TP, along with the MS/MS spectra, indicated the presence of a carboxylic acid group (**Fig. S3.4**, Section S3.4). Only one structure from the suspect database, CTR carboxylic acid, corresponds to the previous molecular formula. Likewise, a fragment ion with  $m/z$  281 ( $C_{18}H_{14}FO_2^+$ ) could be observed and the subsequent loss of  $CO_2$

resulted in the formation of the major fragment  $m/z$  237 ( $C_{17}H_{14}F^+$ ). The standard of CTR carboxylic acid was purchased and the structure was confirmed, achieving identification level 1.

#### 3.3.2.3 CTR 311 ( $C_{19}H_{20}FN_2O^+$ )

This compound lacks one carbon atom and two hydrogens in comparison to CTR, suggesting the loss of a methyl group. MS/MS spectra (**Fig. S3.5**, Section S3.4) presented the subsequent eliminations of  $H_2O$  and  $NH_2CH_3$  resulted in the formation of the ion  $m/z$  262 ( $C_{18}H_{13}FN_2^+$ ). The absence of the fragment  $m/z$  58 ( $C_3H_8N^+$ ) implied the transformation of the tertiary amino group into a secondary one. The identity of N-desmethylCTR was confirmed through the purchase and analysis of a reference standard. This compound is not only a TP that was formed during biodegradation experiments, but also a major metabolite of humans which is further metabolized into N-didesmethylCTR. However, the latter was not detected in the investigated treatment process, indicating that N-desmethylCTR was subjected to a transformation pathway that differs from human metabolism.

#### 3.3.2.4 CTR 329 ( $C_{19}H_{22}FN_2O_2^+$ )

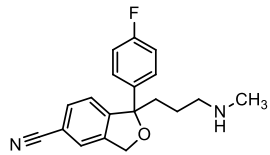
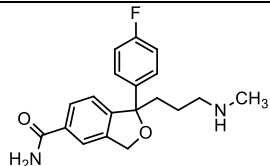
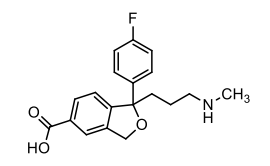
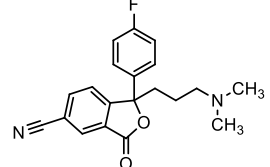
The fragment ions of this TP show similarities to those observed for CTR 343 and CTR 311 (**Fig. S3.6**, Section S3.4). The loss of the  $NHCO$  group from the fragment 280 that was formed through the elimination of  $H_2O$  and  $NH_2CH_3$ , resulting in the most abundant fragment ( $m/z$  237 ( $C_{17}H_{14}F^+$ )), could be attributed to the presence of the amide group. Moreover, the absence of  $m/z$  58 indicated the N-demethylated amide derivative. Thus, CTR 329 was proposed to be N-desmethylCTR amide, with an identification level 2b.

#### 3.3.2.5 CTR 330 ( $C_{19}H_{21}FNO_3^+$ )

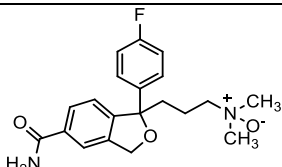
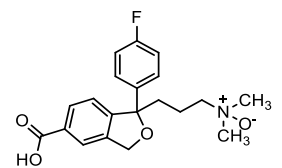
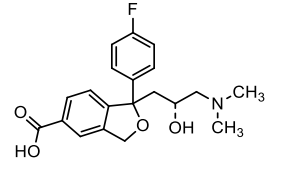
The MS/MS spectra of this TP (**Fig. S3.7**, Section S3.4) showed the initial losses of  $H_2O$  and  $NH_2CH_3$ . Then, the abundant fragment ion  $m/z$  237 ( $C_{17}H_{14}F^+$ ) was formed by decarboxylation, in accordance with the carboxylic acids' fragmentation pattern. These evidences, along with the lack of the fragment  $m/z$  58, suggested N-desmethylCTR carboxylic acid as the most plausible structure, with an identification level 2b.



**Table 3.1:** Identified transformation products (TPs) of citalopram (CTR) during biodegradation batch experiments.

TP	Theoretical Mass of [M+H] <sup>+</sup>	Molecular Formula	Time Trend	First appearance (h)	Appearance of max. intensity (h)	Identification level	Proposed Structure
CTR 311	311.1554	C <sub>19</sub> H <sub>19</sub> FN <sub>2</sub> O	↗	0	144	1	
CTR 329	329.1660	C <sub>19</sub> H <sub>21</sub> FN <sub>2</sub> O <sub>2</sub>	↗	72	144	2b	
CTR 330	330.1500	C <sub>19</sub> H <sub>20</sub> FNO <sub>3</sub>	↗	72	144	2b	
CTR 339A	339.1503	C <sub>20</sub> H <sub>19</sub> FN <sub>2</sub> O <sub>2</sub>	↗	4	144	2b	
CTR 339B	339.1867	C <sub>21</sub> H <sub>23</sub> FN <sub>2</sub> O	↗	6	144	4	-

CTR 341	341.1660	$C_{20}H_{21}FN_2O_2$	$\nearrow \searrow$	2	72	2a	
CTR 343	343.1816	$C_{20}H_{23}FN_2O_2$	$\nearrow$	4	144	1	
CTR 344	344.1656	$C_{20}H_{22}FNO_3$	$\nearrow \searrow$	6	120	1	
CTR 355	355.1452	$C_{20}H_{19}FN_2O_3$	$\nearrow$	24	144	2b	
CTR 357	357.1609	$C_{20}H_{21}FN_2O_3$	$\nearrow$	96	144	2b	
CTR 359A	359.1765	$C_{20}H_{23}FN_2O_3$	$\nearrow$	72	144	3	

CTR 359B					48	96	3
CTR 360A	360.1606	C <sub>20</sub> H <sub>22</sub> FNO <sub>4</sub>			-	144	2b
CTR 360B					6	144	3

### 3.3.2.6 CTR 341 (C<sub>20</sub>H<sub>22</sub>FN<sub>2</sub>O<sub>2</sub><sup>+</sup>)

The elemental composition has an additional oxygen atom, in comparison to CTR and suggested a compound which could correspond to either an N-oxygenated or a hydroxylated TP according to the suspect list. The fragmentation pattern (**Fig. S3.8**, Section S3.4) showed the direct cleavage of the NH(CH<sub>3</sub>)<sub>2</sub>O group, forming the fragment ion  $m/z$  280 (C<sub>18</sub>H<sub>15</sub>FNO<sup>+</sup>), and the subsequent cleavage of H<sub>2</sub>O forming  $m/z$  262. Moreover, the absence of the characteristic fragment  $m/z$  58 indicated the position of the additional oxygen, revealing that the structural change occurred in the tertiary amino group. Theoretically, the compound could be hydroxylated at the  $\alpha$ -C position of the aliphatic chain, resulting in a hemiaminal which is rather unstable. Consequently, CTR 341 was proposed to be CTR-N-oxide, reaching an identification level 2a since the spectra were in agreement with available literature data [34]. CTR-N-oxide is a human metabolite formed from CTR *via* N-oxidation. It was the most dominant compound in these experiments and peaked at 72 hours after its appearance, indicating further transformation.

### 3.3.2.7 CTR 359A and CTR 359B (C<sub>20</sub>H<sub>24</sub>FN<sub>2</sub>O<sub>3</sub><sup>+</sup>)

Two TPs with the same elemental composition were eluted at  $t_R$  4.7 and 5.6 min in RPLC system (**Fig. S3.9**, Section S3.4). The differences in the MS/MS spectra proved their different identity. However, both MS/MS spectra showed similarities with the fragmentation pattern of amides, implying the presence of an amide moiety (**Fig. S3.10** and **Fig.S3.11**, Section S3.4).

More specifically, the MS/MS spectra of CTR 359A (**Fig. S3.10**, Section S3.4) exhibited fragment ions at  $m/z$  341 (C<sub>20</sub>H<sub>22</sub>FN<sub>2</sub>O<sub>2</sub><sup>+</sup>) and  $m/z$  323 (C<sub>20</sub>H<sub>20</sub>FN<sub>2</sub>O<sup>+</sup>), both generated by one or two cleavages of H<sub>2</sub>O. The cleavage of NH(CH<sub>3</sub>)<sub>2</sub>O from  $m/z$  341 produced the fragment  $m/z$  280 (C<sub>18</sub>H<sub>15</sub>FNO<sup>+</sup>), which along with the presence of the fragment  $m/z$  58 (C<sub>3</sub>H<sub>8</sub>N<sup>+</sup>) indicated two possible positions for the hydroxylation. Thus, CTR 359A was identified as a hydroxylated derivative of CTR amide ( $\alpha$ - or  $\beta$ - hydroxylation of the aliphatic chain;  $\alpha$ -hydroxylation could result in a hemiaminal, which are usually unstable compounds), remaining at identification level 3.

The fragmentation pattern of the second-eluted TP (**Fig. S3.11**, Section S3.4) showed a direct loss of  $\text{NH}(\text{CH}_3)_2\text{O}$  at  $m/z$  298 ( $\text{C}_{18}\text{H}_{17}\text{FNO}_2^+$ ). Further on, the absence of  $m/z$  58 ( $\text{C}_3\text{H}_8\text{N}^+$ ) suggested the formation of an N-oxygenated amide derivative, in accordance with the N-oxides' fragmentation pattern. With these evidences, CTR 359B was proposed to be the amide of CTR-N-oxide with an assigned identification level 2b.

#### 3.3.2.8 CTR 360A and CTR 360B ( $\text{C}_{20}\text{H}_{23}\text{FNO}_4^+$ )

Only one TP was detected with this elemental composition in RPLC mode. However, when HILIC analysis was performed, two different compounds with the same elemental composition were detected (**Fig. S3.12**, Section S3.4). Both MS/MS spectra presented the characteristic fragmentation pattern of carboxylic acids (**Fig. S3.13** and **Fig. S3.14**, Section S3.4). CTR 360A spectra presented also the direct elimination of  $\text{NH}(\text{CH}_3)_2\text{O}$  at  $m/z$  299 ( $\text{C}_{18}\text{H}_{16}\text{FO}_3^+$ ) which along with the absence of  $m/z$  58 ( $\text{C}_3\text{H}_8\text{N}^+$ ), implied the presence of an N-oxide group. So, CTR 360A was proposed to be the carboxylic acid of CTR-N-oxide (level 2b). The MS/MS spectra of CTR 360B showed similarities with the fragmentation pattern of the hydroxylated compounds, with the cleavage of two  $\text{H}_2\text{O}$  molecules and further loss of  $\text{NH}(\text{CH}_3)_2\text{O}$ . Thus, CTR 360B was suggested to be a hydroxylated derivative of CTR carboxylic acid ( $\alpha$ - or  $\beta$ -hydroxylation of the aliphatic chain;  $\beta$ -hydroxylation is more likely due to instability of hemiaminals) (level 3).

#### 3.3.2.9 CTR 339A ( $\text{C}_{20}\text{H}_{20}\text{FN}_2\text{O}_2^+$ )

The elemental composition of this TP contains one additional oxygen atom and two hydrogen atoms less than the one corresponding to CTR. It can be observed (**Fig. S3.15**, Section S3.4) that the crucial fragment ions at  $m/z$  258 ( $\text{C}_{18}\text{H}_9\text{FN}^+$ ) and  $m/z$  248 ( $\text{C}_{17}\text{H}_{11}\text{FN}^+$ ), associated with the elimination of  $\text{H}_2\text{O}$  and CO, respectively, indicated the oxidation of the furan ring and denoted the proposed structure of 3-oxo-CTR. It should be noticed that the fluorinated analogue with  $m/z$  109 ( $\text{C}_7\text{H}_6\text{F}^+$ ), which was a diagnostic fragment of CTR and its TPs, was absent here. A commercial standard of 3-oxo-CTR was purchased and the identity of the compound was confirmed *via* appropriate MS/MS and  $t_R$  matching, reaching finally identification level 1.

#### 3.3.2.10 CTR 357 ( $C_{20}H_{22}FN_2O_3^+$ )

Although the suspect database included several double-hydroxylated substituted compounds, the fragmentation pattern of this TP (**Fig. S3.16**, Section S3.4) did not correspond to any of them. The absence of the characteristic fragment  $m/z$  109 was associated with oxidations in the furan ring as observed for CTR 339A, while the diagnostic loss of  $NHCO$  suggested the presence of an amide group. As a result, CTR 357 was proposed to be the oxidized derivative of CTR amide, allowing the assignment of an identification level 2b.

Apart from the compounds present in the suspect list, two additional TPs were detected and evaluated through non-target screening:

#### 3.3.2.11 CTR 355

An unequivocal molecular formula corresponding to  $C_{20}H_{19}FN_2O_3$  was assigned to this TP, involving two additional oxygen atoms and two hydrogen atoms less in comparison to CTR. The MS/MS spectra (**Fig. S3.17**, Section S3.4) displayed two distinct features: on one hand, the direct cleavage of  $NH(CH_3)_2O$  along with the absence of  $m/z$  58 provided strong evidence for the formation of an N-oxide moiety; on the other hand, the lack of the fragment  $m/z$  109, together with the two  $H_2O$  losses, implied the formation of a 3-oxo-CTR derivative. Moreover, the conserved fragment ions at  $m/z$  294 and 276 clearly indicated that the second oxidation occurred in the furan ring. Thus, CTR 355 was tentatively identified as a double-oxidized TP of CTR (level 2b).

#### 3.3.2.12 CTR 339

An unequivocal molecular formula corresponding to  $C_{21}H_{23}FN_2O$  was annotated for this non-target TP. This elemental composition suggested the introduction of a methyl group in the initial structure. However, taking into account the MS/MS spectra (**Fig. S3.18**, Section S3.4), it was not possible to go beyond the determination of the unequivocal molecular formula (level 4).

### 3.3.3 Proposed transformation pathway of CTR

A pathway for the biotic transformation of CTR, based on both the chemical structures of the identified TPs and the sequence of TP formation in the batch

system, was proposed and is shown in **Fig.3.6**. Oxidative reactions, such as hydroxylation, oxidation, N-oxidation and N-demethylation, were observed as the primary biotransformation mechanisms as well as nitrile hydrolysis and amide hydrolysis. All these processes were reported recently in a comprehensive study for amine-containing compounds [73] and previously for amide-containing compounds [45].

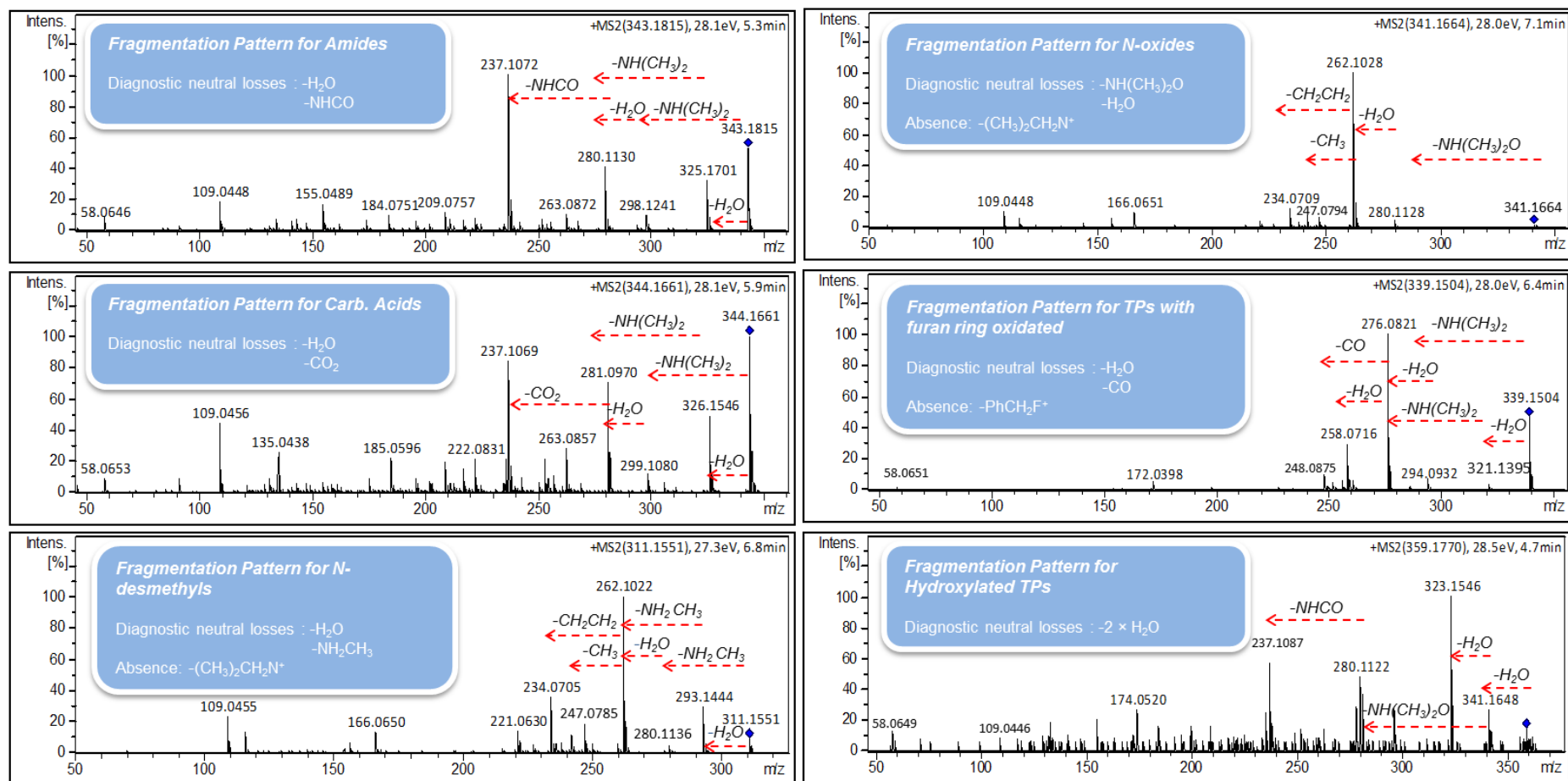


**Fig. 3.5:** Observed fragmentation patterns in selected MS/MS spectra of the formed TPs of CTR.





### 3.3.4 Retrospective analysis of CTR and its TPs in real wastewater samples

The occurrence of the identified TPs was assessed in real wastewater. To this end, a total of 32 samples from the WWTP of Athens (16 IWW and 16 EWW samples), previously analyzed by RPLC-QTOF-MS, were retrospectively screened without the need for additional injections of sample extracts.

The parent compound CTR along with its primary metabolite N-desmethylCTR (CTR 311) was found in all evaluated wastewater samples. 3-oxo-CTR (CTR 339A) was the second most frequently detected compound, as it was present in 26 out of 32 wastewater samples analyzed, including IWW and EWW. CTR-N-oxide (CTR 341) was also detected in all EWW and in 7 out of 16 the IWW. This fact can be easily explained since this compound is also a human metabolite. The intra-week concentration profiles of these three TPs were qualitatively consistent with the one corresponding to the parent compound in the EWW samples, as it can be observed in **Fig. S3.19-S3.20** (Section S3.5). This TP/parent compound agreement in the daily or weekly concentration profile has been previously described by Gago-Ferrero et al. [64] as a valid strategy to obtain extra confidence in the identification of TPs. The same weekly concentration profile was also observed for N-desmethylCTR and CTR in the evaluated IWW samples (the other two TPs were not detected so the trend could not be evaluated; this could be the result of the higher matrix effect of the influent extracts) (**Fig. S3.21-S3.22**, Section S3.5). Finally, the compounds CTR amide (CTR 343) and CTR carboxylic acid (CTR 344) were only found in 3 and 1 EWW samples, respectively, as a result of the biotransformation of CTR during the activated sludge process.

The presence of TPs of CTR in wastewater samples can be attributed to three sources: (1) the direct input from human excreted metabolites in IWW, (2) the biological activity of microorganisms in the sewage system and (3) the biotransformation of CTR and metabolites during wastewater treatment. The first two sources are responsible for the detection of CTR metabolites in the IWW, while the third one is responsible for the presence of biotransformation products in EWW. To assess the origin of CTR TPs, transformation ratios were calculated by divided the peak area of each TP of CTR with the peak

area of CTR, both for IWW and EWW samples of 2014 and 2015. These ratios were compared with those derived from pharmacokinetic studies for CTR excretion and metabolism (**Table S3.5**, Section S3.5). The ratios in urine presented higher uncertainty than the ratios in the IWW and EWW due to the multiple factors that affect the human metabolism of drugs [14]. According to **Table S3.5** (Section S3.5), the ratios for N-desmethyl CTR were similar in urine, IWW and EWW samples, denoting that the concentrations detected in the samples are originated mainly from the input of human excretions. CTR-N-oxide ratios were slightly lower in the IWW samples than in urine and EWW. Especially, the ratios in EWW of 2014 were relatively elevated. Thus, the detected concentrations of CTR-N-oxide could be attributed to the biological activity during wastewater treatment. For the other three detected TPs, no pharmacokinetic data were available since they are not human metabolites and it is the first time that they are reported. The ratios of 3-oxo-CTR were the same in the IWW of both years and in the EWW of 2014, but presented a slight increase in the EWW of 2015, indicating the biotransformation of the parent compound either in the sewer system or during the wastewater treatment. CTR amide and CTR carboxylic acid were only detected in the EWW samples, denoting that they are products of the biotransformation of CTR during the wastewater treatment. Finally, the excretion rate of N-didesmethylCTR was 0.15, thus its presence could be expected in the IWW, but it was not detected in any sample.

### **3.3.5 Environmental risk assessment of CTR and its confirmed TPs**

Semi-quantitation of the identified TPs in the EWW sample collected on March 8, 2015 was performed in order to obtain the MEC values (**Table S3.6**, Section S3.6). The concentrations of CTR and its TPs in the EWW sample, PNEC values and RQ estimated for each analyte are shown in **Table S3.7**, (Section S3.6). It should be taken into account that the choice of data can obviously affect the outcome. According to these results, both CTR and its TPs have RQs lower than 1 and therefore no risk is expected from single compounds. However, given that a mixture of these compounds with the same pharmacological mechanisms exists in the environment, additive effects

could be expected, making the real hazard potentially higher than calculated for the individual compounds [63].

### 3.4 Conclusions

- The observed elimination rate (70%) for CTR in batch experiments with activated sludge can be associated with biological activity as control reactors showed insignificant removal of the parent compound.
- LC-QTOF-MS proved to be a powerful tool for the structure elucidation of the TPs; the orthogonal confirmation by RPLC and HILIC analysis, along with  $t_R$  prediction models, proved to be complementary strategies in the identification workflow. The importance of HILIC is emphasized in the detection of an additional TP (enabling the separation from its isomer), which could not be detected through RPLC analysis.
- In total, fourteen TPs were formed during the biodegradation experiments of CTR. Four out of them were confirmed with reference standards (N-desmethylCTR, CTR amide, CTR carboxylic acid and 3-oxo-CTR). A probable structure based on diagnostic evidence and tentative candidates were proposed for the additional seven and two TPs, respectively, while only one remained unidentified at identification level 4. N-desmethylCTR and CTR-N-oxide have been previously reported as human metabolites, whereas 3-oxo-CTR was an oxidative TP. To the authors' knowledge, this is the first study dealing with the identification of biotransformation TPs of CTR and eleven TPs are reported for the first time.
- Twelve TPs of CTR were identified through the use of suspect screening, and two additional TPs were detected by non-target screening. The performance of suspect screening (using *in silico* prediction software for the creation of the database) and non-target screening as independent and complementary approaches resulted in comprehensive identification of the formed TPs within specific biotransformation systems. Structure-based interpretation of the results was achieved for identification of preferences in biotransformation pathways of CTR.
- Two human metabolites (N-desmethylCTR and CTR-N-oxide) and three biotransformation TPs (3-oxo-CTR, CTR amide and CTR carboxylic acid)

of CTR were detected in EWW samples through retrospective suspect screening. It confirms that monitoring solely the presence of the parent compound CTR is not enough to assess the impact of this widely consumed pharmaceutical in the aquatic ecosystem.

- Risk quotients indicated no potential threat for the exposure of aquatic organisms regarding CTR and its TPs. However, available data regarding toxicity of CTR and its TPs in aquatic biota is very limited and further research is required on this aspect.

## **CHAPTER 4.**

### **Identification of biotransformation products of several emerging pollutants from different chemical classes**

#### **4.1 Introduction**

The integrated workflow presented previously can be used for the identification of biotransformation products from different chemical classes. It is suggested to be used as it is to assure the completeness on the identification of the formed TPs. However the workflow can be used partially and skip certain steps as HILIC or/and non-target screening, depending on the scope of the research. In this chapter, the developed workflow was used for the identification of bio-TPs of pharmaceuticals, illicit drugs and industrial chemicals.

The complete workflow was adopted for the identification of four frequently consumed pharmaceuticals in Greece, namely; metformin (MTF), ranitidine (RAN), lidocaine (LDC) and atorvastatin (ATR). Following, the workflow was used for the identification of bio-TPs of a psychotropic drug (p-methoxy methamphetamine, PMMA) and on the major phase I human metabolite of mephedrone (dehydromephedrone, DHM) in batch reactors seeded with activated sludge.

Lastly, the workflow was used for the identification of bio-TPs of micropollutants that occur in wastewater from domestic and industrial activities (six compounds; benzotriazole (BTR), 4-tolytriazole (4TTR), 5-tolytriazole (5TTR), xylytriazole (XTR), 5-chlorobenzotriazole (CBTR) and 2-hydroxybenzothiazole (OHBT)) in laboratory scale hybrid moving bed biofilm reactor (HMBBR) system.

On the last two studies only suspect screening was performed by using data obtained only from RP chromatographic system.

## 4.2 Identification of biotransformation products of pharmaceuticals

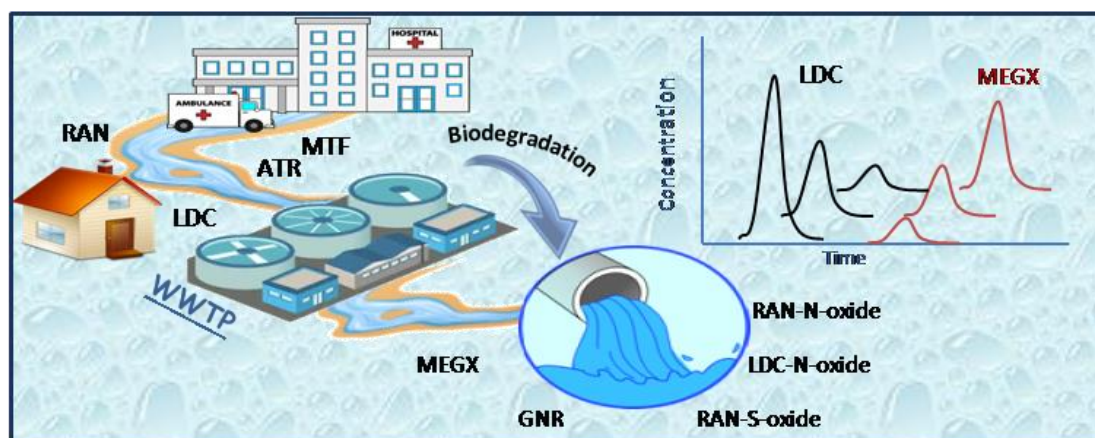


Fig.4.1: Graphical abstract of chapter 4.2.

### 4.2.1 Introduction

Over the last decade, pharmaceuticals have attracted broad scientific interest as a new class of emerging pollutants since they enter into the local sewer system via direct disposal, excretion via urine or/and hospital wastes [43, 74]. Due to the biotic and abiotic processes that take place in a WWTP (hydrolysis, photolysis, microbial metabolism, oxidation) the degradation of pharmaceuticals may result in the formation of transformation products (TPs) [15]. TPs are often more stable and biologically recalcitrant than the parent compounds (PCs) and as a consequence cannot be considered less harmful to the aquatic environment [15, 20, 28].

The selected pharmaceuticals for this study are among the most frequently consumed pharmaceuticals in Greece and have been detected in elevated concentrations both in influent and effluent wastewater (IWW & EWW) samples and seawaters in Greece [13, 72, 75, 76]. Metformin is among the top antidiabetic drugs. Microbial degradation of MTF has been studied previously, indicating the formation of a dead-end TP, known as guanyurea (GNR), that seems to be a very recalcitrant TP against further photo- and biodegradation [64, 77-80]. Ranitidine reversibly inhibits the action of histamine at the histamine H<sub>2</sub>-receptors [81]. Ranitidine-N-oxide (RAN-N-oxide) is the major phase I metabolite in the human body followed by the S-oxide and desmethyl RAN [81]. Several studies have been carried out for the

biotransformation of RAN under aerobic conditions, reporting the already known human metabolites as microbial TPs [68, 81]. Concerning the metabolism of lidocaine, a local anesthetic drug, oxidative N-dealkylation seems to be the major pathway in humans and animals [82]. Numerous studies reported the occurrence of lidocaine and its metabolites in IWW and EWW [72, 76, 82, 83]. The fate of lidocaine, during treatment with activated sludge, was recently investigated by Gulde et al [73]. One of the most prescribed lipid regulator drugs of the statins class, atorvastatin, has not yet been studied for the identification of biodegradation products formed in the aeration tanks of the WWTPs [84].

High-resolution mass spectrometry (HRMS) is the key element for the identification of TPs that are still unknown [13, 15]. Hence, the number of publications dealing with the fate and identification of TPs of pharmaceuticals through suspect and non-target screening has increased significantly over the past few years, following a more holistic approach in environmental analysis [13, 15, 20, 22, 24, 28, 64, 74, 85-89].

Furthermore, appropriate analytical strategies can be applied to support the identification for the candidate TPs. Hydrophilic interaction liquid chromatography (HILIC) can be used complementarily to RPLC for the identification of more polar TPs that cannot be retained in C18 columns addressing in this way the problem of completeness on the identification of TPs [64, 65, 86]. Moreover, the utilization of retention time prediction models can provide additional confidence for the assignment of a structure to a candidate TP detected through suspect and non-target screening [64, 66, 71, 83, 86, 90].

Environmental fate models can promote the quantitative estimation of toxicity of newly identified TPs and thus trigger the establishment of precautionary measurements against their occurrence, if this is indicated. At the same time, innovative and accurate approaches with defined applicability domain (AD) like Quantitative Structure-Toxicity Relationship (QSTR) could be useful to estimate the toxicity of TPs in aquatic multispecies [91]. Therefore, a QSTR model could be suitable to predict the toxicity and to prioritize TPs on the basis of their environmental risk.



In the current study, the transformation of selected pharmaceuticals during wastewater treatment was assessed. The selection of the compounds aimed to cover a wide range of polarities and different pharmaceutical classes. Batch-reactors were designated, with activated sludge under aerobic conditions, to simulate the operating conditions of a WWTP. An integrated workflow was developed through suspect and non-target screening for the identification of novel bio-TPs. The complementarity of HILIC was also evaluated to enhance the completeness of the developed workflow by investigating the possibility to find additional more polar TP. An in-house developed quantitative structure-retention relationship (QSRR) prediction model was used supportively to enhance the identification confidence for the proposed structures of the candidate TPs.

Finally, the occurrence of the identified TPs was estimated in real influent (IWW) and effluent wastewater (EWW) samples, for four consecutive years, through retrospective analysis. The origin of the TPs was assessed by comparing the formation ratios in the IWW and EWW with those in urine reported in literature. Since the biotransformation products of a parent compound could be more toxic and environmental persistent, risk assessment was performed to assess the potential threat for aquatic organisms. Two different toxicity models were used namely, ECOSAR and ToxTrAMS for the calculation of risk quotients (RQs).

## **4.2.2 Material and methods**

### **4.2.2.1 Chemicals, reagents and substance selection**

Details on the used chemicals and reagents are provided in the Electronic Supplementary Material section 4.1.1. A summary of the physicochemical properties of the investigated pharmaceuticals are presented in **Table S4.1** (Section 4.1.1).

### **4.2.2.2 Sampling**

The sampling of this experiment was in line with the previous one and details have been discussed extensively in Chapter 3, section 3.2.2. Two more

sampling campaigns were added and therefore IWW and EWW samples from 2014 to 2017 were screened for the detection of the target compounds and their TPs.

#### **4.2.2.3 Biotransformation batch experiments**

Two separate experiments were carried out for each pharmaceutical to investigate both the degradation kinetics and the biotransformation pathways. A detailed overview on the performed experimental set up, so as to accomplish the aforementioned objectives, presented in **Table 4.1**.

#### **4.2.2.4 Analysis of WWTP samples**

For the analysis of IWW and EWW samples, the protocol developed by Kern et al. [70] was adopted in a slightly modified version. UHPLC-QTOF-MS system in RPLC mode was used for samples analysis. Detailed information about instrumental analysis and sample preparation is given Chapter 3, section 3.2.5.

#### **4.2.2.5 Workflow for suspect and non-target screening for the identification of TPs**

A tiered post-acquisition data processing approach was implemented for the detection and identification of TPs [17, 86] (**Fig.4.2**). Details on the applied workflow can be found on Chapter 3, section 3.2.6.

#### **4.2.2.6 Retrospective suspect screening of the identified TPs in real wastewater**

A retrospective suspect screening was performed in order to evaluate the occurrence of the identified TPs in real wastewater samples. The criteria for the tentative identification (or confirmation when standards were available) of these TPs were mass accuracy of the precursor ion ( $\leq 5$  ppm), isotopic fit ( $m\text{Sigma} \leq 100$ ), identical chromatographic retention time ( $\pm 0.2$  min) and the presence of at least two qualifier ions in the MS/MS spectra.

#### **4.2.2.7 Environmental risk assessment**

Acute toxicity data were estimated by using two different prediction models. The predictive ECOSAR model (US EPA) was used for three different trophic

**Table 4.1:** Overview on the experimental set up was performed to investigate both the degradation kinetics and the biotransformation of the selected compounds.

Reactor	Spiked Concentration	Content	Duration	Application
Biotic	200 $\mu\text{g L}^{-1}$	Spiked mixed liquor	MTF 2 days RAN 3days LDC 12 days ATR 2 days	Degradation kinetics estimation
Biotic	2 $\text{mg L}^{-1}$	Spiked mixed liquor		Monitoring & identification of TPs
Sorption	2 $\text{mg L}^{-1}$	Spiked autoclaved sludge diluted with WWTP effluent (0.3 gss $\text{L}^{-1}$ )		Check for sorption to suspended sludge particles
Control	2 $\text{mg L}^{-1}$	Spiked WWTP effluent		Check for abiotic degradation processes
Blank	-	Non spiked mixed liquor		Check for contamination between sampling & blank subtraction

levels (daphnid, fish and green algae) to assess the potential risk of the pharmaceuticals and their identified TPs (id. level 1, 2a and 2b) in the aquatic environment. The second model that was used was ToxTrAMS. The acute

toxicity of all the identified TPs and parent compounds were predicted with ToxTrAMS, an in-house risk assessment program. Acute toxicity values were predicted towards three aquatic species; *daphnia magna* (planktonic crustacean, measurement was based on  $LC_{50}$  ( $mg\ L^{-1}$ ) after 48 h of exposure), *pseudokirchneriella subcapitata* (algae, measurement was based on  $EC_{50}$  ( $mg\ L^{-1}$ ) after 72 h of exposure) and *Pimephales promelas* (fish, measurement was based on  $LC_{50}$  ( $mg\ L^{-1}$ ) after 96 h of exposure). A wide scope model, which was built based on 1353 emerging contaminants with their experimental  $pLC_{50}$  information, was used to estimate acute toxicity in *daphnia magna*. The molecular features behind the model were hydrophobicity, polarizability, summation of solute-hydrogen bond basicity and minimum atom-type E-state of  $-OH$  [91, 92]. The models used to predict the toxicity in algae and fish were also built based on a large set of 537 and 4060 emerging contaminants, respectively [59]. In the case of algae model, molecular features were  $\log P$ , number of nitrogen, number of rotatable bonds and excessive molar refraction [93]. For risk assessment in fish, the molecular features were hydrophobicity, sum of atom-type E-state of  $=CH-$  and  $-OH$ , modified information content index (neighborhood symmetry of 1-order), molecular distance edge between all tertiary carbons, number of 6-membered rings [94] 3D topological distance based autocorrelation - lag 6 / weighted by covalent radius. The applicability domains of the applied models over the identified TPs with unknown toxicity were carefully studied considering the effect of chemical structure similarity (or chemical space failure) to avoid using any incorrect prediction results [91].

For a compound with unknown experimental toxicity measurement, the only way to address the applicability domain is to study the chemical space. Therefore, if the error is the function of chemical space failure, hat values, warning leverage values and also normalized mean distance can be used to define the applicability domain. To this end, we used a robust method to show if the error is a function of chemical space failure, using hat values (a threshold applied by warning leverage value) versus normalized mean distance. This method offers several conditions where chemical space failure of a compound with unknown toxicity could be addressed: (a) the chemical

space failure zone is the area above the normalized mean distance of 1 and leverage values higher than the warning leverage cut off. Any compounds found to be there are outside of the applicability domain of the proposed QSTR model and should not be predicted with this model; (b) the safe zone is the area where compounds are within the warning leverage and normalized mean distance limit. These predictions are accepted because these compounds are highly similar to the compounds in the training set used to build the model; (c) for compounds in the area that is exceeding the warning leverage cut-off limit, but they are within the limit of normalized mean distance and the maximum leverage value (derived from the training set), the prediction results are less reliable and in case of a resulting concern, values should be verified experimentally.

For both models risk quotients (RQ) were calculated and compared. Baseline toxicity predicted by ECOSAR was used to evaluate the potential risk due to the simultaneous presence of all the PCs and their TPs in wastewater ( $RQ_{mix}$ ) and the possible environmental hazard of the mixture when wastewater is released in Greek rivers ( $RQ_{mix,river}$ ) was also estimated [72].

The ECOSAR program predicts toxicity by assessing the structural similarity of a given compound with compounds whose toxicity to aquatic organisms has already been experimentally determined [72]. The output of ECOSAR was the baseline toxicity (in  $mg\ L^{-1}$ ) and the lethal or effective concentration ( $LC_{50}$  or  $EC_{50}$ , in  $mg\ L^{-1}$ ) of three different trophic levels (daphnid, fish and green algae).

According to the Technical Guidance Document of the European Commission (European Commission, 2003), the risk quotient (RQ) was calculated as the maximum Measured Environmental Concentration (MEC) of a contaminant, divided by the Predicted No Effect Concentration (PNEC), which was calculated as the  $EC_{50}$  or  $LC_{50}$  value divided by a safety factor of 1000 for the case of acute toxicity data (Equations 4.1-4.2). RQs greater than 1 were considered indicative of an ecotoxicological risk for the aquatic environment [72].

$$PNEC = \frac{LC_{50} \text{ or } EC_{50}}{1000} \quad (4.1)$$

$$RQ = \frac{MEC}{PNEC} \quad (4.2)$$

The risk due to the simultaneous presence of all the PCs and their TPs in wastewater ( $RQ_{mix}$ ) was calculated as following (Eq. 4.3)

$$RQ_{mix} = \sum_{i=1}^n RQ_i = \sum_{i=1}^n \frac{MEC_i}{PNEC_i} \quad (4.3)$$

To estimate the possible environmental hazard of the mixture of all the PCs and their TPs when wastewater is released in Greek rivers the  $RQ_{mix,river}$  was calculated using Eq. 4.4.

$$RQ_{mix,river} = \frac{RQ_{mix}}{DF}, \quad DF = \text{Dilution factor} \quad (4.4)$$

For  $RQ_{mix}$  and  $RQ_{mix,river}$  calculations baseline toxicity predicted by ECOSAR program (also known as narcosis or nonspecific toxicity) was used. Dilution factors were adopted by the study of Thomaidi et al. [72] for 25 Greek rivers that received treated wastewater.

## 4.2.3 Results and discussion

### 4.2.3.1 Degradation of the selected pharmaceuticals in batch experiments with activated sludge

All the selected pharmaceuticals degraded as shown in the concentration time courses in **Fig. 4.2**. The degradation rate and extent of degradation differed among the compounds. The studied concentration ( $0.2 \text{ mg L}^{-1}$  with a TSS concentration of  $3 \text{ g L}^{-1}$ ) disappeared for MTF and ATR within 4 h and RAN was completely degraded (>99%) after 24 h. LDC was dissipated by approximately 64% within 6 days. The removal of the PCs followed pseudo-first order kinetic with observed reaction constants presented in the Electronic Supplementary Material (**Table S4.2**, Section S4.1.2). The half-lives were calculated to be 0.71 h, 1.27 h, 5.43 h and 108.2 h for MTF, ATR, RAN and LDC, respectively (**Table S4.2**, Section S4.1.2).

Sorption control experiments revealed only little sorption onto the sludge particles for MTF (2%), LDC (10%) and ATR (14%) (**Fig. 4.3**). Although RAN presented the greatest sorption among the studied PCs at the end of the

experiment (23% in 48 h), only 10% of the initial concentration were sorbed onto the sludge within the 24 h where complete removal was achieved. Therefore, sorption in the batch reactors was neglected when deriving the kinetic data. Controls with spiked EWW showed <8% losses due to abiotic processes (hydrolysis and volatilization) for all the studied compounds (**Fig. 4.3**). Thus, the disappearance of the pharmaceuticals can be clearly associated with biotic processes.

#### **4.2.3.2 Identification of biotransformation products**

Full-scan data was acquired from LC-QTOF-MS operating in broad band collision induced dissociation (bbCID) mode. Data-dependent acquisition obtained from AutoMS mode supported the structure elucidation of the candidate TPS. Twenty-two TPs stemming from four pharmaceuticals were identified in total. All the TPs were detected in positive (+ESI) mode while negative (-ESI) mode did not provide additional TPs. Seventeen TPs were identified through suspect screening and five more through non target screening. Five out of the 22 TPs were confirmed by corresponding reference standards whereas no standards were available for the remaining TPs. For additional 3 potential TPs, a molecular formula was suggested but no additional structural information could be generated. Moreover, one additional TP (RAN317B) was identified in HILIC but not in RP. For RAN, HILIC enabled the separation and characterization of isomeric TPs (RAN 301A & B). Besides, the TP peaks of RAN and MTF (both very polar compounds) in HILIC had a clearer MS/MS spectra for interpretation. As an additional confirmation step for the assignment of a structure in a candidate TP, in-house QSRR prediction models were used for retention time prediction both in RPLC and HILIC (**Table S4.3** SectionS4.1.3). The QSRR prediction model cannot predict the retention time of compounds that their structure are out of the applicability domain of the model (e.g. N-oxides). On this basis, the identification of these TPs was only supported by the MS/MS spectra and retention time prediction filtering step did not apply. All the detected TPs are listed in **Table 4.2** along with their corresponding theoretical mass of the precursor ions ( $[M+H]^+$ ), molecular formula, the time trend, the time of first appearance, the time corresponding to the maximum intensity, the reached

identification levels and the proposed structures. The time-courses of the degraded PCs and the corresponding formed TPs are illustrated in **Fig. 4.3**.

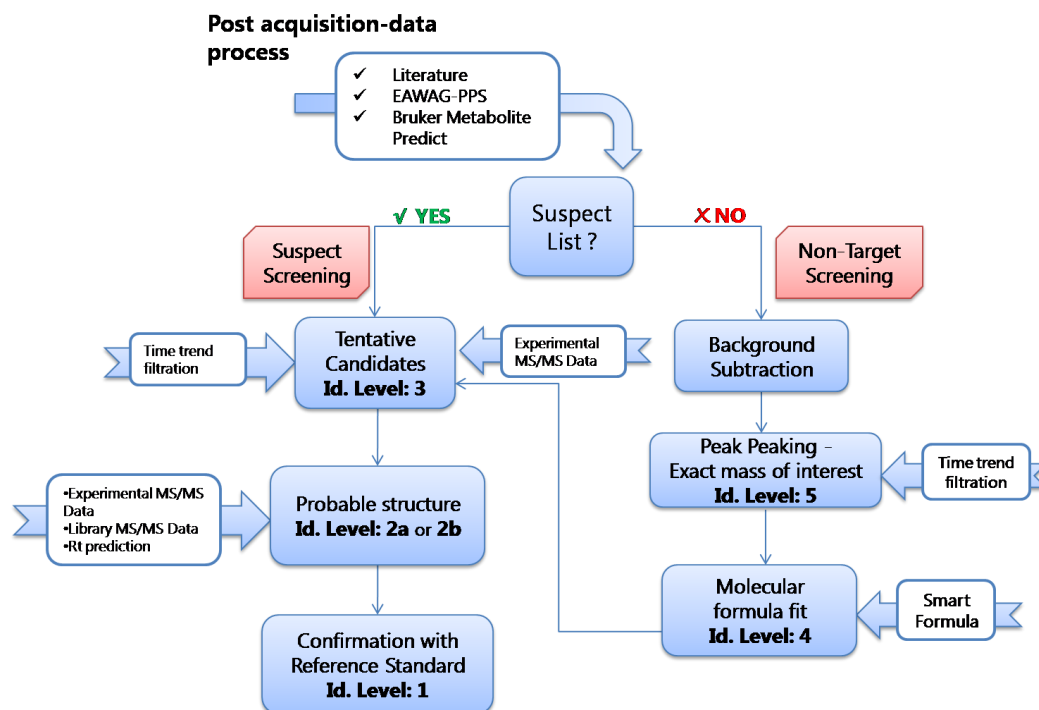


**Fig.4.2:** Developed workflow for suspect and non-target screening for the identification of TPs.

#### 4.2.3.2.1 Biotransformation of MTF

Metformin is a very polar compound and therefore eluted during the first minutes in RPLC. As a consequence, MTF TPs which can be expected to be eluted earlier than the PC, would be hard to identify. The initial concentration of the compound disappeared within 6 hours. The 48-hours experiment revealed only the formation of MTF103 (**Fig. S4.1**, Section S4.1.3). Even though HILIC provided better peak shapes for MTF103, no more additional TPs were identified through suspect and non-target screening. Fragmentation verified that MTF103 was the microbial TP of MTF, guanylurea. The identification of guanylurea (GNR) was confirmed through the analysis of a reference standard. To assess the further biotransformation of GNR, separate batch reactors were run in parallel. GNR was spiked in  $2 \mu\text{g L}^{-1}$  and the



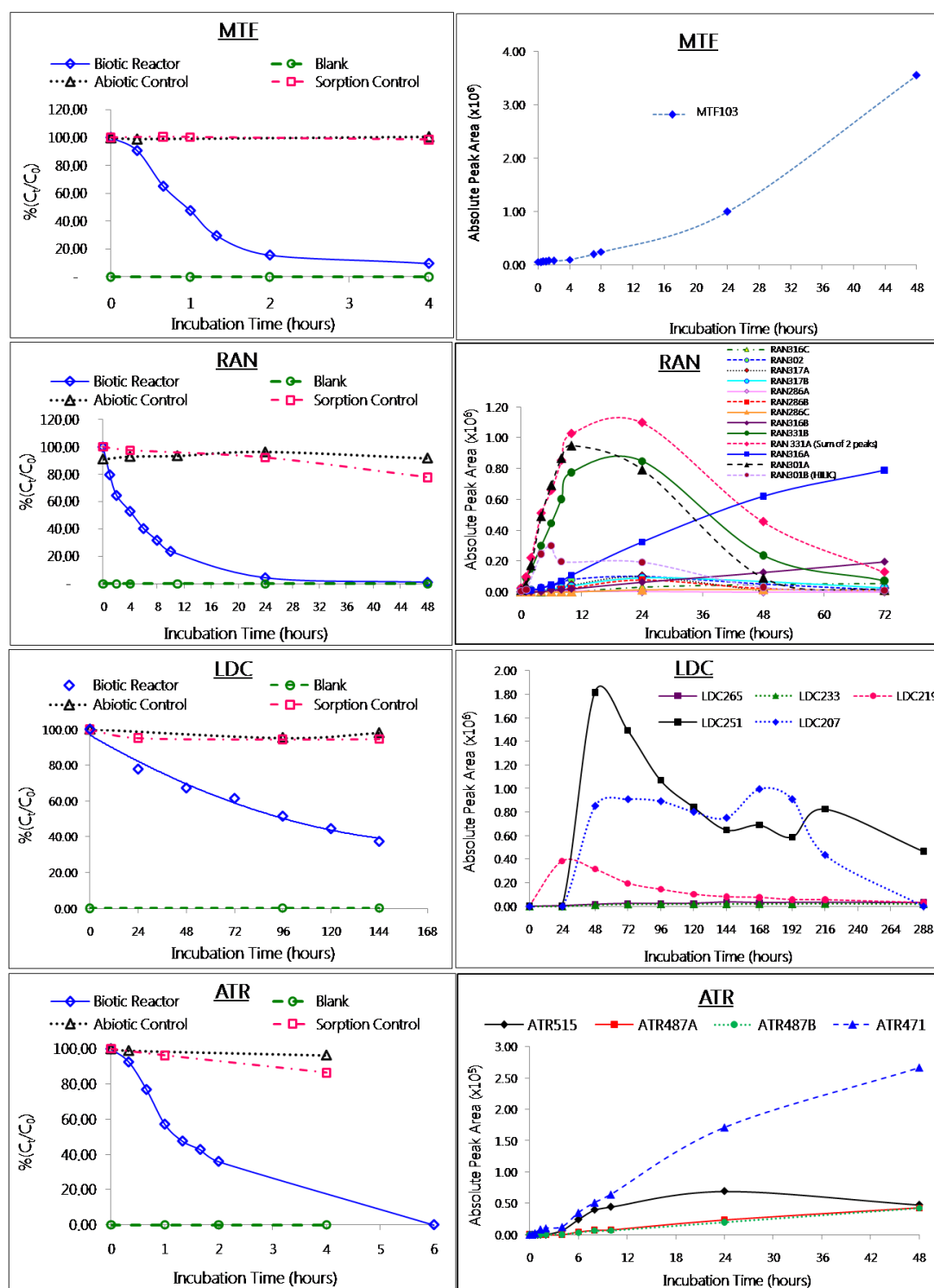


**Fig.4.3:** Time courses of pharmaceuticals concentrations in activated sludge, blank, sorption, and abiotic controls for metformin, ranitidine, lidocaine and atorvastatin along with the respective formed transformation products are depicted in plots by peak area.

incubation time was 5 days. The obtained time trends (Fig. S4.2, Section S4.1.3) showed no significant degradation of GNR. Consequently, GNR was considered the dead-end bioTP of MTF. It is very recalcitrant and expected to

be omnipresent in all aquatic compartments in elevated concentrations [77-79].

#### 4.2.3.2.2 Biotransformation of RAN

Ranitidine was fully degraded within 24 hours. Twelve candidate TPs emerged during the 72-hours experiment. Suspect screening revealed 9 candidate TPs while the non-target approach showed the formation of RAN316A-C. RAN286 was foreseen from the suspect list to be formed as a second generation bioTP by hydroxylation of RAN followed by hydrolysis and oxidative deamination on the hydroxylated carbon. This candidate TP was predicted only by Metabolite Predict software. The accurate mass of the protonated ion 286.0856 presented three different peaks, RAN286A, RAN286B and RAN286C with retention times of 3.0 min, 3.4 min and 4.2 min, respectively (**Fig. S4.3**, Section S4.1.3) However, the  $m/z$  286.0856 was not present in HILIC. Poor fragmentation in the MS/MS spectra did not allow the verification of the predicted structure and thus only an unequivocal molecular formula corresponding to  $C_{11}H_{15}N_3O_4S$  was attributed to these masses (level 4). RAN301 lacks one carbon atom and two hydrogens in comparison to the PC, suggesting the loss of a methyl group which was in agreement with the suspect list. The loss could have occurred either at the secondary or the tertiary amine of the parent molecule. RPLC presented only one peak with elemental composition  $C_{12}H_{20}N_4O_3S$ . Contrary, two different peaks were detected in HILIC with retention times of 6.3 and 6.7 min and the same elemental composition, respectively (**Fig. S4.4**, Section S4.1.3) Obtained MS/MS spectra interpretation denoted slight differences in the fragmentation. The  $m/z$  85.0760, 117.0481  $m/z$  and 170.0634 were the keys to assign the formation of desmethyl-RAN at the tertiary and the secondary amine moiety in RAN301A and RAN301B, respectively (level 2b). Desmethyl-RAN is thus a good example to point out the complementarity of HILIC. The separation of the isomers was achieved with HILIC, whereas co-elution of the isomers occurred in RPLC. MS/MS spectra further provided the necessary information for assigning the TPs to their respective peaks in HILIC. The elemental composition of RAN302 ( $C_{11}H_{15}N_3O_5S$ ) along with the MS/MS spectra indicated the presence of a carboxylic acid group (**Fig. S4.5**, Section S4.1.3)

which was demonstrated by the presence of the fragment ion with  $m/z$  125.0233 ( $C_6H_5O_3^+$ ) (level 2b).

The theoretical mass of  $[M+H]^+$  331.1434 was represented by several isomeric TPs in the suspect list derived from S-, N-oxidation and hydroxylation reactions in the parent molecule. Suspect screening showed the existence of three peaks with retention times 1.4, 2.0 and 3.5 min in RPLC whereas only one peak was found in HILIC (**Fig. S4.6**, Section S4.1.3) The MS/MS spectra of the peaks at 1.4 and 2.0 min obtained in RPLC were identical. The spectrum of the peak that eluted in 3.5 min was rather different. Surprisingly, the MS/MS spectrum in HILIC was a mix of the two aforementioned spectra. In the first two spectra, the fragment with  $m/z$  138.0907 implied that the part of the parent molecule with the furan ring and the tertiary amine remained intact. After the cleavage of the furan ring, the fragment 110.0960 amplified that hypothesis and thus the possible TPs were reduced to three; two hydroxylations and one S-oxidation. In the third spectrum, the fragments with  $m/z$  270.0903 and 224.0983 indicated that the oxygen was added in the part of the molecule with the tertiary amine.

This could have been form either the N-oxide or of a hydroxylated TP in the tertiary amine. Since RAN-S-oxide and RAN-N-oxide have been previously identified in biodegradation experiments [43] with activated sludge, the corresponding reference standards were analyzed as the most plausible TPs to have been formed. As it was expected (**Fig. S4.7**, Section S4.1.3) two TPs were confirmed as RAN-S-oxide and RAN-N-oxide (level 1). RAN-S-oxide reference standard presented two peaks in RPLC ( $R_t$  1.4 and 2.0 min) presumably due to the chromatographic system used which is generic and not optimized for all the TPs. Both RAN-S-oxide and RAN-N-oxide eluted at 6.7 minutes in HILIC, denoting the insufficient separation of the TPs when co-existing in a sample and justifying the obtained spectra.

The molecular formula of RAN317 ( $C_{12}H_{20}N_4O_4S$ ) indicated the demethylation of the PC and the simultaneous addition of an oxygen. According to the suspect list, the demethylation can be occur either at the secondary or in the tertiary amine comparable to RAN301. Proportionally to RAN331, the oxygen can enter to the molecule through an oxidation reaction (hydroxylation or S-

/N-oxidation) and thus a few candidate TP's should be considered. RAN317 presented two peaks, in RPLC and HILIC (**Fig. S4.8**, Section S4.1.3)

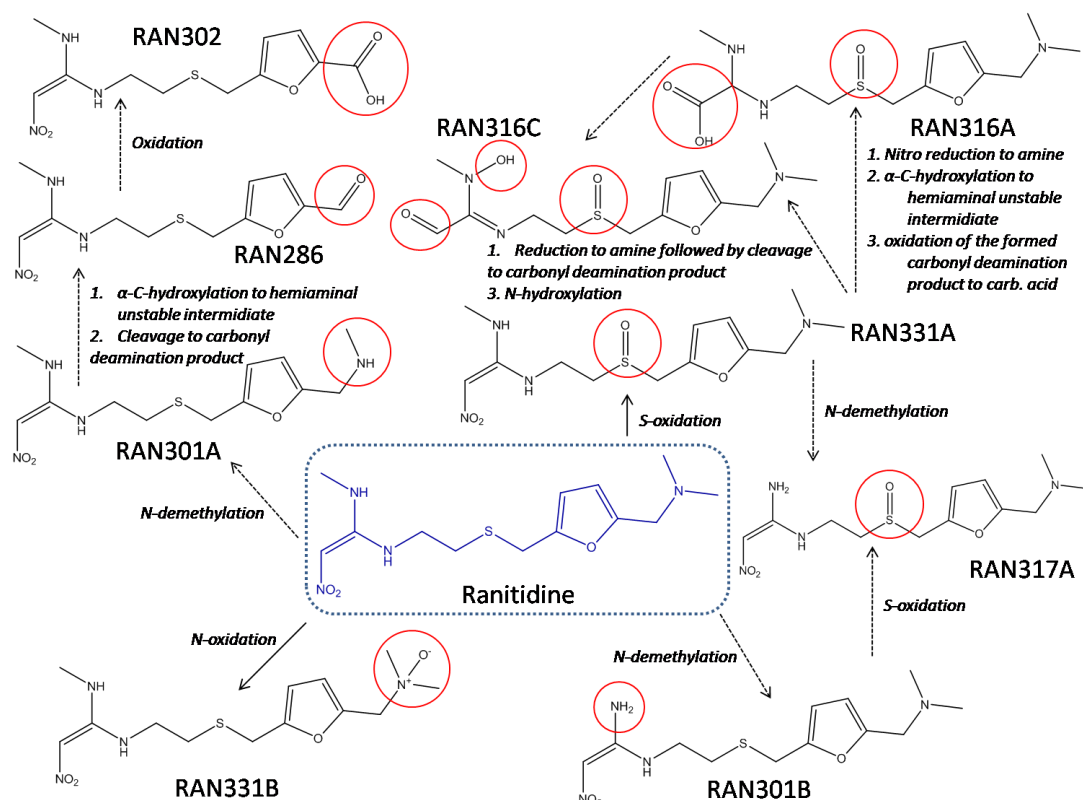


**Fig.4.4:** Proposed biotransformation pathway of ranitidine. Dotted arrows indicate proposed structures of the TP's while line arrows indicate confirmed TP's.

The spectrum of the second peak ( $R_t = 7.9$  min) in HILIC could not be obtained due to low intensity. Both spectra in RPLC (RAN317A and RAN317B) showed significant similarities particularly comparing to the spectra of RAN-S-oxide. Considering the similar fragmentation we result to that; an S-oxidation has taken place ( $m/z$  192.0456, 110.0967 and 138.0919) instead of a hydroxylation. The fragment with  $m/z$  138.0919 was the key point to support that the demethylation in RAN317A occurred at the secondary amine, as the part of the molecule with the furan ring and the tertiary amine remained intact (level 2b). The MS/MS spectra of RAN317B in HILIC did not show rich fragmentation and only three common fragments were presented. As a result, no specific structure could be proposed for RAN317B (level 3).

Non-target screening revealed the occurrence of three chromatographic peaks with theoretical mass of  $[M+H]^+$  316.1331 (RAN316A-C). SmartFormula

assigned the same elemental composition for the three peaks with retention times 1.4, 1.9 and 2.9 min, possibly indicating the formation of isomers. The elemental composition of RAN316 ( $C_{13}H_{21}N_3O_4S$ ) lacks a nitrogen and involves one oxygen more in comparison with the PC. The MS/MS fragmentation of RAN316C was really poor while the MS/MS spectra of RAN316A and RAN316B presented substantial similarities (**Fig. S4.9**, Section S4.1.3) RAN316A and RAN316B spectra presented comparable fragmentation with RAN-S-oxide and RAN317A. In the full-scan MS spectrum of RAN316A, the transition of 316.1329 to 272.1431 was displayed denoting the neutral loss of  $CO_2$ . The loss caused by the in-source fragmentation of the precursor ion and thus a formation of a carboxylic acid TP is possible. The fragment with  $m/z$  138.0913 implied also that the part of the molecule that remained intact is the furan ring with the secondary amine. Subsequently, the formation of the carboxylic acid in RAN316A is considered to have taken place in the nitro group position in the previously formed TP RAN331A (level 2b). A similar pathway (oxidative deamination after rearrangement has been previously proposed by Men et al. [95] for the formation of a RAN carboxylic acid TP by ammonia-oxidizing archaea. MS/MS spectra did not provide additional information for the TP RAN316B. As a consequence, RAN316B was assumed part of the peak RAN316A, eluted 0.2 min later due to the chromatographic system used which is generic and not optimized for all the TPs, as it was mentioned before. RAN316C fragmentation both in RPLC and HILIC was not rich. Very few fragments were available for interpretation to suggest a structure. The similarity of the obtained spectra with the spectra of the ozonation by-product of ranitidine P-315b reported by Christoforidis et al. lead to the proposal of the structure (level 2a) [69].

The biodegradation pathway of RAN was depicted (**Fig. 4.4**) according to the proposed structures of the identified TPs. The observed biotransformation reactions include dealkylation (demethylation), S-oxidation, N-oxidation, hydroxylation and deamination, some of them most likely proceeded by nitro reduction.

#### 4.2.3.2.3 Biotransformation of LDC

Five TPs were identified for LDC. Two of the TPs were in the suspect database and the remaining three were identified through non target screening. According to the suspect list, a single or double deethylation was an expected way of biotransformation for the PC. LDC207 was identified as the mono-deethylated TP of LDC since the fragmentation matched the proposed structure well (**Fig. S4.10**, Section S4.1.3). The molecular formula of LDC251 ( $C_{14}H_{22}N_2O_2$ ) denoted the insertion of an oxygen atom in the PC presumably via a hydroxylation or oxidation reaction. The  $m/z$  74.0596 and 130.0846 indicated the formation of N-oxide (**Fig. S4.11**, Section S4.1.3). Analysis of the corresponding reference standards confirmed the formation of LDC207 and LDC251 as norlidocaine (or monoethylglycinexylidide) and lidocaine-N-oxide, respectively (**Fig. S4.12**, Section S4.1.3) (Id. level 1).

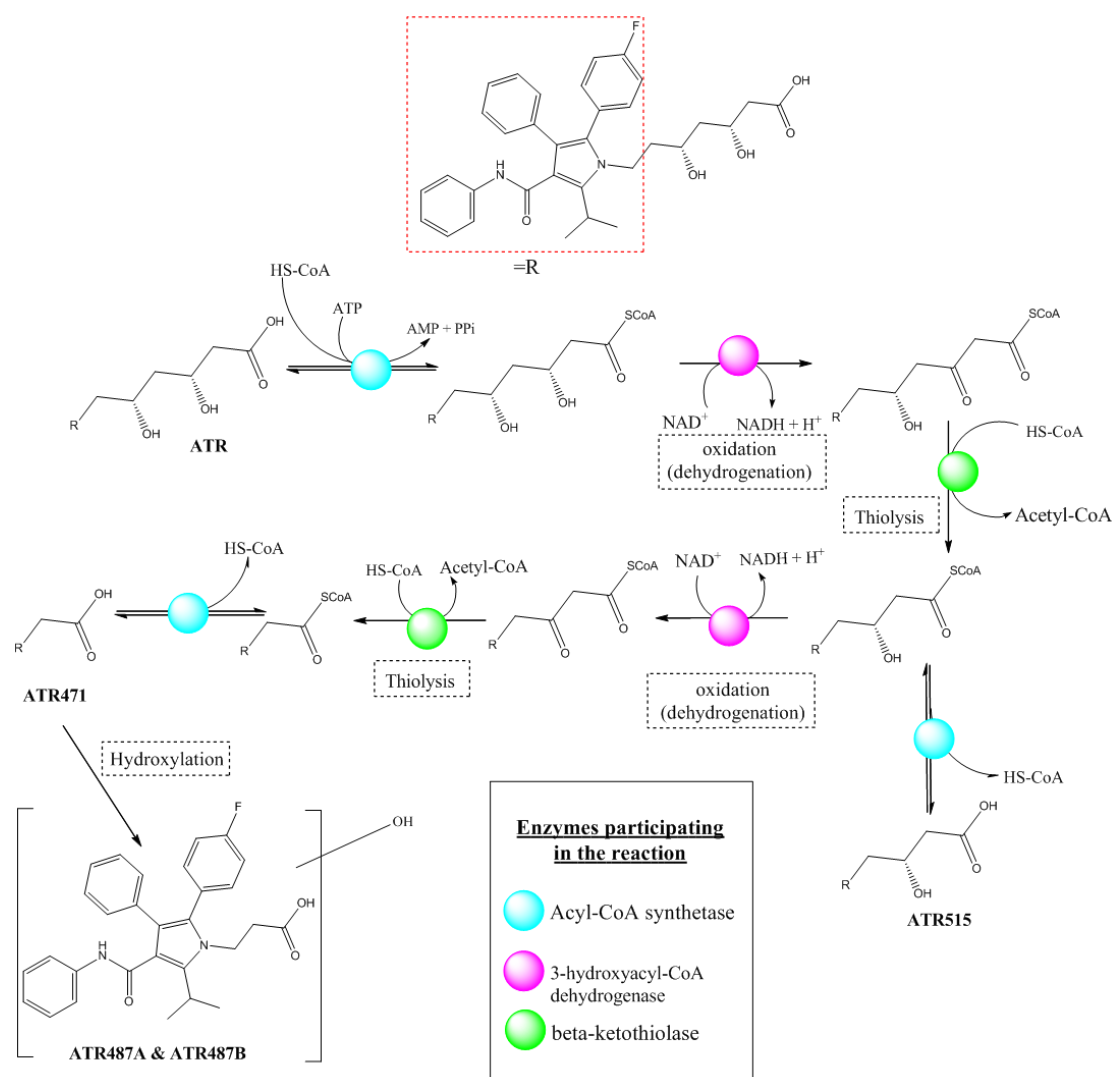
Non-target screening revealed the formation of three additional TPs, namely LDC219, LDC233 and LDC265 both in RPLC and HILIC. LDC219 was formed within the first 24 hours, reached the maximum intensity and then decreased but did not disappear. Molecular formula of LDC219 ( $C_{13}H_{18}N_2O$ ) indicated the loss of one carbon atom and four hydrogens and thus a cyclized TP was proposed (**Fig. S4.13**, Section S4.1.3). LDC233 formation started at the second day and continuously increased until the twelfth day when the experiment was stopped. This TP had a different accurate mass and molecular formula than LID\_233.1648 reported by Gulde et al. [73]. LDC233 presented spectra similarities both with LDC251 and LDC219 (**Fig. S4.14**, Section S4.1.3) LDC233 started to be formed after the second incubation day where both LDC219 and LDC251 have already reached their maximum formation. The formation of LDC233 involved presumably the formation of a cyclized TP from LDC-N-oxide or the N-oxidation of the cyclized TP LDC219 (level 3). Lastly, the elemental composition of LDC265 ( $C_{14}H_{20}N_2O_3$ ) involved two additional oxygen atoms compared to the PC and so the formation of a carboxylic acid was very feasible. While the fragmentation in RPLC was limited, the fragmentation in HILIC was adequate (**Fig. S4.15**, Section S4.1.3). The modification indicated the formation of a carboxylic acid. A neutral loss of  $CO_2$ , in the full-scan MS spectrum of LDC265 was recognized by the transition of 265.1540 to 221.1696, due to in-source fragmentation. Therefore, the

formation of a carboxylic acid was likely. The observed MS/MS fragments with accurate mass 58.0651 and 86.0964 denoted that the diethylmethylamine group remained intact. The findings were in agreement with the recent study by Gulde et al. [73] reported the possible formation of LDC carboxylic acid (Id. level 3). Here, two representative fragments with  $m/z$  73.0291 and 99.0441, proved that the carboxylation occurred at the aromatic amide part of the molecule.

#### 4.2.3.2.4 Biotransformation of ATR

ATR degraded completely within 6 hours resulting in the formation of four TPs. The first formed TP was ATR515 (2 hours) followed by ATR471 (4 hours) and then simultaneously ATR487A and B (6 hours). All the formed TPs had been included in the suspect list and no additional TPs were identified through non target screening or HILIC analysis. ATR515 lacks of an acetyl moiety compared to the PC. The suspect TP had been predicted to be formed through  $\beta$ -oxidation with the involvement of co-enzyme A (CoA). In  $\beta$ -oxidation a new carboxylic acid was further composed, liberating two carbon units. ATR515 predicted by both Eawag-BBD/PPS (1<sup>st</sup> generation TP;  $\beta$ -oxidation rule) and MetPred (2<sup>nd</sup> generation TP; a. alcohol dehydrogenation to keto- group and b.  $\beta$ -oxidation cleavage) and the proposed structure was in agreement with the findings in the MS/MS spectra (**Fig. S4.16**, Section S4.1.3). ATR471 was also in the suspect database, but this time it was predicted only by Eawag-PPS (2<sup>nd</sup> generation TP;  $\beta$ -oxidation rule). A consecutive single  $\beta$ -oxidation took place in the already formed TP ATR515 (or double  $\beta$ -oxidation in ATR) and thus as a 4<sup>th</sup> generation TP, was out of the reaction depth in MetPred. Once more, two carbon units (four carbon units in total compared to ATR molecular formula) were released and a new carboxylic acid was formed. The MS/MS spectra of ATR487 (**Fig. S4.17**, Section S4.1.3) presented significant similarities in the formed fragments with the spectra of ATR515 differing per 44 Da which was attributed to the leaving acetyl group. A hydroxylation occurred in ATR471 gave as an outcome the formation of ATR487A-B. Two possible isomers were formed, as it can be observed in the XICs both in RPLC and HILIC (**Fig. S4.17**, Section S4.1.3) where different fragmentation patterns were observed. The characteristic

fragments of ATR487A were 142, 212 and 394. The  $m/z$  142 and 212 possibly indicate that the monohydroxylation did not take place at the propionic acid group. On the other hand the  $m/z$  394 and 368 fragments indicated that the monohydroxylation could not have occurred in the benzamide group. For ATR487B, the fragments  $m/z$  352 and 366 indicated that there was no possibility of the hydroxylation to have occurred in the benzamide group. Along with fragment 352, which further supports this assumption, the hydroxylation did also not seem to have taken place in the propionic acid chain.

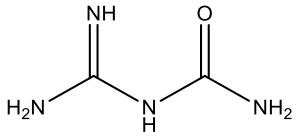
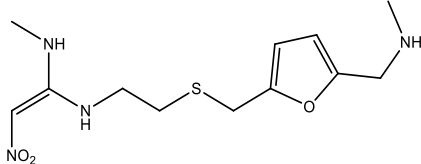


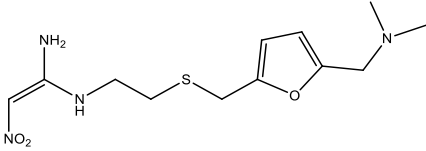
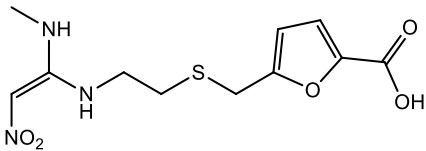
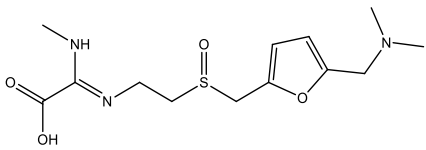
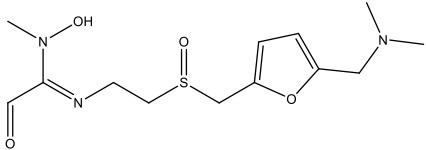
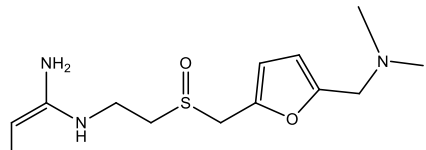
**Fig.4.5:** Proposed biodegradation pathway of ATR. The formation of TP ATR515 and ATR471 are driven by single and double  $\beta$ -oxidation, respectively. The steps followed for  $\beta$ -oxidation are the same with the catabolism of fatty acids in animal metabolism.

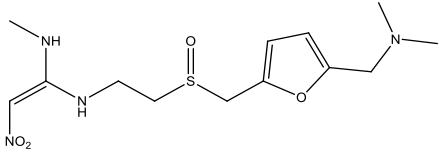
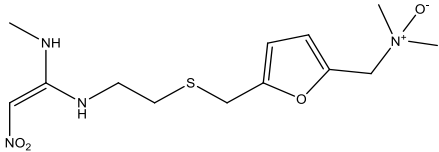
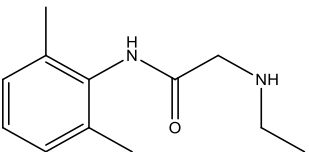
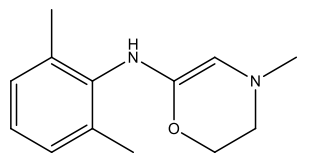
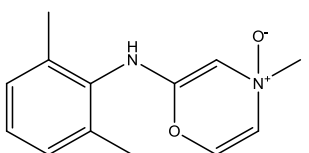


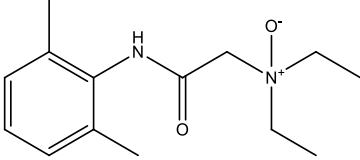
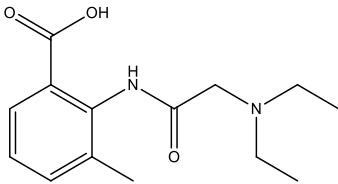
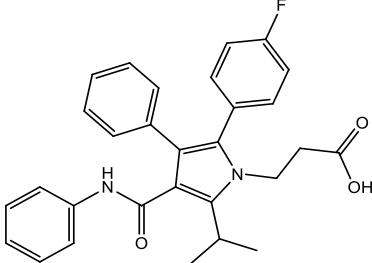
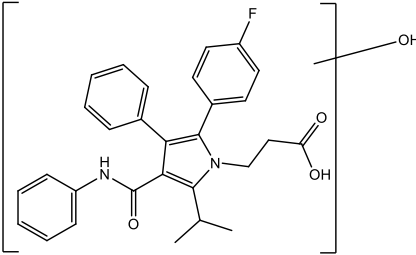
Therefore, it is believed that hydroxylation occurred at one of the two benzene groups for both of the formed TPs. The biotransformation pathway of the identified TPs of ATR is illustrated in Fig. 4.5.

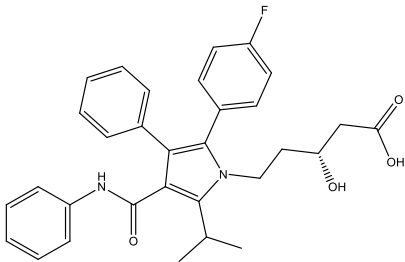
**Table 4.2:** Identified transformation products (TPs) of the selected pharmaceuticals during biodegradation batch experiments.

PC	TP	Theoretical Mass of [M+H] <sup>+</sup>	Molecular Formula	Time Trend	First appearance	Appearance of max. intensity	Id. level	Proposed Structure
Metformin	MTF103	103.0614	C <sub>2</sub> H <sub>7</sub> N <sub>3</sub> O	↗	20min	2d	1	
Ranitidine	RAN286A	286.0856	C <sub>11</sub> H <sub>15</sub> N <sub>3</sub> O <sub>4</sub> S	↗↘	6h	1d	4	-
	RAN286B			↗↘	1d	2d	4	-
	RAN286C			↗↘	1h	10h	4	-
	RAN301A	301.1329	C <sub>12</sub> H <sub>20</sub> N <sub>4</sub> O <sub>3</sub> S	↗↘	4h	10h	2a	 <p>(MassBank Record: ET300103)</p>

	RAN301B (HILIC)			↗↘	t <sub>0</sub>	1d	2b	
	RAN302	302.0805	C <sub>11</sub> H <sub>15</sub> N <sub>3</sub> O <sub>5</sub> S	↗↘	1h	1d	2b	
	RAN316A-B	316.1331	C <sub>13</sub> H <sub>21</sub> N <sub>3</sub> O <sub>4</sub> S	↗	1h	3d	2b	
	RAN316C			↗	6h	3d	2a [69]	
	RAN317A-B (RPLC)	317.1278	C <sub>12</sub> H <sub>20</sub> N <sub>4</sub> O <sub>4</sub> S	↗↘	4h	1d	2b	
	RAN317B			↗↘	4h	1d	3	-

	(HILIC)							
	RAN331A	331.1434	$C_{13}H_{22}N_4O_4S$	$\nearrow \searrow$	t <sub>0</sub>	1d	1	
	RAN331B			$\nearrow \searrow$	1h	1d	1	
Lidocaine	LDC207	207.1504	$C_{12}H_{18}N_2O$	$\nearrow \searrow$	1d	7d	1	
	LDC219	219.1485	$C_{13}H_{18}N_2O$	$\nearrow \searrow$	1d	1d	3	
	LDC233	233.1282	$C_{13}H_{16}N_2O_2$	$\nearrow \rightarrow$	2d	7d	3	

	LDC251	251.1756	$C_{14}H_{22}N_2O_2$	$\nearrow \searrow$	1d	2d	1	
	LDC265	265.1547	$C_{14}H_{20}N_2O_3$	$\nearrow \rightarrow$	2d	9d	2b	
Atorvastatin	ATR471	471.2078	$C_{29}H_{27}FN_2O_3$	$\nearrow$	4h	2d	2b	
	ATR487A	487.2028	$C_{29}H_{27}FN_2O_4$	$\nearrow$	6h	2d	3	
	ATR487B			$\nearrow$	6h	2d	3	

	ATR515	515.2341	$C_{31}H_{31}FN_2O_4$	$\nearrow \rightarrow$	2h	1d	2b	 <p>The chemical structure of ATR515 is a complex molecule. It features a central indole ring system. The indole ring is substituted with a phenyl group at the 2-position, a 4-fluorophenyl group at the 3-position, and a 2-hydroxy-3-phenylpropanoate group at the 4-position. The indole ring is also substituted with a 2-phenylpropanoate group at the 5-position. The molecule is shown in a 3D representation with stereochemistry indicated by wedges and dashes.</p>
--	--------	----------	-----------------------	------------------------	----	----	----	---

#### 4.2.3.3 Retrospective analysis of the selected pharmaceuticals and their TPs in real WW samples

Real wastewater samples were retrospectively screened for the occurrence of the identified TPs. In total, 62 samples, distributed equally in influents and effluents (31 IWW and 31 EWW) were screened. The samples were collected from the WWTP of Athens during spring champing campaigns (March or April) for 8 consecutive days from 2014 to 2017. The samples have been previously analyzed by RPLC-QTOF-MS and so no additional sample treatment or/and analysis were needed.

MTF, RAN and LDC were present in all the IWW and EWW samples indicating partial elimination through the WW treatment (**Fig.S4.19**, Section S4.1.4) ATR was found in all IWW samples but not in the EWW apart from the EWW of 2017 which was detected at a concentration of  $0.254 \pm 0.075 \mu\text{g L}^{-1}$ . Guanylurea was the most frequently detected TP as it was present in 55 out of 62 IWW and EWW samples. Ranitidine's TPs RAN-S-oxide, Ran-N-oxide and desmethyl RAN were detected in 22, 16 and 6 out of 31 IWW and EWW samples, respectively. The positive detected samples for the TPs of LDC, LDC-N-oxide and MEGX were 7 and 2, respectively for the IWW samples while in EWW samples the positive samples were 10 and 14, respectively. None of the TPs of ATR were detected in the IWW samples, but in EWW ATR51, ATR 471, ATR487A and ATR 487b were detected in 8, 12, 17 and 17 samples out of 31. The rest of the TPs identified in this study were not detected either in the IWW or EWW samples. The average calculated concentrations as long as with the minimum and maximum values are presented in **Table S4.4** (Section S4.1.4).

The presence of the detected TPs in the IWW originated either from direct input (excretion of human metabolites) or/and the biotic processes occurred in the sewage system by microorganisms while the detected TPs in the EWW can be attributed to the biotransformation during secondary (or/and tertiary) treatment in the WWTP. Transformation ratios (ratio of the peak area of the TP to PC peak area) were calculated to evaluate the origin of the TPs formation. These ratios compared with pharmacokinetic data for excretion and

metabolism of the PCs available in literature **Table S4.5** (Section S4.1.4). As it has been previously reported, the ratios in urine presented higher uncertainty than the ratios in the IWW and EWW due to the multiple factors that affect the human metabolism of drugs [86].

According to **Table S4.5** (Section S4.1.4), the ratios for RAN-S-oxide, RAN-N-oxide, desmethyl-RAN and MEGX were higher than in urine both in IWW and EWW. The high ratios in IWW could be explained by the occurrence of biotic processes in the sewage system by microorganisms. The ratios in EWW were significantly elevated for RAN-S-oxide and MEGX that could be attributed to the biological activity during wastewater treatment. The ratio of RAN-N-oxide was also higher in EWW than in IWW. However it is highlighted that the ratios of desmethyl RAN were the same both in IWW and EWW. For GNR, LDC-N-oxide, desacetyl ATR and didesacetyl ATR no pharmacokinetic data were available since they are not reported as human metabolites. The detection of GNR, LDC-N-oxide and desacetyl ATR in IWW was related to biotransformation in the sewage system. Moreover, the significantly elevated ratio of GNR and the detection of desacetyl ATR and didesacetyl ATR in more than one samples in EWW denoted that the TPs were produced during wastewater treatment. LDC-N-oxide was detected in more EWW than IWW but the ratio in effluents was lower. This may be explained by further biotransformation of the TP in the aeration tank to other bioTPs (LDC 233) with lower sensitivity which were not detected.

#### **4.2.3.4 Environmental risk assessment of MTF, RAN, LDC, ATR and their TPs**

A semi-quantitation was performed for the detected TPs in the IWW and EWW for the years from 2014 to 2017. Maximum environmental concentrations of the TPs were calculated from the response factor of the parent compounds. PNEC and RQ values for both PCs and their TPS are shown in **Table S4.6** (Section S4.1.5.) for the ECOSAR model and in **Table S4.7** (Section S4.1.5.) for ToxTrAMS model for the three trophic levels.

To assess the threat towards the aquatic environment from the occurrence of a single compound RQ values were initially calculated with both toxicity



models. The compounds that showed possible hazard effect for the aquatic organisms were ATR and its TPs desacetyl ATR and didesacetyl ATR for both models, as their RQs were >1. For the ECOSAR model, only the two lower trophic levels (*daphnia magna* and algae) presented potential risk. On ToxTrAMS model, ATR presented the same results as those calculated by ECOSAR model. However, ATR TPs desacetyl ATR and didesacetyl ATR presented possible toxic effects for *pimephales promelas* (Fish) and *daphnia magna* but not for algae. An RQ value greater than one was also calculated for GNR by ToxTrAMS and seems to present an ecotoxicological threat. The remain PCs and TPs detected in the EWW do not seem to pose risks to all aquatic organisms as their RQ were lower than one.

Even if the PCs and their TPs are more possible to exhibit a baseline mechanism of action when occurred in mixture in the aquatic environment, there is still a possible hazard effect. According to the results (**Table S4.8**, Section S4.1.5), the most sensitive aquatic organisms in the presence of the mixture was *daphnia magna* ( $RQ_{mix} = 42.30$ ), followed by fish ( $RQ_{mix} = 37.59$ ) and algae ( $RQ_{mix} = 9.30$ ). It is highlighted that the 99.9% of the toxicity of the mixture was attributed to ATR and its TPs. After release to the aquatic compartment (rivers), treated wastewater poses risk to all aquatic organisms in streams with small flows. Specifically, for dilution factor up to 22 for fish and *daphnia magna* and up to 3 for algae, respectively the mixture of the PC and their TPs remain an ecological hazard.

#### 4.2.4 Conclusions

- The degradation rate differed among the compounds.
- Abiotic and sorption processes in the batch reactors were neglected when deriving the kinetic data.
- In total, twenty two TPs were formed during the biodegradation experiments. Seventeen TPs were identified through suspect screening and five more through non target screening while five TPs were confirmed by corresponding reference standards. LC-QTOF-MS

technique proved to be a powerful tool for the structure elucidation of the TPs.

- The complementarity of HILIC is summarized in the detection of an additional TP (RAN 301A & B) enabling the separation from its isomer).
- The retrospective analysis revealed the occurrence of certain identified TPs in IWW and EWW and moreover, some of them presented possible hazard effect for the aquatic organisms, as their RQs were >1.

### 4.3 Identification of biotransformation products p-methoxy methylamphetamine (PMMA) and dihydromephedrone (DHM)

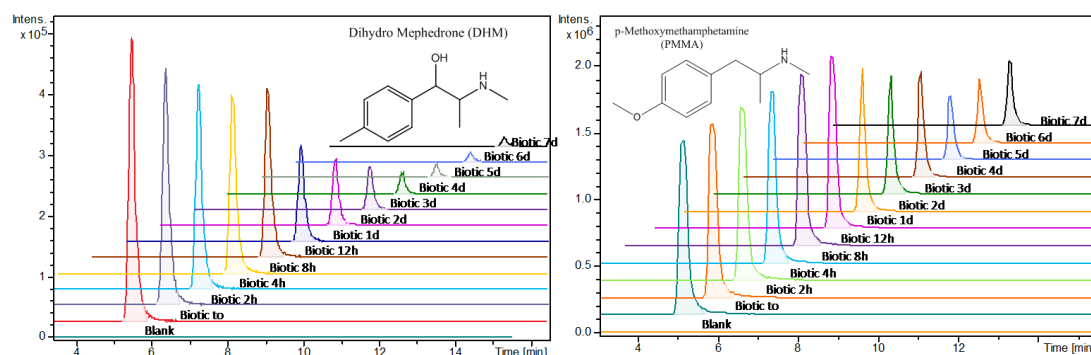


Fig.4.6: Graphical abstract of Chapter 4.3.

#### 4.3.1 Introduction

*p*-methoxymethylamphetamine (PMMA) is a synthetic phenethylamine drug structurally related to methamphetamine. It has been found in tablets and capsules of the 3,4-methylenedioxymethamphetamine (MDMA) sold as "ecstasy" [96]. Mephedrone (4-methylmethcathinone) is a synthetic drug structurally derived from cathinone, and its metabolite, dihydromephedrone (DHM) has been identified in *in vitro* [97, 98], and *in vivo* [98, 99] human metabolism studies. Additionally, DHM was identified as a major transformation product of mephedrone in a study involving in-sewer incubations in the presence of biofilm [68]. Both PMMA and mephedrone are older designer drugs that have been associated with intoxication cases in European countries [96, 100, 101], however, are now been banned in European Union and United Kingdom.

There have been many studies on fate and transport of emerging pollutants (EPs) that are released into the environment via discharges of municipal wastewater effluents. However, the research on TPs of illicit drugs novel psychoactive substances (NPs) has received little attention [19, 25]. It is highlighted through several studies that research on the metabolism and biotransformation of NPs and illicit drugs should be encouraged due to the existing need to select the most representative analytes for wastewater based

epidemiology (WBE) and to identify possible overlapping microbial and mammalian biotransformation pathways [25].

Previous studies have investigated the presence of PMMA in influent wastewater to determine community use [102, 103], however, PMMA levels have been reported as very low only [103]. In-sewer stability of PMMA in the presence of biofilm has been reported as stable [104, 105] within 24 h indicating it is stable before WW treatment processes.

Several studies have investigated the presence of mephedrone in wastewater [106-112]. In some studies mephedrone levels in wastewater have been reported as below quantification level or absent [106, 107, 109], more likely due to its significant (bio)transformation under aerobic conditions in-sewer system, as it has been reported [104, 113, 114]. Additionally, DHM was identified as a major TP from an in-sewer stability experiments and determined to be a reliable biomarker due to its levels within a 24 h residence time [104]. Though DHM has not been monitored in wastewater studies it has been proposed as a biomarker of exposure for mephedrone use in wastewater based epidemiology [104] and has been previously detected in pooled urine samples from UK [115].

The aims of the study were to explore the fate and transformation of PMMA and DHM during the biological treatment process, due to their stability in wastewater. On this basis, suspect screening was performed for the identification of the formed TPs, along with structure elucidation for the candidate TPs, based on accurate mass and isotopic pattern measurements by HRMS and tentative interpretation of MS/MS spectra, using *in silico* fragmentation tools.

### **4.3.2 Material and methods**

#### **4.3.2.1 Chemicals and reagents**

PMMA, and DHM were obtained from LGC Standards SARL (Molsheim, France) and Cerilliant (Round Rock, Texas, USA), respectively, at the concentration of 1 mg mL<sup>-1</sup> or 100 µg mL<sup>-1</sup> in methanol. Stock standard solutions of individual compounds (1000 µg mL<sup>-1</sup>) were prepared in MeOH

and stored at  $-20\text{ }^{\circ}\text{C}$  in amber glass bottles to prevent photodegradation. The solvents as well as the salts for the mobile phase's buffers that were used for the LC analysis and preparation of the callibrant have been discussed in Chapter 3, section 3.2.1.

Details on the used chemicals and reagents are provided in the

#### **4.3.2.2 Sampling**

Sampling was performed on April 2016 and was the same that was followed for the experiments conducted on the study of chapter 3 (section 3.2.2) and on the study of chapter 4 (section 4.2.2.2), where more details can be found.

#### **4.3.2.3 Biotransformation batch experiments**

Biotransformation batch experiments were set up in the line of the setup of the previously experimental sections; Chapter 3, section 3.2.3 and Chapter 4, section 4.2.2.3. Sampling was performed immediately after spiking and after 2, 4, 8 and 12 hours and after 1, 2, 3, 4, 5, 6 and 7 days.

#### **4.3.2.4 Workflow for suspect screening for the identification of TPs**

The applied workflow that was used was the one that was developed and described on Chapter 3, section 3.2.6. and has been applied also in Chapter 4, section 4.2.2.4 and it was followed partially regarding the fact that, only suspect screening and no non-target screening was performed.

### **4.3.3 Results and discussion**

#### **4.3.3.1 Degradation of PMMA and DHM in batch experiments with activated sludge**

The experiments run successfully with the vital parameters (pH and temperature) remaining consistent over the seven-day period in all reactors.

Eight TPs were identified in total both for PMMA and DHM. Determination of the major and minor TPs based on their stability during the six-day incubation was performed, however, it should be noted that, while useful for discussion purposes, a higher abundance does not always guarantee a higher

concentration of the TPs since different ESI ionization efficiencies may be expected for different chemical structures.

#### 4.3.3.2 Identification of biotransformation products of PMMA

PMMA levels decreased approximately to 20% in the biotic reactor and to 80% in both the sorption and abiotic reactors over the 7-day period of incubation (**Fig.4.7**). Therefore, only 60% of PMMA was (bio)transformed as the sorption and abiotic reactors were used to account for losses through abiotic processes. It is likely that PMMA has a higher rate of degradation in an activated sludge reactor as a previous study involving in-sewer incubation of PMMA in the presence biofilm had 20% loss over 24 h incubation [104]. Two TPs were detected and identified (TP-166 and TP-196) in the biotic reactor (Table 4.3).

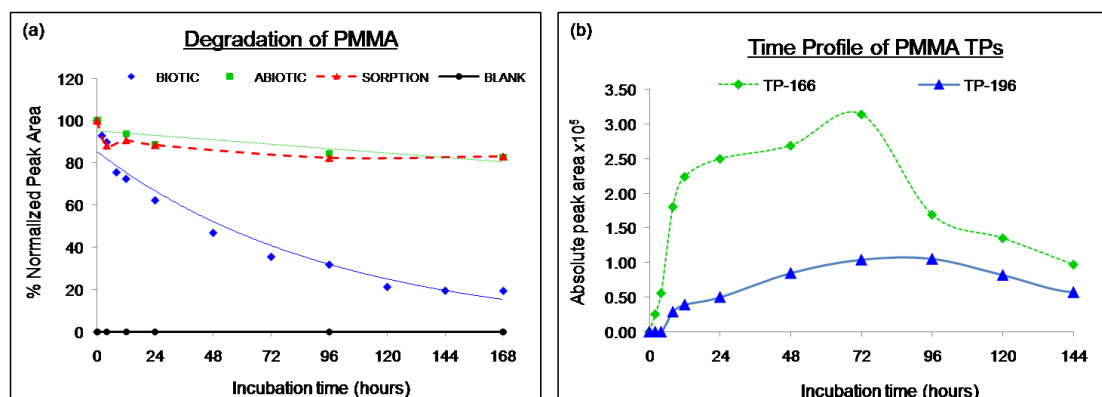


**Fig.4.7:** (a) The degradation of PMMA in four reactors; (b) Formation of PMMA TPs in the biotic reactor over a 7-day incubation period.

TP-166 with  $m/z$  166.1215 at  $t_R$  3.01 min was detected after 2h at relatively low levels (**Fig.4.7**). Based on the accurate mass,  $t_R$  and MS/MS spectra we identified TP-166 as the O-demethylation product of PMMA (**Fig. S4.21**, Section S4.2.1). TP-166 corresponds to p-OH-methamphetamine which has been previously confirmed as human metabolite [116, 117], as well as an in-sewer [104] TP of PMMA. Additionally, p-OH-methamphetamine has also been identified as a metabolite of methamphetamine [117]. Furthermore, the product ions acquired for TP-166 at  $m/z$  135.0797 which corresponds to loss of  $NH_2CH_3$ , and a further loss of an ethylene group ( $C_2H_4$ ) results in  $m/z$

107.0491 (**Fig. S4.21**, Section S4.2.1) match product ions for p-OH-methamphetamine in the previous studies [104, 116].

TP-196 with  $m/z$  196.1317 at  $t_R$  3.96 min was detected after 8h and its low levels (<1 %) remained throughout the 96h (**Fig.4.7**). Using accurate mass, and MS/MS spectra we identified the TP-196 as a hydroxylation product of PMMA. It was assigned an Id. Level 3, because we could not confirm the position of the hydroxyl group (**Fig. S4.21**, Section S4.2.1). Three possible structures formed through aliphatic hydroxylation reactions, and N-hydroxylation were proposed (**Fig. 4.8**). The product ions with  $m/z$  178.1216 resulted from the loss of a hydroxyl and a methyl group, further loss of the (N) methyl group resulted in  $m/z$  163.0981 and an additional (O) methyl loss resulted in the  $m/z$  148.0736. Additionally, product ions with  $m/z$  121.0654, and  $m/z$  135.0774 corresponded to the alkyl benzene moieties with an intact methoxy group (**Fig. S4.21**, Section S4.2.1). These product ions acquired for TP-196 were not unique to any of the three proposed isomeric forms and their proposed fragmentation only shifts depending on the position of the hydroxyl substituent. Furthermore, using retention time prediction analysis the query structures were within  $t_R$  3.1-4.7 min, as such, we could not significantly discern the likely isomeric form of TP-196.

Previous in-sewer incubations in the presence of biofilm identified three TPs for PMMA over a 24h period, with only one TP (TP-166) matching this study. To the best of our knowledge, TP-196 has not been previously identified in relation to PMMA degradation.

#### 4.3.3.3 Identification of biotransformation products of DHM

Dihydromephedrone levels were gradually decreased to completion over the six-day incubation in the biotic reactor. The levels of DHM reduced to approximately 90% and 70% in the abiotic and sorption reactors, respectively. This showed that 30% of DHM degradation was subject to abiotic process and sorption (**Fig. 4.9 (a)**). This stability data is comparable with a study showed DHM as the major TP formed from mephedrone incubation and increasing levels over a 24h period. In total, six TPs were detected and identified in the biotic reactor (**Table 4.3**).

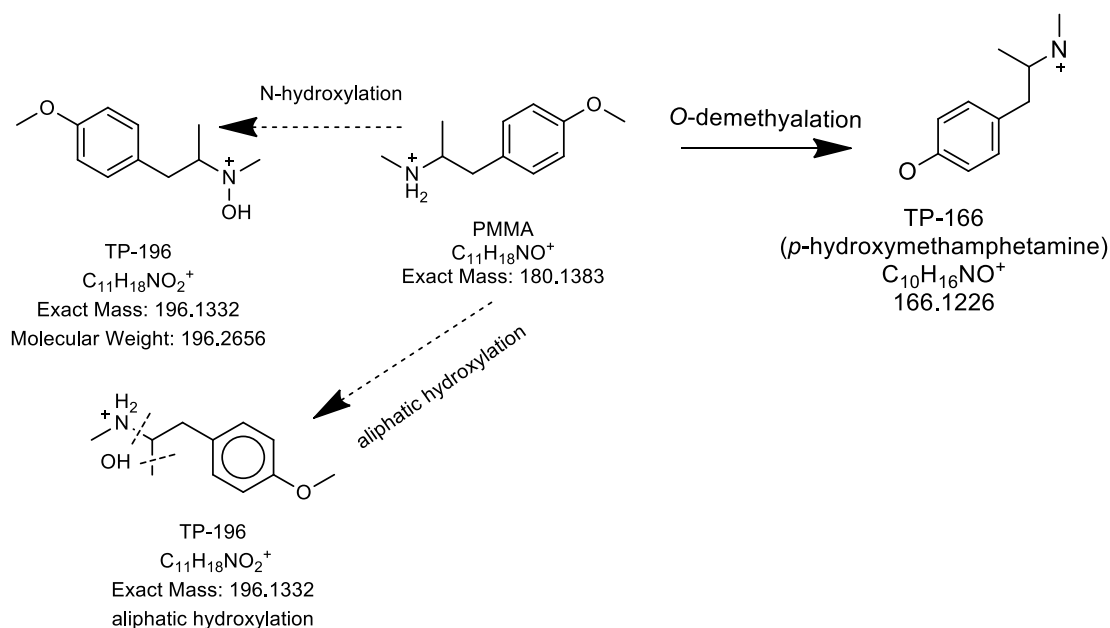


**Fig.4.8:** Proposed (bio)transformation pathway for PMMA. Dotted arrows indicate the possible reactions that can lead to the formation of a single TP. Based on their abundance, TP-210 and TP-178 were identified as the major TPs and TP-166, TP-164, TP-192a, and TP-192b, as the minor TPs (Fig. 4.9 (b)).

TP-210 with  $m/z$  210.113 at  $t_R$  1.74 min was detected after 8h of incubation. It was assigned an Id. Level 3 because, the position of the substituent hydroxyl group on the three proposed isomeric forms could not be confirmed (**Fig. S4.23**, Section S4.2.1). Two biotransformation pathways were proposed for the formation of TP-210; firstly the oxidation of the primary alcohol on DHM to form a ketone group on the  $\beta$ -carbon (forming TP-178), then subsequent dihydroxylation. In this pathway, two structural forms of TP-210 were possible: a hydroxylation on methylphenyl and primary amine groups; or a hydroxylation on the benzene ring and methylphenyl group. The second possible pathway for TP-210, was formed through three reactions involving the hydroxylation on the aliphatic methyl group and subsequent oxidation of the alcohol to form an aldehyde group and lastly a carboxylate formation (**Fig.4.10**). This structural form matched 4-carboxy dihydromephedrone which has been identified, previously, in human *in vivo* samples [65, 66]. Furthermore, using retention time prediction analysis the query structures



were within  $t_R$  3.1-3.2 min, as such, we could not significantly discern the likely isomeric form of TP-210. Although, based on the fragmentation of TP-210 the most probable structure could be the carboxylated form.

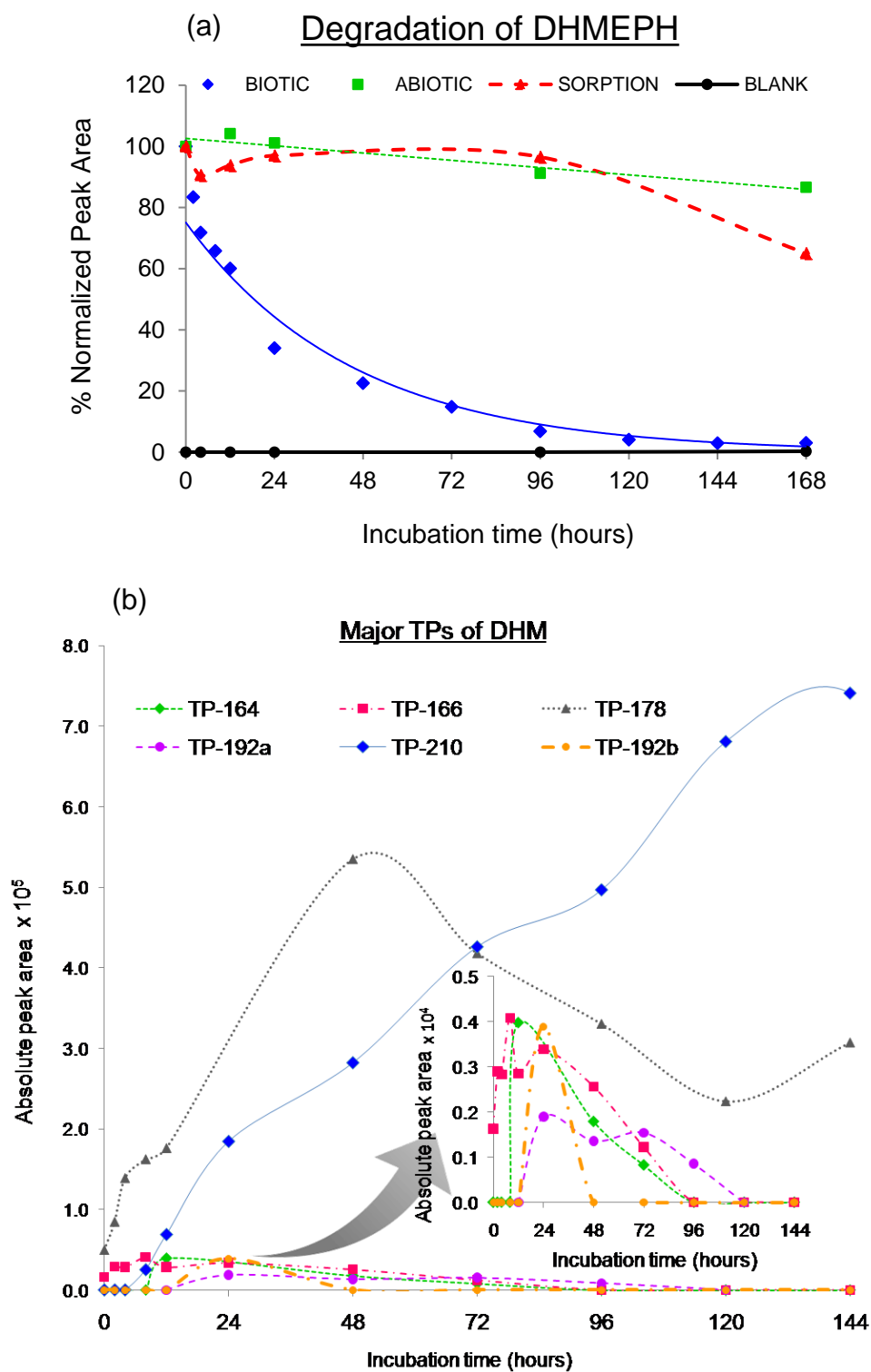


**Fig.4.9:** (a) The degradation of DHM in the four reactors; (b) Formation of DHM TPs in the biotic reactor over a 7-day incubation period.

TP-166 with  $m/z$  166.1228 at  $t_R$  4.49 min was detected at 2h and increased to its peak at 12h and diminished over 96 h (**Fig. 4.9**) TP-166 was identified as the *N*-demethylated form of DHM (**Fig. S4.22**, Section S4.2.1) which has previously been identified as nor-dihydromephedrone in rat and human urine [97]. TP-178 with  $m/z$  178.1212 at  $t_R$  4.64 min was detected at 2h time-point, reaching its peak around 48h and gradually decreasing thereafter over the 144h incubation period (**Fig 4.9**). TP-178 corresponds to the oxidation of the primary alcohol of DHM. Using  $t_R$  and MS/MS spectra, TP-178, was confirmed as mephedrone (**Fig. S4.23**, Section S4.2.1). Mephedrone was reported as highly unstable *in-sewer* in the presence of biofilm and led to formation of DHM [104]. The dynamics of mephedrone and DHM in a biotic reactor indicate their presence in effluent samples.

TP-164 with  $m/z$  164.1071 at  $t_R$  6.5 min was detected at the 24h time point and only present for an additional 72 hours (**Fig 4.9 (b)**). TP-164 could have resulted from two pathways, the *N*-demethylation of TP-178 and/or the oxidation of alcohol on TP-166 to form a  $\beta$ -ketone group. A metabolite (*in vitro* and *in vivo*) [97-99] and TP (*in-sewer*) [104] with the same  $m/z$  has been identified as nor-mephedrone. Product ions acquired for TP-164 with  $m/z$  146.0968 ( $H_2O$  loss) and  $m/z$  131.0727 ( $CH_5O\cdot$  loss) match *in vivo* and *in-sewer* studies [104, 118], however, without a commercial reference standard could not be confirmed (**Fig. S4.22**, Section S4.2.1). The *N*-demethylation pathway was proposed to be the main metabolic pathway in *in vivo* metabolism of mephedrone [99] (**Fig.4.10**).

TP-192a and TP-192b with  $m/z$  192.1024 at  $t_R$  5.10 min and  $m/z$  192.1022 at  $t_R$  6.15 min, respectively were detected at the 24h time point. Levels of TP-192a diminished over the following 72 hours whereas TP-192b was absent after 48h (**Fig 4.9 (b)**). The MS/MS spectra of both TPs are illustrated on **Fig. S4.23** (Section S4.2.1), along with the representative fragmentations.

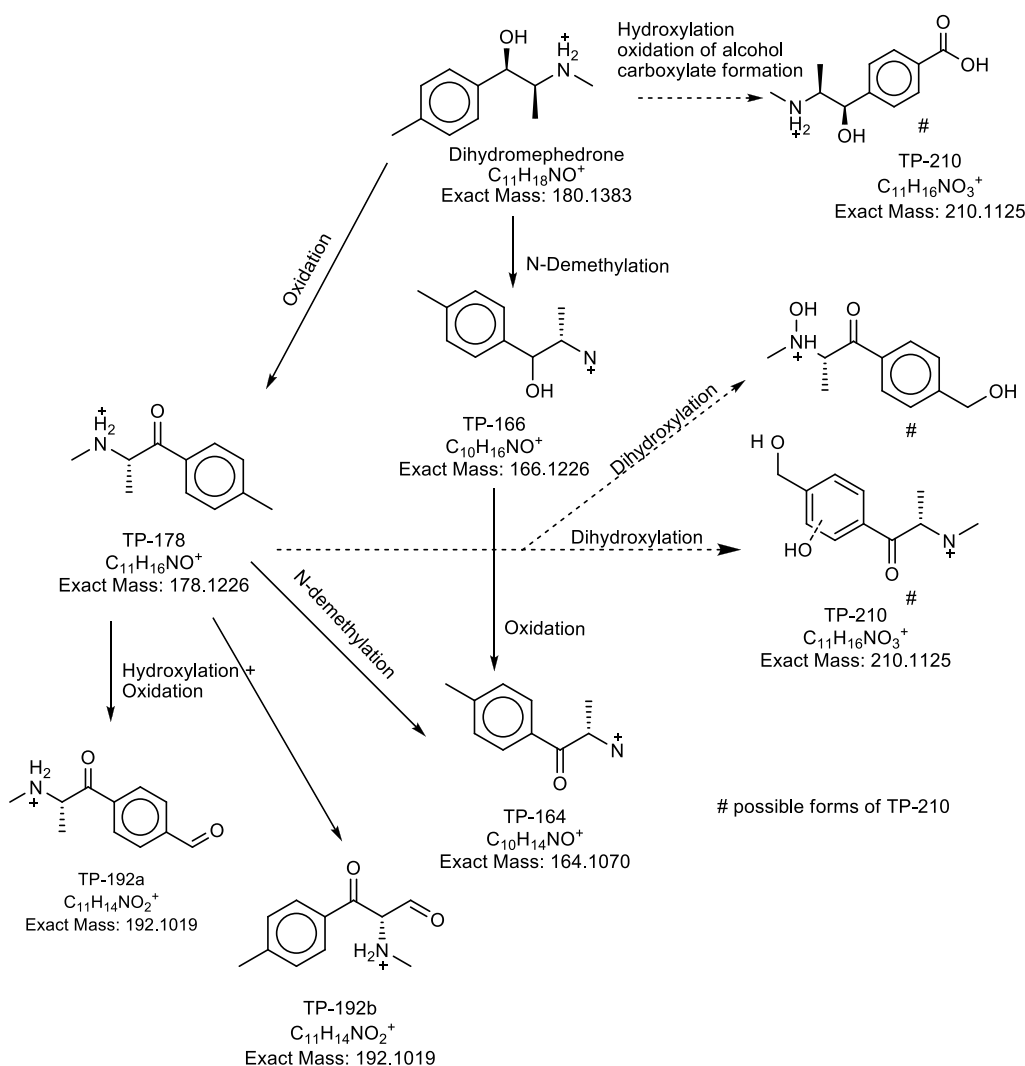


**Fig.4.10:** Proposed (bio)transformation pathway for DHM. Dotted arrows indicate the possible reactions that can lead to the formation of a single TP.

Two forms of TP-192 were proposed to be formed from TP-178 with two different reaction pathways (**Fig. 4.10**). Firstly, the formation of TP-192a involved the hydroxylation and subsequent oxidation of the aromatic methyl group on TP-178 forming a ketone. Secondly, formation of TP-192a involved the hydroxylation and subsequent oxidation on the aliphatic methyl of TP-178 forming a ketone. TP-192 isomers have not previously mentioned in mephedrone studies, the proposed isomer TP-192a is closest to hydroxytolyl-mephedrone with a further oxidation of the primary alcohol.

#### 4.3.4 Conclusions

- The observed elimination rate (80%) for PMMA and (90%) for DHM in batch experiments with activated sludge associated in a great extent with biological activity as control reactors showed lower rates of removal (20% for PMMA and 30% for DHM).
- In total, eight TPs were formed during the biodegradation experiments. One of them was confirmed with reference standard (Mephedrone). A probable structure based on diagnostic evidences and tentative candidates were proposed for the additional two and four TPs, respectively, while for one of them spectrum match with literature was achieved (TP-196, p-OH-methamphetamine).
- TP-166 (PMMA), TP-210, TP-164 and TP-166 (DHM) have been previously reported as human metabolites in vivo studies.
- Three TPs have not been reported previously on literature (TP196, TP-192a and TP-192b).
- The main bioreactions for PMMA TPs was O-demethylation and hydroxylation, while for DHM TPs the major bioreactions that were occurred were oxidation, hydroxylation and N-demethylation.
- Mephedrone and few of its reported metabolites (TP-164 and TP-210) were formed back from DHM incubation indicated that the dynamics of mephedrone and DHM in a biotic reactor denoted their presence in EWW.

**Table 4.3:** Biotransformation products (TPs) identified for PMMA and DHM over a 7-day incubation in the activated sludge reactor.

Compound	t <sub>R</sub> (min)	Theoretical <i>m/z</i> [M+H] <sup>+</sup>	Measured <i>m/z</i> [M+H] <sup>+</sup>	Δ <i>m</i> (ppm)	Diagnostic product ions	Chemical Formula	Id. Level
PMMA	4.38	180.1383	180.1376	-3.89	149.0953, 121.0650, 109.0661, 91.0544	[C <sub>11</sub> H <sub>18</sub> NO] <sup>+</sup>	PC
TP-166	3.01	166.1226	166.1215	-6.62	135.0797, 107.0491	[C <sub>10</sub> H <sub>16</sub> NO] <sup>+</sup>	2a
TP-196	3.96	196.1332	196.1317	-7.65	178.1216, 163.0981, 148.0736, 135.0774, 121.0654	[C <sub>11</sub> H <sub>17</sub> NO <sub>2</sub> ] <sup>+</sup>	3
DHM	4.64	180.1383	180.1382	-0.56	162.1286, 147.1047, 131.0861	[C <sub>11</sub> H <sub>18</sub> N O] <sup>+</sup>	PC

TP-210	1.74	210.1125	210.1130	2.38	192.1011, 177.0722, 161.0577	[C <sub>11</sub> H <sub>16</sub> NO <sub>3</sub> ] <sup>+</sup>	3
TP-166	4.49	166.1226	166.1228	1.20	148.112, 131.0848, 116.063	[C <sub>10</sub> H <sub>16</sub> NO] <sup>+</sup>	2b
TP-178	4.64	178.1226	178.1212	-7.86	162.1269, 145.0883, 132.0826	[C <sub>11</sub> H <sub>16</sub> NO] <sup>+</sup>	1
TP-164	6.5	164.1070	164.1071	0.61	146.0968, 131.0727, 120.0798	[C <sub>10</sub> H <sub>14</sub> NO] <sup>+</sup>	2b
TP-192a	5.1	192.1019	192.1024	2.60	119.049	[C <sub>11</sub> H <sub>14</sub> NO <sub>2</sub> ] <sup>+</sup>	3
TP-192b	6.2	192.1019	192.1022	2.62	148.1112, 135.0432, 119.049	[C <sub>11</sub> H <sub>14</sub> NO <sub>2</sub> ] <sup>+</sup>	3

#### 4.4 Identification of biotransformation products of benzotriazoles and hydroxyl-benzothiazole in laboratory scale hybrid moving bed biofilm reactor (HMBBR) system

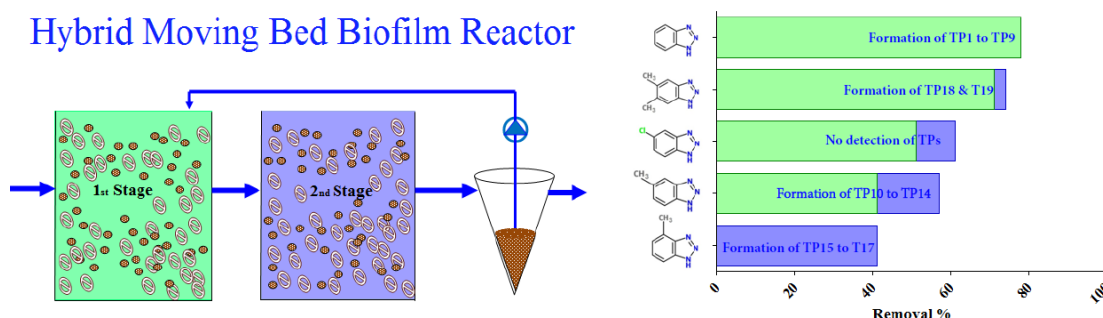


Fig.4.11: Graphical abstract of chapter 4.4.

##### 4.4.1 Introduction

Growing demand for more efficient wastewater treatment is leading to new technologies for treatment as well as improvement of existing ones. Concerning biological treatment, the Hybrid Moving Bed Biofilm Reactor (HMBBR) is an approach that was introduced two decades ago for the first time in wastewater engineering [119]. The HMBBR is a combination of a typical activated sludge (AS) system with a Moving Bed Biofilm Reactor (MBBR), in which biofilm attached on biocarriers and AS flocs co-exist in the bioreactor, contributing to wastewater treatment. The main advantages of such a system compared to AS are the lower requirement for process volume, the increased nitrification capacity and the lower sludge load on the secondary clarifier [120]. Due to the above, HMBBR systems have been successfully used for upgrading of conventional AS systems [121, 122]. Beside the above, so far, only few studies have focused on the ability of this system to remove micropollutants from wastewater.

Benzotriazoles (BTRs) and Benzothiazoles (BTHs) are two groups of micropollutants that occur in wastewater from domestic and industrial activities [6]. BTRs are found in corrosion-inhibiting products, cooling fluids, de-icing fluids and dishwashing detergents [123], while BTHs are used as

vulcanization accelerators and stabilizers in the photo industry [124]. Both groups are highly soluble in water and highly polar, leading to their persistence in the water cycle [125]. The partial removal of some of them in AS systems has been documented in monitoring studies [126-128] and laboratory biodegradation experiments [129, 130]. Moreover, information on the biotransformation products of specific BTRs (1H-benzotriazole, BTR; 4-methyl-1H-benzotriazole, 4TTR; 5-methyl-1H-benzotriazole, 5TTR) has been reported in activated sludge experiments [22, 129]. In recent studies, Mazioti et al., [130, 131] compared the ability of AS and pure MBBR systems to biodegrade six of these compounds (BTR; 4TTR; 5TTR; xylotriazole, XTR; 5-chlorobenzotriazole, CBTR; 2-hydroxybenzothiazole, OHBTH) and reported that attached biomass had higher biodegradation potential for the target compounds comparing to AS.

The aim of this study was to investigate the potential of a laboratory scale HMBBR system, consisting of two bioreactors in series, to remove BTR, 4TTR, 5TTR, XTR, CBTR and OHBTH from domestic wastewater and to compare observed removal efficiencies with those reported in a previous study using AS and MBBR systems [130, 131]. Finally, batch experiments were conducted and for the first time biotransformation products formed in a HMBBR reactor were identified.

#### **4.4.2 Material and methods**

##### **4.4.2.1 Chemicals and reagents**

Analytical standards of XTR and CBTR were supplied by Sigma-Aldrich (USA). BTR was purchased from Merck (Germany), 4TTR by Fluka (Switzerland), 5TTR by Acros Organics (Belgium); whereas OHBTH was purchased from Alfa Aesar (USA). Stock solutions of individual compounds were prepared in methanol (MeOH) at 1000 mg L<sup>-1</sup> and kept at -18 °C. Working solutions of 10 mg L<sup>-1</sup> were prepared when needed and were kept at -18 °C for a time period not exceeding three months. Methanol (MeOH, HPLC-MS grade) and acetonitrile (ACN, HPLC grade) were purchased from Merck (Germany) and Fisher (USA), respectively. The solid phase extraction (SPE) cartridges used for samples' clean-up were polymer-based with surface



modified styrene divinylbenzene phase (Strata-X, 33u Polymeric Reversed Phase 200mg/6ml) and they were supplied by Phenomenex (USA). HPLC grade water was prepared in the laboratory using a MilliQ/MilliRO Millipore system (USA). Ultra-pure HCl (32%), used for samples acidification, was purchased from Merck (Germany).

#### **4.4.2.2 Batch biodegradation experiments for biotransformation products identification**

To identify the biotransformation products of target compounds in HMBBR system, aerated batch experiments were conducted using biomass from BC1 where the greatest part of biodegradation was observed during continuous flow experiments. Mixture of AS and biocarriers from BC1 was transferred to seven different glass bottles at a final volume of 200 mL. Each target compound was spiked in a different bottle at an initial concentration of 10 mg L<sup>-1</sup>, while a control flask was also prepared containing biomass and methanol at an amount equal to that added in other reactors. All bottles were covered with aluminium foil and constantly agitated on a shaking plate. The total duration of the experiment was 24 h. Three homogenized samples (10 mL each) were taken from each reactor at 0, 6 and 24 h.

#### **4.4.2.3 Analytical method**

The instrumental parameters as well as the applied protocol for the identification of the TPs were the same as reported previously in Chapter 3, sections 3.2.4 and 3.2.6. On this study only RP mode was used in positive and negative ionization and only the first tier of the developed protocol was used; suspect screening.

Details on the continuous flow systems set-up and operation can be found in Electronic Supplementary Material section 4.3.1.

#### **4.4.2.4 Results and discussion**

Twenty two transformation products were tentatively identified in total with mass accuracy  $\pm 5$  ppm. The  $m/z$  range of the candidate TPs ranged from 132.0567 (TP14) to 245.9536 (TP22) (**Table 4.4**). For the majority of the

candidates, retention times showed the formation of more polar TPs than the parent compounds. A distinctive time trend (absent in the blank, increasing peak over incubation time) was observed for all candidate TPs. All information about TPs is summarized in **Table 4.4**. As identification confidence in HR-MS is sometimes difficult to communicate in an accurate way [45], in the present work we used the levels of identification confidence proposed by Schymanski et al. [48].

BTR presented the higher degree of biotransformation compared to the other BTRs [65]. Five candidate TPs were found in positive ionization mode (TP1-TP5) and 4 more (TP6-TP9) in negative ionization mode. Hydroxylation was the dominant reaction mechanism followed by oxidation and methylation. Previously reported TPs for BTR [64, 65] were among the tentatively identified TPs (TP1-TP7, TP9). In total, five TPs (TP3-TP7) were identified by library spectrum match and the records from the online mass spectra database, MassBank, were reported. Two TPs (TP2 and TP8) were tentatively identified and probable structures were proposed. TP1 (1-OH BTR) was confirmed by a reference standard and for TP9 an unequivocal molecular formula was reported (id. level 1 and 4, respectively).

Biotransformation of 4TTR showed 5 candidate TPs (TP10-TP14). Hydroxylation and oxidation were found to be the most probable reaction mechanisms for the formation of the TPs. In positive mode only TP10 ( $C_7H_5N_3O_2$ ) was identified with a tentative structure that is illustrated in **Table 4.4**. In negative ionization mode, 4 more TPs were identified. Hydroxylation of the benzene ring was identified for TP14 whereas mono-hydroxylation of the methyl group was identified for TP13. Both hydroxylation and oxidation reactions were involved in formation of TP11-TP12. For TP12 the probable structure of 4-COOH BTR was proposed by a library spectrum match (Id. level 2a).

5TTR degradation revealed the formation of 3 candidate TPs (TP15-TP17). TP15 was identified to be 5-COOH BTR by a library spectrum match (Id. level 2a). The tentative structure of TP16 ( $C_7H_7N_3O$ ) corresponds to mono-hydroxylation, whereas TP17 ( $C_7H_7N_3O_2$ ) corresponds to a dihydroxylation of the benzene ring (Id. level 3). To our knowledge, biodegradation products of

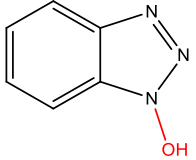
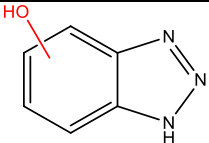
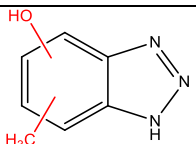
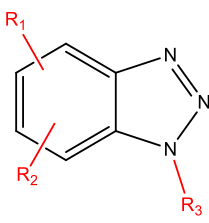
XTR has not been studied before, and this is the first report of its biotransformation products. Two candidate TPs (TP18-TP19) were found for XTR and tentative structures were proposed (Id. level 3). TP18 ( $C_8H_7N_3O_2$ ) corresponds to the formation of carboxylic acid XTR, while TP19 ( $C_8H_9N_3O$ ) indicates either the mono-hydroxylation of a methyl group or mono-hydroxylation of the benzene ring of XTR, which was detected in both ionization modes. CBTR did not show any potential TP according to the screened database either in positive or negative ionization mode.

Finally, OHBTH has also not been studied before, and this is the first report of its biotransformation products. Three candidate TPs (TP20-TP22) were identified and tentative structures were proposed for OHBTH (Id. level 3). TP20 of OHBTH ( $C_8H_7NO_2S$ ) indicates methoxylation of the benzene ring, whereas the candidate TPs in negative mode TP21 ( $C_7H_5NO_2S$ ) and TP22 ( $C_7H_5NO_5S_2$ ) correspond to a hydroxylation of the benzene ring followed by the formation of a sulfonic ester in one of the two hydroxyl groups, respectively.

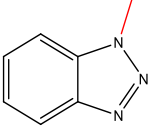
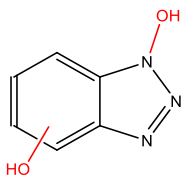
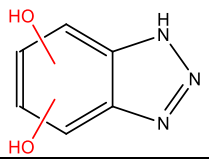
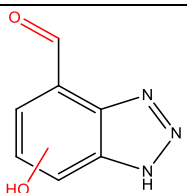
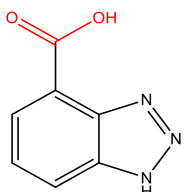
#### 4.4.3 Conclusions

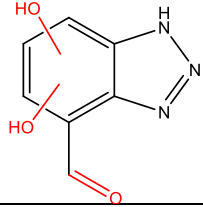
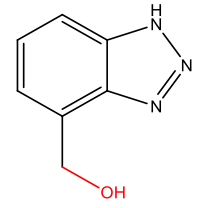
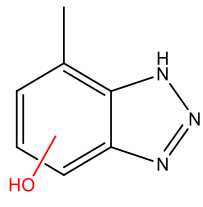
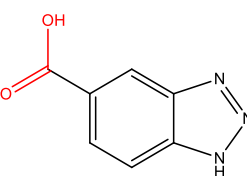
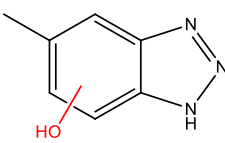
- HMBBR partially removed all target micropollutants.
- Twenty two transformation products were tentatively identified in total.
- Three TPs were identified by library spectrum match (TP6; 1-Methyl-1H-benzotriazole, TP11; 4-COOH BTR and TP15; 5-COOH BTR), one TP (TP1) was identified by the analysis of reference standard (1-Hydroxy benzotriazole), for TP9 only the molecular formula was estimated and for the remained seventeen TPs probable structures were proposed.
- Hydroxylation was the dominant reaction mechanism followed by oxidation and methylation.
- BTR presented more biotransformation products among all target compounds.

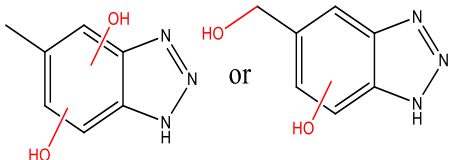
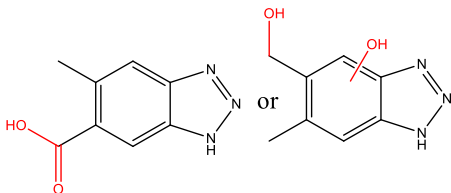
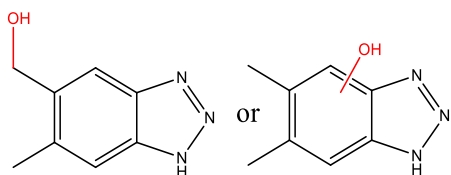
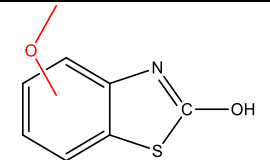
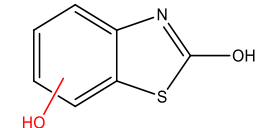
**Table 4.4:** Biotransformation products (TPs) identified for BTR, 4TTR, 5TTR, XTR, CBTR and OHBTH, over a 24-hour incubation in BC1.

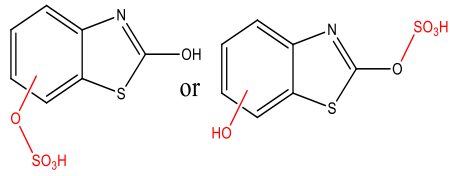
Parent compound	TP	ESI polarity/ Precursor ion	m/z	Rt (min)	Molecular Formula	Tentative Structures	Id. Level (MassBank Record)	Time trend <sup>a</sup>	Reported in Literature
BTR	TP1	[M+H] <sup>+</sup>	136.0505	3.8	C <sub>6</sub> H <sub>5</sub> N <sub>3</sub> O		1	↗	[26]
	TP2	[M+H] <sup>+</sup>	136.0505	4.1	C <sub>6</sub> H <sub>5</sub> N <sub>3</sub> O		3	↗	[26]
		[M-H] <sup>-</sup>	134.0360	4.0				↗	
	TP3	[M+H] <sup>+</sup>	150.0662	5.1	C <sub>7</sub> H <sub>7</sub> N <sub>3</sub> O		3 (ETS00101)	↗	[26, 98]
	TP4	[M+H] <sup>+</sup>	178.0611	3.5	C <sub>8</sub> H <sub>7</sub> N <sub>3</sub> O <sub>2</sub>		3 (ETS00108)	↗	[26]
	TP5	[M+H] <sup>+</sup>	178.0611	4.2			3 (ETS00109)	↗	[26]

R<sub>1</sub>, R<sub>2</sub>, R<sub>3</sub>: H, CH<sub>3</sub>, COOH

	TP6	[M-H] <sup>-</sup>	132.0567	3.7	C <sub>7</sub> H <sub>7</sub> N <sub>3</sub>		2a (ETS00115)	↗	[26, 98]
	TP7	[M-H] <sup>-</sup>	150.0309	1.6	C <sub>6</sub> H <sub>5</sub> N <sub>3</sub> O <sub>2</sub>		3 (ETS00103)	↗	[26, 98]
	TP8	[M-H] <sup>-</sup>	150.0309	3.1	C <sub>6</sub> H <sub>5</sub> N <sub>3</sub> O <sub>2</sub>		3	↗	-
	TP9	[M-H] <sup>-</sup>	182.0207	1.2	C <sub>6</sub> H <sub>5</sub> N <sub>3</sub> O <sub>4</sub>	-	4	↗	[26]
4TTR	TP10	[M+H] <sup>+</sup>	164.0455	4.1	C <sub>7</sub> H <sub>5</sub> N <sub>3</sub> O <sub>2</sub>		3	↗	[26]
		[M-H] <sup>-</sup>	162.0309	3.2					
	TP11	[M-H] <sup>-</sup>	162.0309	2.3	C <sub>7</sub> H <sub>5</sub> N <sub>3</sub> O <sub>2</sub>		2a (ETS00107)	↗	[26]

	TP12	[M-H] <sup>-</sup>	178.0258	1.3	C <sub>7</sub> H <sub>5</sub> N <sub>3</sub> O <sub>3</sub>		3	↗	-
	TP13	[M-H] <sup>-</sup>	148.0516	3.9	C <sub>7</sub> H <sub>7</sub> N <sub>3</sub> O		3 (ETS00102)	↗↘	[26]
	TP14	[M-H] <sup>-</sup>	148.0516	4.7	C <sub>7</sub> H <sub>7</sub> N <sub>3</sub> O		3 (ETS00102)	↗↘	[26]
5TTR	TP15	[M+H] <sup>+</sup>	164.0455	3.7	C <sub>7</sub> H <sub>5</sub> N <sub>3</sub> O <sub>2</sub>		2a (ETS00121)	↗	[26]
		[M-H] <sup>-</sup>	162.0309	3.7					
	TP16	[M+H] <sup>+</sup>	150.0662	4.6	C <sub>7</sub> H <sub>7</sub> N <sub>3</sub> O		3 (ETS00102)	↗	[26]

	TP17	[M-H] <sup>-</sup>	164.0466	2.9	C <sub>7</sub> H <sub>7</sub> N <sub>3</sub> O <sub>2</sub>		3	↗	-
XTR	TP18	[M+H] <sup>+</sup>	178.0611	3.8	C <sub>8</sub> H <sub>7</sub> N <sub>3</sub> O <sub>2</sub>		3	↗	-
	TP19	[M+H] <sup>+</sup>	164.0818	5.4	C <sub>8</sub> H <sub>9</sub> N <sub>3</sub> O		3	↗	-
		[M-H] <sup>-</sup>	162.0673	4.9					
CBTR			-						
OHBTH	TP20	[M+H] <sup>+</sup>	182.0270	3.1	C <sub>8</sub> H <sub>7</sub> NO <sub>2</sub> S		3	↗	-
	TP21	[M-H] <sup>-</sup>	165.9968	5.8	C <sub>7</sub> H <sub>5</sub> NO <sub>2</sub> S		3	↗	-

	TP22	[M-H] <sup>-</sup>	245.9536	4.2	C <sub>7</sub> H <sub>5</sub> NO <sub>5</sub> S <sub>2</sub>		3	↗↘	-
--	------	--------------------	----------	-----	--	---	---	----	---



## **CHAPTER 5.**

### **Environmental fate of selected pharmaceuticals under nitrifying and denitrifying conditions: comparison of aerobic, anaerobic degradation and formation of biotransformation products**

#### **5.1 Introduction**

Pharmaceuticals (Phs) as a class of emerging contaminants have been studied thoroughly the last years [43, 83, 132, 133]. Elevated concentrations of pharmaceuticals and their metabolites have been found in several environmental compartments such as rivers, lakes, sea water, biosolids, waste water and sludge [75, 83, 134-137]. Pharmaceuticals' wide range of chemical properties resulted in their insufficient removal by the conventional wastewater treatment plants (WWTPs), designed to degrade simple organic loading [74]. As it is reflected by the vast knowledge about aerobic degradation mechanisms in comparison to anaerobic ones, aerobic conditions are generally reported to be more effective for the removal of most organic contaminants [133]. However, anaerobic degradation of micropollutants has been reported in literature especially for compounds that present environmental persistence under aerobic conditions [129, 138-140].

The target compounds on this study namely, metformin (MTF), ephedrine (EPH), ranitidine (RAN), lidocaine (LDC), citalopram (CTR), tramadol (TRA) and topiramate (TOP) are highly prescribed and consumed drugs in Greece and have been reported in elevated concentration in IWW and EWW [43, 72, 75, 76, 78]. Aerobic microbial degradation of MTF, RAN, LDC, TRA and CTR have been studied previously [68, 73, 77, 81, 86]. Although literature scarce on studies regarding degradation of these compounds under anoxic and anaerobic conditions.

Nowadays, removal mechanisms for conventional contaminants under different redox conditions are understood in detail and have been efficiently applied in most full scale STPs, although not the same can be said for the EPs. For the latter, the contribution of anoxic and anaerobic conditions to their

overall removal was usually not analyzed, since only influent and effluent concentrations of micropollutants have been normally considered in the monitoring of STPs [141, 142]. Understanding the behavior of EPs under different redox conditions is not only essential for achieving deeper knowledge of the whole wastewater treatment process, but also, in order to predict further pathways of those contaminants once released into the environment. In fact, different transformation products could be formed under aerobic and anoxic conditions, as previously indicating differences in degradation pathways in anoxic and aerobic processes. This could explain why some pollutants are better removed under anoxic conditions despite the common evidence that higher oxidation potentials in aerobic environments should favor their degradation [143, 144].

The main objective of the current study was to contribute in the lack of data for the biodegradation of the target compounds during wastewater treatment under aerobic/anoxic conditions and sludge anaerobic digestion. In this line, the biodegradation of 7 pharmaceuticals in activated sludge process and sludge anaerobic digestion (target compounds in **Table S5.1**, Section S5.1) was investigated. The effect of aerobic and anoxic conditions on biotransformation kinetics was investigated in activated sludge experiments. Experiments were also conducted using digested sludge under anaerobic conditions and the kinetics was calculated. Finally, for the first time biotransformation products formed by different types of sludge were tentatively identified.

## **5.2 Materials and methods**

### **5.2.1 Analytical standards and reagents**

Metformin, ranitidine, lidocaine hydrochloride, tamadol, topiramate and ephedrine pharmaceutical standards were of high-purity grade (more than 95 %) and were purchased from Sigma-Aldrich (Steinheim, Germany). Methanol (MeOH) LC-MS grade was purchased from Merck (Darmstadt, Germany), whereas 2-propanol LC-MS grade was purchased from Fisher Scientific (Geel, Belgium). Sodium hydroxide monohydrate for trace analysis  $\geq 99.9995\%$ , ammonium formate  $\geq 99.0\%$  and formic acid 99% were

purchased from Fluka (Buchs, Switzerland). Sodium azide and sodium nitrate were also purchased from Sigma-Aldrich (Steinheim, Germany). Distilled water was provided by a Milli-Q purification apparatus (Millipore Direct-Q UV, Bedford, MA, USA).

The amber Schott glass bottles used for the biotransformation batch experiments were purchased from ISOLAB (Wertheim, Germany). Glass fiber filters (GFF, pore size 0.7  $\mu\text{m}$ , diameter 47 mm) used in wastewater filtration and disposable GFF syringe filters (pore size 1.0  $\mu\text{m}$ , diameter 25 mm) were obtained from Whatman (Maidstone, UK). Regenerated cellulose syringe filters (RC, pore size 0.2  $\mu\text{m}$ , diameter 15mm) were purchased from Phenomenex (Torrance, CA, USA).

Stock standard solutions of individual compounds (1000  $\mu\text{g mL}^{-1}$ ) were prepared in MeOH and stored at  $-20\text{ }^{\circ}\text{C}$  in amber glass bottles to prevent photodegradation.

Detailed information on the physicochemical properties of the selected analytes can be found in **Table S5.1** (Section S5.1).

### 5.2.2 Biodegradation experiments

Mixed liquor and anaerobic digested sludge were used as inoculums for aerobic/anoxic and anaerobic microcosms, in order to assess the fate of the selected pharmaceuticals under nitrifying and denitrifying conditions. The previously described samples were withdrawn from the aeration tanks and the anaerobic digester of the WWTP of Athens, Greece, respectively.

The residential population connected to the WWTP of Athens is 3,700,000. The WWTP is designed to serve a population equivalent of 5,200,000 and thus is by far the largest in Greece and one of the largest in Europe. The WWTP has an estimated incoming sewage flow of 750,000  $\text{m}^3 \text{ day}^{-1}$  and implements primary sedimentation, activated sludge process with biological nitrogen (nitrification, denitrification) and phosphorus removal and secondary sedimentation. The operational parameters of the WWTP can be summarized to the following; 7-d Sludge Retention Time (SRT) of activated sludge and 18-d of the anaerobic digester, 12-h Hydraulic Retention (HRT),  $326 \pm 5 \text{ mg L}^{-1}$

BOD and  $N_{\text{tot}}$   $52 \pm 6 \text{ mg L}^{-1}$  of incoming wastewaters and mixed liquor suspended solids (MLSS)  $3680 \pm 102 \text{ mg L}^{-1}$ .

The experimental conditions used in different biodegradation batch experiments (A to L) are presented in Table 5.1. Experiments were conducted in stoppered glass bottles that were constantly agitated on a shaking plate and under dark conditions. The working volume in each reactor for the aerobic and anoxic experiments (A to H) was 0.2 L and the MLSS concentration  $2000 \text{ mg L}^{-1}$ . The working volume on anaerobic reactors was 15 mL and the suspended solids (SS) concentration  $30 \text{ g L}^{-1}$ . The investigated compounds were spiked using methanol solutions to obtain an initial concentration of around  $1 \text{ mg L}^{-1}$  for each microcontaminant in the reactors. The concentrations of target compounds were determined in the dissolved phase using the analytical methods described below.

In aerobic experiments (Experiments A - D), dissolved oxygen concentrations higher than  $4 \text{ mg L}^{-1}$  were achieved by using aeration through porous ceramic diffusers. In anoxic experiments (Experiments E - H), the reactors were initially purged with  $N_2$  gas and a solution of  $NaNO_3$  was added to provide an initial concentration of  $NO_3\text{-N}$  equal to  $40 \text{ mg L}^{-1}$ . In anaerobic experiments (Experiments I - L), the reactors were also purged with  $N_2$  gas for dissipation of dissolved oxygen. Finally, to investigate the effect of sorption of target compounds onto the sludge particles, batch experiments were performed with sodium azide ( $NaN_3$ , 0.2% w/v) to inactivate the bioactivity (Experiments C, G and K). In aerobic and anoxic experiments the temperature was  $25 \pm 2 \text{ }^\circ\text{C}$ , while pH was  $7.3 \pm 0.2$  and  $6.7 \pm 0.5$ , respectively. In anaerobic experiments the temperature was  $35 \pm 1 \text{ }^\circ\text{C}$ .

### **5.2.3 Analytical Method**

Samples were taken immediately after spiking, 1, 2, 6, 8 and 10 hours later and after 1, 2, 3, 4 and 6 days for aerobic and anoxic experiments, while in anaerobic experiments the samples were withdrawn immediately after spiking and after 1, 3, 5, 7, 10 and 12 days. 1 mL was sampled from each reactor and was filtered through pre-ashed glass fiber filters (GF-3 Macherey Nagel) and then through a  $0.2 \text{ }\mu\text{m}$  regenerated cellulose (RC Macherey Nagel) syringe

**Table 5.1:** Experimental conditions used in the different biodegradation batch experiments (A to L).

		Content	Spiked Concentration	T (°C)
<b>Aerobic experiment</b>				
A	Biotic reactor	sludge from the aeration tanks	1 mg L <sup>-1</sup>	25
B	Blank	sludge from the aeration tanks	-	25
C	Sorption Control	sludge from the aeration tanks + NaN <sub>3</sub> (1 g L <sup>-1</sup> )	1 mg L <sup>-1</sup>	25
D	Abiotic Control	tap water	1 mg L <sup>-1</sup>	25
<b>Anoxic experiment</b>				
E	Biotic reactor	sludge from the aeration tanks + NaNO <sub>3</sub> (40 mg L <sup>-1</sup> )	1 mg L <sup>-1</sup>	25
F	Blank	sludge from the aeration tanks + NaNO <sub>3</sub> (40 mg L <sup>-1</sup> )	-	25
G	Sorption Control	sludge from the aeration tanks + NaNO <sub>3</sub> (40 mg L <sup>-1</sup> ) + NaN <sub>3</sub> (1 g L <sup>-1</sup> )	1 mg L <sup>-1</sup>	25
H	Abiotic Control	tap water	1 mg L <sup>-1</sup>	25
<b>Anaerobic experiment</b>				
I	Biotic reactor	sludge from the anaerobic digester	1 mg L <sup>-1</sup>	35
J	Blank	sludge from the anaerobic digester	-	35
K	Sorption Control	sludge from the anaerobic digester + NaN <sub>3</sub> (1 g L <sup>-1</sup> )	1 mg L <sup>-1</sup>	35
L	Abiotic Control	tap water	1 mg L <sup>-1</sup>	35

filter. The extracts were diluted with MeOH to achieve an in-vial composition of 50:50 MeOH:H<sub>2</sub>O and were stored at -18 °C prior to analysis. More details on the HR-MS conditions performed only in RP chromatographic system can be found on electronic Electronic Supplementary Material Section S3.3.

#### 5.2.4 Calculation and modelling equations

The dissipation time of target compounds in biodegradation experiments were estimated using first-order kinetics, (Equations 5.1, 5.2):

$$C_t = C_o e^{-kt} \quad (5.1)$$

$$DT50 = \frac{\ln 2}{k} \quad (5.2)$$

Where  $C_t$  and  $C_o$  are the target compound concentrations in batch experiment at time  $t$  and  $t = 0$ , respectively,  $k$  is the biodegradation coefficient and DT50 is the dissipation time; the time it takes until the concentration of the compound has decreased by 50%.

#### 5.2.5 Suspect screening for the identification of TPs

The post-acquisition data processing approach was the same with the previous described in Chapter 3, Section 3.2.6, and it was followed partially regarding the fact that only suspect screening and no non-target screening was performed.

### 5.3 Results and Discussion

#### 5.3.1 Biodegradation experiments

The removal of the target compounds was assessed under aerobic and under pure anaerobic conditions (total absence of free oxygen –O<sub>2</sub> or bound oxygen –NO<sub>2</sub>, NO<sub>3</sub>) and under anoxic conditions (in the presence of NO<sub>3</sub>). Biotic processes are expected to be the main removal mechanism of the target compounds in contact with activated sludge since their physicochemical properties and chemical structure (**Table S5.1**, Section S5.1) indicate insignificant volatilization and hydrolysis as well as low adsorption from the sludge and high solubility in aqueous phase.

Time profiles of the sterile (sorption reactor) and non-sterile (biotic reactor) experiments for the selected pharmaceuticals under aerobic, anoxic and anaerobic conditions are presented in **Fig. 5.1** and **Fig.5.2**, respectively. Furthermore, the estimated dissipation times and pseudo- first order rate

constants, in the cases that could be estimated, are presented in **Table 5.1**.  $k_{\text{ABIOTIC}}$  is the rate of sorption calculated from the experiments with the sterilized sludge (based on the assumption that sorption is the main abiotic mechanism which takes place in the system). In addition,  $k_{\text{TOTAL}}$  is the rate calculated from the experiments with the activated sludge and expresses the total degradation of the compounds in the system (including abiotic and biotic processes). Finally, dissipation time of the compounds was corrected for the DT50 derived from the sterile experiments in order to exclusively reflect the dissipation that can be attributed to biological transformation ( $\text{DT50}_{\text{BIOTIC}}$ ).

Under aerobic conditions, as it can be observed (**Fig.5.1** and **Fig.5.2**) the sterile experiments revealed insignificant adsorption (lower than 20%) of the target compounds onto the sludge particles and most of their content remains in the aqueous phase. TRA and EPH as exceptions, presented a sorption rate around 50% and 40% from the first day, respectively. Sorption of TRA remained steady after the first day, however EPH present further decrease up to 60% (**Fig.5.2**) until the end of the incubation time. Although the sorption rate recorded for EPH was very high the first day, completely elimination of the compound was achieved within the first 10 hours of the incubation, indicating that the major elimination mechanism was biodegradation. For EPH no sorption studies were found in the literature but the findings for TRA were in contrast with previous publications by Horsing et al. [59] and Bergheim et al. [81] who reported low affinity of TRA with the sludge. Similar contrary results have been reported for CTR sorption in the study of Horsing et al. [59] in long age and short age sludge. This behavior give rise to speculations like there was something within the sludge which prevented sorption to occur or enhanced sorption based on unknown similarities and differences within the sludges, however no clear explanation could be found. Another explanation that has been previously reported, is that losses could also be explained by a partial reactivation of the autoclaved sludge as the sludge could be contaminated by active bacteria each time it was sampled [22, 86]. The removals on the sterile (sorption reactor) and non-sterile (biotic reactor) experiments for RAN, LDC and CTR were in accordance with previous studies [60, 82, 86, 145].

By comparing the rate constant values for all target compounds (**Table 5.1**) it is clearly noticed that the highest biodegradability among the analytes was presented for MTF followed by EPH, RAN, CTR, TOP and LDC. TRA presented  $k_{\text{biot}}$  greater than  $k_{\text{total}}$  and as a result a negative value for  $k_{\text{biot}}$  was calculated. MTF and EPH were almost completely degraded within the first 12 hours of incubation while CTR and LDC degraded up to 80% and 60%, respectively after 3d incubation time and their percentage remained steady until the end of the experiment. The estimated rate constant values ( $k_{\text{BIOTIC}}$ ), for RAN, CTR and LDC were in agreement with previous studies [146], but it should be mentioned that differences may occur due to the different experimental conditions (incubation time, incubation temperature, concentration of the analyte, MLSS concentration) [139]. TOP was presented the lowest removal rate between the analytes.

For the compounds that were not eliminated completely after the incubation time of 5 days, it was hypothesized that maybe anaerobic conditions worked efficiently for their removal. However MTF, EPH and RAN were also included in the experiments for comparison. Since there are very few studies in the literature regarding removal rates of PPCPs under anaerobic conditions, especially for the target analytes, no further evaluation with experimental data could be achieved. It should be noted that high DT50 values reflect low removal of the target compound. MTF observed to be also high biodegradable under anoxic conditions and no any significant difference presented in DT50. Increase of the DT50 under anoxic conditions was observed for CTR and RAN approximate in 5.6 and 9.2 days, respectively.

EPH and TRA concentrations were reduced in half after almost 10h of anoxic incubation followed by LDC and TOP with DT50 equal to 53.3. It is clear that anoxic conditions did not improve the removal rate of the compounds that did not degrade efficiently under aerobic conditions (LDC and TOP) but increased further the time needed for elimination. CTR presented approximately the same  $k_{\text{sorption}}$  under all the conditions. LDC, TOP and MTF presented a constant sorption profile of 20% under all the experimental conditions apart from LDC which increased the sorption losses up to 60% after 12d under anaerobic conditions. Sorption mechanism removed 40% of the initial RAN



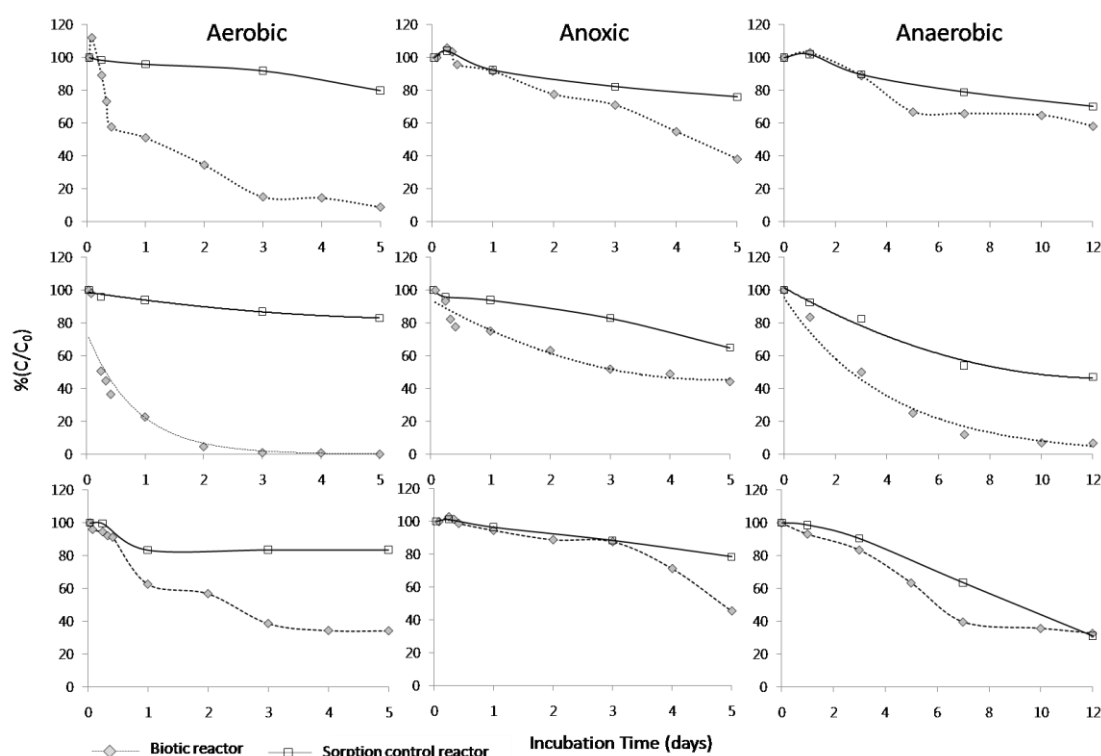


**Fig.5.1:** Time profiles of CTR, RAN and LDC under aerobic, anoxic and anaerobic conditions, respectively.

concentration under anoxic (after 5d) and under anaerobic conditions (after 5d and remained steady until 12d).

Although the sorption was greater under anoxic than aerobic conditions, the removal of RAN was in total higher (60%) indicating a small percentage of 20% which implied biotic degradation. TRA and EPH were the two compounds that their sorption losses under anaerobic and anoxic conditions were lower than in the sorption reactor operate aerobically.

In general, reduction of the dissolved oxygen concentration resulted in lower removal rate and thus greater DT50 for all the compounds. Only for two analytes, namely TOP and RAN the removal rate was higher under anaerobic than under anoxic conditions. More specifically, TOP showed slightly higher removal rate in anaerobic than in anoxic reactor, since overall removal was higher under anaerobic conditions and sorption losses were almost the same both in anoxic and anaerobic conditions and thus a percentage of 20% estimated to be biodegraded under total absence of free oxygen. In addition, RAN which presented a constant sorption both under anoxic and anaerobic conditions (40%) the total removal rate in anaerobic reactor was higher than

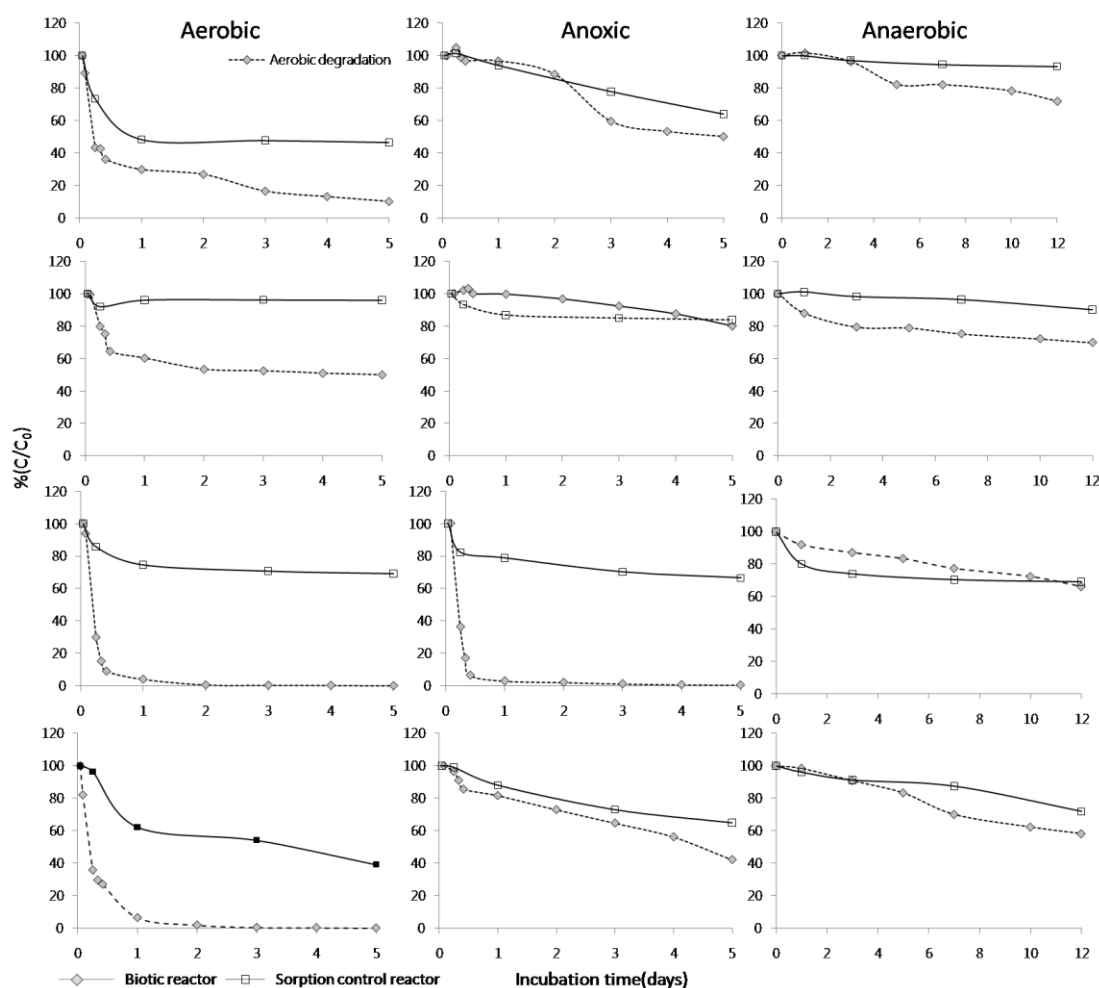


**Fig.5. 2:** Time profiles of TRA, TOP, MTF and EPH under aerobic, anoxic and anaerobic conditions, respectively.

in anoxic reactor, indicating more efficient elimination of RAN and thus higher biodegradation rate under total absence of free oxygen.

### 5.3.2 By –products formation

All the time intervals of the three experimental conditions were screened for the identification of TPs. For the suspect screening, individual suspect databases for the target compounds were compiled based on reported TPs from the literature, already known human metabolites, findings of our previous research not published yet, and finally, predicted TPs provided by *in silico* prediction tools under aerobic and anaerobic conditions. The detected TPs under the three different conditions along with the corresponding reactions are summarized comparatively in **Table S5.2** (Section S5.2).

**Table 5.2:** Estimated dissipation times and pseudo- first order rate constants under different redox conditions for the study analytes

		<b>k<sub>ABIOTIC</sub> (d<sup>-1</sup>)</b>	<b>DT<sub>50, ABIOTIC</sub> (d)</b>	<b>k<sub>TOTAL</sub>(d<sup>-1</sup>)</b>	<b>DT<sub>50, TOTAL</sub> (d)</b>	<b>k<sub>BIOTIC</sub> (d<sup>-1</sup>)</b>	<b>DT<sub>50, BIOTIC</sub> (d)</b>
<b>CTR</b>	Aerobic	0.041	16.8	0.524	1.3	0.483	1.4
	Anoxic	0.061	11.4	0.184	3.8	0.123	5.6
	Anaerobic	0.039	17.6	0.045	15.4	0.006	116
<b>RAN</b>	Aerobic	0.035	19.8	1.21	0.57	1.175	0.6
	Anoxic	0.081	8.6	0.156	4.4	0.075	9.2
	Anaerobic	0.066	10.5	0.239	2.9	0.173	4.0
<b>LDC</b>	Aerobic	0.201	3.4	0.317	2.2	0.116	6.0
	Anoxic	0.050	13.8	0.079	8.8	0.029	23.9
	Anaerobic	0.098	7.1	0.103	6.7	0.005	138.6
<b>TRA</b>	Aerobic	0.706	1.0	0.384	4.0	-0.322	-2.2
	Anoxic	0.093	7.5	0.16	4.3	0.067	10.3
	Anaerobic	0.006	115	0.029	24.1	0.023	30.1
<b>TOP</b>	Aerobic	0.013	53.3	0.29	2.4	0.277	2.5
	Anoxic	0.030	23.1	0.043	16	0.013	53.3
	Anaerobic	0.009	77.0	0.025	27.5	0.016	43.3
<b>MTF</b>	Aerobic	0.273	2.5	2.55	0.27	2.277	0.3
	Anoxic	0.259	2.7	3.57	0.19	3.311	0.2
	Anaerobic	0.019	36.5	0.032	21.7	0.013	53.3
<b>EPH</b>	Aerobic	0.178	3.9	1.52	0.46	1.342	0.5
	Anoxic	0.089	7.8	0.153	4.5	0.064	10.8

---

Anaerobic	0.026	27	0.043	16	0.017	40.8
-----------	-------	----	-------	----	-------	------

Since the reduction of free oxygen found not to improve significant the removal of the compounds, specifically, the removal rate decreased in anoxic conditions than in aerobic and was limited further under anaerobic conditions, no extended biotransformation was expected under anoxic/anaerobic conditions.

Metformin was the compound that presented the greater removal under both aerobic and anoxic conditions within the first 10h. As it has been previously mentioned in chapter 4.2, which is in line with literature [77, 78], aerobic biotransformation of MTF resulted in the formation of MTF103 (guanylurea, GNR). Indeed, the aerobic and anoxic removal of MTF in this experiment revealed the formation of GNR. The long incubation time (5d) showed that under aerobic conditions GNR reached its maximum formation at 10h and then started to decrease contrary to anoxic formation of GNR which after reaching its maximum at 10h remained steady until the end of experiment. The behavior observed in the aerobic reactor was not expected as GNR has been characterized as a recalcitrant dead-end by-product of GNR very stable to further bio- and photo- degradation [77]. Surprisingly, the strictly anaerobic conditions did not promote the reactions of double N-demethylation and oxidative deamination to ketone needed for the formation of GNR, even though in general reductive deamination is a common reaction for small molecules organic compounds under aerobic conditions [133].

Similarly to MTF, EPH was removed very quickly under aerobic conditions and sorption have not presented as significant degradation mechanism. The removal rate, under anoxic and anaerobic conditions, was calculated around 60% and 40%, respectively. Although, significant sorption occurrence, especially under anaerobic conditions, where elevated concentration of MLSS have been applied, denoted only a low percentage of the parent compound ready to biotransformed in the anoxic reactor. As it was expected no TPs formation observed in the time interval samples withdrawn from the anaerobic reactor. The formation of the oxidative by-product of EPH, EPH164 (ephedrone) was detected based on spectra diagnostic evidences (Id. level 2b) under aerobic and anoxic conditions.

Little is known for TOP, since the literature lacks biotransformation studies. TOP presented rather stable under aerobic conditions and more stable under anoxic/anaerobic conditions presented a total removal of 40% and 20% respectively. Sorption did not occur in great extent, with almost 10% and 20% in the aerobic and anoxic/anaerobic sterile control reactor, respectively. Thus, only a small fraction of the parent compound remained available for biotransformation under aerobic conditions. However, no TPs were found to be formed during 5 days incubation time under aerobic conditions according to the suspect screening performed for TOP.

Ranitidine is a highly degraded compound under aerobic conditions as it has been mentioned elsewhere within this study but also according to the literature [68, 81] and thus experimental data for its removal under anoxic/anaerobic conditions are scarce. Its high degradability under aerobic conditions was also confirmed and in this experiment. RAN presented a total removal of 90% and 50% under total absence of free oxygen or bound oxygen, respectively. The removal attributed to sorption mechanism counted for 50% and 30% in the anaerobic and anoxic sterile control reactors, respectively, denoted that a percentage between 20-40% biotransformed under absence of oxygen. Suspect screening performed for the sample points from the anaerobic reactor did not reveal any RAN TP formation. In addition, under anoxic and anaerobic conditions, as it was expected several TPs were formed. Six TPs were identified under aerobic whereas only four under anoxic conditions. Namely the TPs identified were, RAN331A (RAN-S-oxide), RAN331B (RAN-N-oxide), RAN301 (desmethyl-RAN), RAN 302 (RAN-carboxylic acid), RAN317 (desmethyl-RAN-S-oxide) and RAN286 under aerobic conditions. The identified TPs formed under anoxic conditions were RAN331A (RAN-S-oxide), RAN331B (RAN-N-oxide), RAN301 (desmethyl-RAN), RAN 302 (RAN-carboxylic acid). RAN-S-oxide was found the most abundant formed TP under both conditions. Since N-demethylation was occurred under anoxic conditions resulted in the formation of the demethylated RAN TP, RAN317 was expected to be formed by N-demethylation of RAN-S-oxide. However an explanation for not being identified it could be that, demethylation followed the formation RAN-S-oxide

under aerobic conditions as it started after 24h where the formation rate of RAN-S-oxide has started to decrease, indicating that S-oxidation occurred firstly. RAN317 reached within the second day of the experiment its highest level and then started to decrease. However, under anoxic conditions, RAN-S-oxide reached the highest formation level after 3d incubation time which may be delayed the formation RAN317.

Biodegradation of citalopram under aerobic conditions has been studied thoroughly in chapter 3 of this doctoral thesis. Regarding the removals calculated for CTR under anoxic and anaerobic conditions on this experiment it was observed that only a percentage of 20% and 10%, respectively, was expected to be removed by biotransformation processes, since around 30% of losses of the target compound was attributed to sorption mechanism. Nine TPs were detected under aerobic conditions, whereas six TPs detected under anoxic conditions and only one TP under anaerobic conditions. Compared to the identified TPs on chapter 3, five TPs were did not detected (CTR339B, CTR355, CTR357, CTR359A and CTR360). The transformation products CTR339B (Id. Level 4) and CTR355 (lactone derivative of CTR-N-oxide) have not been included in the suspect list since the studies run in parallel and the aforementioned TPs detected after non target screening. CTR360B (hydroxylated derivative of CTR-carboxylic acid) could not have been identified, as in the previous study, was identified dew to implementation of HILIC analysis as an isomer of the TP360A (carboxylic acid of CTR-N-oxide) which was detected. For the last two TPs CTR357 (lactone derivative of CTR-amide) and 359A (hydroxylated derivative of CTR-amide) it was hypothesized that the precursor substrates for their formation may have been produced in lower concentrations or later than the experiment in chapter 3 and as a consequence could not have been detected. The TPs that were not formed under anoxic conditions were CTR329 (amide of desmethyl-CTR), CTR359B (amide of CTR-N-oxide) and CTR360A (carboxylic acid of CTR-N-oxide). For this it was assumed that, the delay on the formation of the precursory molecules for their formation (for CTR360; CTR343 should be formed and then CTR344 or CTR341 and then CTR359B and for CTR329; CTR343 should be formed firstly) under anoxic conditions compared to aerobic ones,

resulted presumably in not sufficient time for their formation. Under anaerobic conditions only one TP was detected namely CTR344 (CTR carboxylic acid). The formation of CTR344 proceed *via* nitrile hydrolysis for the formation of the corresponding amide (CTR343; was not detected) and further amide hydrolysis and formation of the carboxylic acid. Since hydrolysis is a relatively simple reaction and not requiring any oxygen or cofactors it was likely to occur under anaerobic conditions [133]. CTR344 was the only TP that was formed and detected under anaerobic conditions in this study.

Lidocaine presented the same removal rate under anaerobic conditions both on the biotic reactor and on the sterile control reactor. Thus, the total elimination of LDC under strictly anaerobic conditions attributed to sorption onto the sludge particles more probably due to the high concentration of MLSS. The calculated fractions of the target compound available for biotransformation under aerobic and anoxic conditions were almost 50% and 40%, respectively. The three TPs identified through suspect screening in chapter 4.2, namely; LDC207 (norlidocaine), LDC251 (LDC-N-oxide) and LDC219 (Id. level 3) were also formed and detected under both aerobic and anoxic conditions.

Tramadol present more liable to biotransformation under aerobic conditions, followed by anaerobic and anoxic conditions, since the percentages were calculated around 30%, 20% and 10%, respectively. No TP was detected to be formed under anaerobic conditions, however, previous studies have been reported a slight removal of TRA and formation of O-desmethyl TRA under anaerobic conditions [147]. Under aerobic conditions the following TPs were detected; TRA250 (N- TRA), TRA280 (hydroxylated derivative of TRA), TRA278 (ketone of TRA), TRA236 (N,O-didemsethyl TRA) while under anoxic conditions TRA280 was not detected. Although the formation of the detected TP TRA278 the formation of TRA280 the last one was not detected, surprisingly.



## 5.4 Conclusions

- The degradation of seven pharmaceuticals was studied under aerobic, anoxic and anaerobic conditions.
- Biodegradation mechanism as well as sorption mechanism studied in parallel for the elimination of the target compounds.
- Aerobic conditions presented more effective for the removal of analytes followed by anoxic conditions.
- Total absence of free oxygen has shown that it does not promote the biotic removal of the PCs.
- Sorption mechanism was found very significant for the elimination process of the target compounds under anaerobic conditions presumably due to the high concentration of the MLSS.
- In most of the study compounds the majority of the TPs formed under aerobic conditions were also formed under anoxic conditions indicating that the occurrence of bonded oxygen can still promote the biotic degradation of the compounds.
- More studies for the elimination and transformation of EPs should be performed to elucidate the transformation pathways, characterize microbial communities and understand the processes involved under anaerobic conditions for the transformation of complex matrix compounds.

## CHAPTER 6. Conclusions

Over the last years advances on the analytical instruments such as high resolution mass analyzers, along with the development of sophisticated software for the post acquisition data treatment of the vast information that is extracted through HRMS analysis, contributed to the field of the environmental analysis and especially to the detection and identification of unknown compounds, the so-called transformation products. Computer-assisted workflows based on *in silico* prediction and *in silico* fragmentation tools promote the compilation of more smart suspect databases and the interpretation of mass spectra as well as and the structure elucidation of the new identified transformation products.

Conventional activated sludge system is the most commonly employed treatment worldwide for processing both urban wastewater and industrial effluents. Identification of TPs of EPs is a challenging task as a consequence of their unknown nature and the absence of analytical standards to confirm their identity.

The removal of certain EPs and their biotransformation during batch experiments with activated sludge (Chapters 3, 4 & 5) and digested sludge under anaerobic conditions (Chapter 5) were in depth investigated in the experimental part of this doctoral thesis. The results have demonstrated that suspect and non-target screening workflows can result in the identification of several transformation products of emerging contaminants (Chapters 3 & 4). LC is the technique of choice for the determination of a wide range of polarities organic compounds. Since bioTPs have been reported to be more polar than their parent compound, the use of HILIC as a complimentary technique to RP was proven meaningful for the detection of polar TPs that were not retained on the RP column and for the separation of isomeric TPs that were co-eluted in the RP system (Chapters 3 & 4). Moreover, the use of quantitative structure-retention relationship (QSRR) prediction model was proved a significant supportive tool to enhance the identification confidence for the proposed structures of the candidate TPs.

Additionally, retrospective analysis of the samples is the greater advantage of HRMS methods, in order to look back in previous samples for new or recently released or reported compounds.

Toxicity assessment results revealed that the formed TPs could be more toxic than their parent compounds. Based on these evidences, there is a need for routine monitoring not only the parent compounds (EPs), but also their TPs.

Finally this doctoral thesis was contributed to the gap presented in the literature for the biodegradation of EPs during wastewater treatment under aerobic/anoxic conditions and sludge anaerobic digestion and study the biotransformation products that were formed by different types of sludge under different redox conditions (Chapter 5). However, we recognized the need that more studies for the elimination and transformation of EPs should be performed to elucidate the transformation pathways, characterize microbial communities and understand the processes involved under anaerobic conditions for the transformation of complex matrix compounds.

To conclude with, there is a general consensus among policy-makers that emerging substances need to be addressed in a systematic and coherent manner. For this reason the ultimate objective should be to advance our knowledge and environmental monitoring abilities to the point, where the need for the term “emerging” disappears altogether and it is anticipated that environmental legislation will be widened to cover a range of municipal derived ECs.

The traditional analytical approach of applying targeted screening with low resolution mass spectrometry results in numerous chemicals such as transformation products going undetected. New analytical techniques such as non-target screening are likely to generate much more chemical monitoring data in the future. The necessity of using integrated analytical approaches which compliments targeted and non-targeted screening with biological assays to measure ecological impact are of high demand. A wider picture of contaminants in the environment will become a challenge for environmental legislation.

There is still a need to better investigate individual chemicals of emerging concern and their transformation products by developing analytical methods to determine occurrence of these compounds in the environment; understanding how they may be released or formed; and identifying their potential environmental effects.

Non-target screening analysis, combined with the integration of high-performance computing, becomes “ready to go” for environmental applications and moves traditional exposure analysis to ‘big data’. Digital Sample Freezing Platforms (DSFP) will host in the near future harmonized format full-scan HR-MS data, allowing for high-throughput processing (including retrospective analysis) of any environmental sample for a wide range of pollutants. Moreover, DSFP will work as an open-access database of mass spectra of environmental contaminants to support the identification of unknowns.

Environmental monitoring must also apply a holistic approach. This involves determining fate and impact of ECs across their complete life cycle which includes the terrestrial environment. Detailed case studies of amended soils in field conditions which investigate leaching and runoff, impact to surrounding surface water quality, in soil degradation, toxicity to terrestrial organisms and the potential uptake by plants and entry into the human food chain are needed. A similar approach can be taken for monitoring other contaminated environmental compartments such as river sediments. Finally, the combined use of chemical and biological analysis to better assess environmental impact from ECs will enable the revision and development of more accurate environmental risk assessment.

.

## ABBREVIATIONS AND ACRONYMS

2-hydroxybenzothiazole	OHBTH
3,4-methylenedioxymethamphetamine	MDMA
4-tolytriazole (or 4-methylbenzotriazole)	4TTR
5-chlorobenzotriazole	CBTR
5-tolytriazole (or 5-methylbenzotriazole)	5TTR
Acetonitrile	ACN
Activated Sludge	AS
Advanced Oxidation Processes	AOPs
Applicability Domain	AD
Atorvastatin	ATR
Benzothiazoles	BTHs
Benzotriazole	BTR
Benzotriazoles	BTRs
Broad Band Collision Induced Dissociation	bbCID
Citalopram	CTR
Conventional Activated Sludge	CAS
Data-Dependent Acquisition	DDA
Data-Independent Acquisition	IDA
Dehydromephedrone	DHM

Dissipation Time	DT50
Dissolved Oxygen	DO
Eawag Biocatalysis/Biodegradation Database	EAWAG-BBD
Eawag Pathway Prediction System	EAWAG-PPS
Ecological Structure Activity Relationships	ECOSAR
Effluent Wastewater	EWV
Electrospray Ionization	ESI
Emerging Pollutants	EPs
Endocrine-Disrupting Chemicals	EDCs
Ephedrine	EPH
European Commission	EC
European Economic Community	EEC
European Inventory of Existing Commercial Chemical Substances	EINECS
European Medicines Agency	EMA
European Union	EU
Full Width at Half Maximum	FWHM
Gas Chromatography	GC
Gas Chromatography-Mass Spectrometry	GC-MS
Glass Fiber Filters	GFFs

Guanylurea	GNR
Half maximal effective concentration	EC50
Half maximal lethal concentration	LC50
High energy	HE
High Resolution Mass Spectrometry	HRMS
High-Density Polyethylene	HDPE
Hybrid Moving Bed Biological Reactors	HMBBRs
Hydrolytic Retention Time	HRT
Hydrophilic Interaction Liquid Chromatography	HILIC
Influent Wastewater	IWW
Ion-trap	IT
Lidocaine	LDC
Liquid Chromatography	LC
Liquid Chromatography - High Resolution Mass Spectrometry	LC-HRMS
Liquid Chromatography-Mass Spectrometry	LC-MS
Low Energy	LE
Maximum Environmental Concentration	MEC
Membrane Bioreactors	MBRs
Metformin	MTF

Methanol	MeOH
Mixed Liquor Suspended Solids	MLSS
Moving Bed Biological Reactors	MBBRs
New Psychoactive Substances	NPs
Organisation for Economic Co-operation and Development	OECD
Parent Compound	PC
Persistent Organic Pollutants	POPs
Pharmaceuticals	Phs
Pharmaceuticals and Personal Care Products	PPCPs
p-methoxy Methamphetamine	PMMA
Polybrominated Diphenyl Ethers	PBDEs
Polychlorinated Biphenyls	PCBs
Polycyclic Aromatic Hydrocarbons	PAHs
Predicted No Effect Concentration	PNEC
Quadrupole Time-of-Flight	Q-TOF
Quadrupole-Linear Ion Trap	Q-LIT
Quantitative Structure-Retention Relationship	QSRR
Quantitative Structure-Toxicity Relationship	QSTR
Ranitidine	RAN



Regenerated Cellulose	RC
Registration, Evaluation, Authorisation and Restriction of Chemicals	REACH
Reversed Phase Liquid Chromatography	RPLC
Risk Quotient	RQ
Selected Reaction Monitoring	SRM
Selective Serotonin Re-uptake Inhibitor	SSRI
Sewage Treatment Plants	STPs
Sludge Retention Times	SRT
Solid-Phase Extraction	SPE
Suspended Solids	SS
Time-of-Flight	TOF
Topiramate	TOP
Total Suspended Solids	TSS
Tramadol	TRA
Transformation Products	TPs
Triple Quadrupole	QqQ
Ultrahigh-Performance Liquid Chromatography	UHPLC
United States Environmental Protection Agency	US EPA
Wastewater Based Epidemiology	WBE

Wastewater Treatment Plants	WWTPs
Xylytriazole	XTR

## REFERENCES

- [1] B.I. Escher, K. Fenner, Recent advances in environmental risk assessment of transformation products, *Environmental science & technology*, 45 (2011) 3835-3847.
- [2] M.Petrovic, D. Barcelo, S. Perez, *Comprehensive Analytical Chemistry: Analysis, Removal, Effects and Risk of Pharmaceuticals in the Water Cycle Occurrence and Transformation in the Environment*, Elsevier, 2013.
- [3] E.C.W. OW/ORD, White Paper Aquatic Life Criteria for Contaminants of Emerging Concern: Part I Challenges and Recommendations, USEPA, (2008).
- [4] K. Fent, A.A. Weston, D. Caminada, *Ecotoxicology of human pharmaceuticals*, *Aquatic toxicology*, 76 (2006) 122-159.
- [5] A. Agüera, M.J. Martínez Bueno, A.R. Fernández-Alba, New trends in the analytical determination of emerging contaminants and their transformation products in environmental waters, *Environmental science and pollution research international*, 20 (2013) 3496-3515.
- [6] M.I. Farré, S. Pérez, L. Kantiani, D. Barceló, Fate and toxicity of emerging pollutants, their metabolites and transformation products in the aquatic environment, *TrAC Trends in Analytical Chemistry*, 27 (2008) 991-1007.
- [7] F.J. Benitez, J.L. Acero, F.J. Real, G. Roldan, E. Rodriguez, Photolysis of model emerging contaminants in ultra-pure water: kinetics, by-products formation and degradation pathways, *Water Res*, 47 (2013) 870-880.
- [8] J. Santiago, A. Agüera, M. del Mar Gómez-Ramos, A.R. Fernández Alba, E. García-Calvo, R. Rosal, Oxidation by-products and ecotoxicity assessment during the photodegradation of fenofibric acid in aqueous solution with UV and UV/H<sub>2</sub>O<sub>2</sub>, *Journal of hazardous materials*, 194 (2011) 30-41.
- [9] A.K. Genena, D.B. Luiz, W. Gebhardt, R.F.P.M. Moreira, H.J. José, H.F. Schröder, Imazalil Degradation upon Applying Ozone—Transformation Products, Kinetics, and Toxicity of Treated Aqueous Solutions, *Ozone: Science & Engineering*, 33 (2011) 308-328.
- [10] B.I. Escher, K. Fenner, Recent Advances in Environmental Risk Assessment of Transformation Products, *Environmental science & technology*, 45 (2011) 3835-3847.
- [11] M. Petrović, S. Pérez, D. Barceló, *Analysis, Removal, Effects and Risk of Pharmaceuticals in the Water Cycle Occurrence and Transformation in the Environment*, Elsevier, 2013.
- [12] S. Suárez, M. Carballa, F. Omil, J.M. Lema, How are pharmaceutical and personal care products (PPCPs) removed from urban wastewaters?, *Reviews in Environmental Science and Bio/Technology*, 7 (2008) 125-138.
- [13] A.A. Bletsou, J. Jeon, J. Hollender, E. Archontaki, N.S. Thomaidis, Targeted and non-targeted liquid chromatography-mass spectrometric workflows for identification of transformation products of emerging pollutants in the aquatic environment, *TrAC Trends in Analytical Chemistry*, 66 (2015) 32-44.

- [14] U.M. Zanger, *Metabolism of Drugs and Other Xenobiotics*, 2012.
- [15] Y. Pico, D. Barcelo, Transformation products of emerging contaminants in the environment and high-resolution mass spectrometry: a new horizon, *Analytical and bioanalytical chemistry*, 407 (2015) 6257-6273.
- [16] C. Prasse, M. Wagner, R. Schulz, T.A. Ternes, Biotransformation of the antiviral drugs acyclovir and penciclovir in activated sludge treatment, *Environmental science & technology*, 45 (2011) 2761-2769.
- [17] D.E. Helbling, J. Hollender, H.-P.E. Kohler, H. Singer, K. Fenner, High-Throughput Identification of Microbial Transformation Products of Organic Micropollutants, *Environmental Science and Technology*, 44 (2010) 6621–6627.
- [18] S. Kern, K. Fenner, H. Singer, R.P. Schwarzenbach, J. Hollender, Identification of transformation products of organic contaminants in natural waters by computer-aided prediction and high-resolution mass spectrometry, *Environmental science & technology*, 43 (2009) 7039-7046.
- [19] A. Wick, M. Wagner, T.A. Ternes, Elucidation of the transformation pathway of the opium alkaloid codeine in biological wastewater treatment, *Environmental science & technology*, 45 (2011) 3374-3385.
- [20] R. Beel, C. Lutke Eversloh, T.A. Ternes, Biotransformation of the UV-filter sulisobenzone: challenges for the identification of transformation products, *Environmental science & technology*, 47 (2013) 6819-6828.
- [21] A. Rubirola, M. Llorca, S. Rodriguez-Mozaz, N. Casas, I. Rodriguez-Roda, D. Barcelo, G. Buttiglieri, Characterization of metoprolol biodegradation and its transformation products generated in activated sludge batch experiments and in full scale WWTPs, *Water research*, 63 (2014) 21-32.
- [22] S. Huntscha, T.B. Hofstetter, E.L. Schymanski, S. Spahr, J. Hollender, Biotransformation of benzotriazoles: insights from transformation product identification and compound-specific isotope analysis, *Environmental science & technology*, 48 (2014) 4435-4443.
- [23] R. Gulde, D.E. Helbling, A. Scheidegger, K. Fenner, pH-dependent biotransformation of ionizable organic micropollutants in activated sludge, *Environmental science & technology*, 48 (2014) 13760-13768.
- [24] T. Kosjek, N. Negreira, M.L. de Alda, D. Barcelo, Aerobic activated sludge transformation of methotrexate: identification of biotransformation products, *Chemosphere*, 119 Suppl (2015) S42-50.
- [25] M. Mardal, M.R. Meyer, Studies on the microbial biotransformation of the novel psychoactive substance methylenedioxypyrovalerone (MDPV) in wastewater by means of liquid chromatography-high resolution mass spectrometry/mass spectrometry, *The Science of the total environment*, 493 (2014) 588-595.
- [26] S. Terzic, I. Senta, M. Matosic, M. Ahel, Identification of biotransformation products of macrolide and fluoroquinolone antimicrobials in membrane bioreactor treatment by ultrahigh-performance liquid chromatography/quadrupole time-of-flight mass spectrometry, *Analytical and bioanalytical chemistry*, 401 (2011) 353-363.

- [27] S. Mejia Avendano, J. Liu, Production of PFOS from aerobic soil biotransformation of two perfluoroalkyl sulfonamide derivatives, *Chemosphere*, 119 (2015) 1084-1090.
- [28] Z. Li, M.P. Maier, M. Radke, Screening for pharmaceutical transformation products formed in river sediment by combining ultrahigh performance liquid chromatography/high resolution mass spectrometry with a rapid data-processing method, *Analytica chimica acta*, 810 (2014) 61-70.
- [29] M. Radke, M.P. Maier, Lessons learned from water/sediment-testing of pharmaceuticals, *Water research*, 55 (2014) 63-73.
- [30] L. Tong, P. Eichhorn, S. Perez, Y. Wang, D. Barcelo, Photodegradation of azithromycin in various aqueous systems under simulated and natural solar radiation: kinetics and identification of photoproducts, *Chemosphere*, 83 (2011) 340-348.
- [31] C. Boix, M. Ibanez, L. Bijlsma, J.V. Sancho, F. Hernandez, Investigation of cannabis biomarkers and transformation products in waters by liquid chromatography coupled to time of flight and triple quadrupole mass spectrometry, *Chemosphere*, 99 (2014) 64-71.
- [32] L. Bijlsma, C. Boix, W.M. Niessen, M. Ibanez, J.V. Sancho, F. Hernandez, Investigation of degradation products of cocaine and benzoylecgonine in the aquatic environment, *The Science of the total environment*, 443 (2013) 200-208.
- [33] A. Muller, S.C. Weiss, J. Beisswenger, H.G. Leukhardt, W. Schulz, W. Seitz, W.K. Ruck, W.H. Weber, Identification of ozonation by-products of 4- and 5-methyl-1H-benzotriazole during the treatment of surface water to drinking water, *Water research*, 46 (2012) 679-690.
- [34] M. Horsing, T. Kosjek, H.R. Andersen, E. Heath, A. Ledin, Fate of citalopram during water treatment with O<sub>3</sub>, ClO<sub>2</sub>, UV and Fenton oxidation, *Chemosphere*, 89 (2012) 129-135.
- [35] F. Hernandez, M. Ibanez, E. Gracia-Lor, J.V. Sancho, Retrospective LC-QTOF-MS analysis searching for pharmaceutical metabolites in urban wastewater, *Journal of separation science*, 34 (2011) 3517-3526.
- [36] E.L. Schymanski, H.P. Singer, P. Longree, M. Loos, M. Ruff, M.A. Stravs, C. Ripolles Vidal, J. Hollender, Strategies to characterize polar organic contamination in wastewater: exploring the capability of high resolution mass spectrometry, *Environmental science & technology*, 48 (2014) 1811-1818.
- [37] M. Gomez-Ramos Mdel, A. Perez-Parada, J.F. Garcia-Reyes, A.R. Fernandez-Alba, A. Aguera, Use of an accurate-mass database for the systematic identification of transformation products of organic contaminants in wastewater effluents, *Journal of chromatography. A*, 1218 (2011) 8002-8012.
- [38] C. Moschet, A. Piazzoli, H. Singer, J. Hollender, Alleviating the reference standard dilemma using a systematic exact mass suspect screening approach with liquid chromatography-high resolution mass spectrometry, *Anal Chem*, 85 (2013) 10312-10320.
- [39] A.C. Chiaia-Hernandez, M. Krauss, J. Hollender, Screening of lake sediments for emerging contaminants by liquid chromatography atmospheric

pressure photoionization and electrospray ionization coupled to high resolution mass spectrometry, *Environmental science & technology*, 47 (2013) 976-986.

[40] F.J. Santos, M.T. Galceran, Modern developments in gas chromatography–mass spectrometry-based environmental analysis, *Journal of Chromatography A*, 1000 (2003) 125-151.

[41] V. Leendert, H. Van Langenhove, K. Demeestere, Trends in liquid chromatography coupled to high-resolution mass spectrometry for multi-residue analysis of organic micropollutants in aquatic environments, *TrAC Trends in Analytical Chemistry*, 67 (2015) 192-208.

[42] F. Hernández, J.V. Sancho, M. Ibáñez, E. Abad, T. Portolés, L. Mattioli, Current use of high-resolution mass spectrometry in the environmental sciences, *Analytical and bioanalytical chemistry*, 403 (2012) 1251-1264.

[43] E.N. Evgenidou, I.K. Konstantinou, D.A. Lambropoulou, Occurrence and removal of transformation products of PPCPs and illicit drugs in wastewaters: a review, *The Science of the total environment*, 505 (2015) 905-926.

[44] M. Krauss, H. Singer, J. Hollender, LC-high resolution MS in environmental analysis: from target screening to the identification of unknowns, *Analytical and bioanalytical chemistry*, 397 (2010) 943-951.

[45] D.E. Helbling, J. Hollender, H.-P.E. Kohler, K. Fenner, Structure-Based Interpretation of Biotransformation Pathways of Amide-Containing Compounds in Sludge-Seeded Bioreactors, *Environ. Sci. Technol.*, 44 (2010) 6628–6635.

[46] C. Noutsopoulos, E. Koumaki, D. Mamais, M.C. Nika, A.A. Bletsou, N.S. Thomaidis, Removal of endocrine disruptors and non-steroidal anti-inflammatory drugs through wastewater chlorination: The effect of pH, total suspended solids and humic acids and identification of degradation by-products, *Chemosphere*, 119 (2015) S109-S114.

[47] D.B. Yolanda Picó, Transformation products of emerging contaminants in the environment and high-resolution mass spectrometry: a new horizon, *Analytical and bioanalytical chemistry*, 407 (2015) 6257-6273.

[48] E.L. Schymanski, J. Jeon, R. Gulde, K. Fenner, M. Ruff, H.P. Singer, J. Hollender, Identifying small molecules via high resolution mass spectrometry: communicating confidence, *Environmental science & technology*, 48 (2014) 2097-2098.

[49] A.B.A. Boxall, C.J. Sinclair, K. Fenner, D. Kolpin, S.J. Maund, What are the absolute fate, effects, and potential risks to humans and the ecosystem?, *Environmental Science and Technology*, 38 (2004).

[50] A.S. Stasinakis, G. Gatidou, D. Mamais, N.S. Thomaidis, T.D. Lekkas, Occurrence and fate of endocrine disruptors in Greek sewage treatment plants, *Water research*, 42 (2008) 1796-1804.

[51] T. Kosjek, E. Heath, Tools for evaluating selective serotonin re-uptake inhibitor residues as environmental contaminants, *TrAC Trends in Analytical Chemistry*, 29 (2010) 832-847.

- [52] L.J. Silva, C.M. Lino, L.M. Meisel, A. Pena, Selective serotonin re-uptake inhibitors (SSRIs) in the aquatic environment: an ecopharmacovigilance approach, *The Science of the total environment*, 437 (2012) 185-195.
- [53] L.J. Silva, A.M. Pereira, L.M. Meisel, C.M. Lino, A. Pena, Reviewing the serotonin reuptake inhibitors (SSRIs) footprint in the aquatic biota: uptake, bioaccumulation and ecotoxicology, *Environmental pollution*, 197 (2015) 127-143.
- [54] B. Subedi, K. Kannan, Occurrence and fate of select psychoactive pharmaceuticals and antihypertensives in two wastewater treatment plants in New York State, USA, *The Science of the total environment*, 514 (2015) 273-280.
- [55] M.P. Schlusener, P. Hardenbicker, E. Nilson, M. Schulz, C. Viergutz, T.A. Ternes, Occurrence of venlafaxine, other antidepressants and selected metabolites in the Rhine catchment in the face of climate change, *Environmental pollution*, 196 (2015) 247-256.
- [56] C.D. Metcalfe, S. Chu, C. Judt, H. Li, K.D. Oakes, M.R. Servos, D.M. Andrews, Antidepressants and their metabolites in municipal wastewater, and downstream exposure in an urban watershed, *Environmental toxicology and chemistry / SETAC*, 29 (2010) 79-89.
- [57] T. Vasskog, T. Anderssen, S. Pedersen-Bjergaard, R. Kallenborn, E. Jensen, Occurrence of selective serotonin reuptake inhibitors in sewage and receiving waters at Spitsbergen and in Norway, *Journal of chromatography. A*, 1185 (2008) 194-205.
- [58] T. Alvarino, S. Suarez, E. Katsou, J. Vazquez-Padin, J.M. Lema, F. Omil, Removal of PPCPs from the sludge supernatant in a one stage nitrification/anammox process, *Water research*, 68 (2015) 701-709.
- [59] M. Horsing, A. Ledin, R. Grabic, J. Fick, M. Tysklind, J. la Cour Jansen, H.R. Andersen, Determination of sorption of seventy-five pharmaceuticals in sewage sludge, *Water research*, 45 (2011) 4470-4482.
- [60] S. Suarez, J.M. Lema, F. Omil, Removal of pharmaceutical and personal care products (PPCPs) under nitrifying and denitrifying conditions, *Water research*, 44 (2010) 3214-3224.
- [61] S. Suarez, R. Reif, J.M. Lema, F. Omil, Mass balance of pharmaceutical and personal care products in a pilot-scale single-sludge system: influence of T, SRT and recirculation ratio, *Chemosphere*, 89 (2012) 164-171.
- [62] J.-W. Kwon, K.L. Armbrust, Degradation of citalopram by simulated sunlight, *Environmental Toxicology and Chemistry*, 24 (2005) 1618–1623.
- [63] A.M. Christensen, S. Faaborg-Andersen, F. Ingerslev, A. Baun, Mixture and single-substance toxicity of selective serotonin reuptake inhibitors toward algae and crustaceans, *Environmental Toxicology and Chemistry*, 26 (2007).
- [64] P. Gago-Ferrero, E.L. Schymanski, A.A. Bletsou, R. Aalizadeh, J. Hollender, N.S. Thomaidis, Extended Suspect and Non-Target Strategies to Characterize Emerging Polar Organic Contaminants in Raw Wastewater with LC-HRMS/MS, *Environmental science & technology*, 49 (2015) 12333-12341.

- [65] B. Zonja, C. Goncalves, S. Perez, A. Delgado, M. Petrovic, M.F. Alpendurada, D. Barcelo, Evaluation of the phototransformation of the antiviral zanamivir in surface waters through identification of transformation products, *Journal of hazardous materials*, 265 (2014) 296-304.
- [66] R. Bade, L. Bijlsma, J.V. Sancho, F. Hernandez, Critical evaluation of a simple retention time predictor based on LogKow as a complementary tool in the identification of emerging contaminants in water, *Talanta*, 139 (2015) 143-149.
- [67] L.S. Clesceri, A.E. Greenberg, A.D. Eaton, *Standard Methods for the Examination of Water and Wastewater*, Washington, DC, 1998.
- [68] S. Kern, Baumgartner, R., Helbling, D. E., Hollender, J., Singer, H., Loos, M. J., Schwarzenbach, R. P. and Fenner, K., A tiered procedure for assessing the formation of biotransformation products of pharmaceuticals and biocides during activated sludge treatment, *Journal of environmental monitoring : JEM*, 12 (2010) 2100-2111.
- [69] C. Christophoridis, M.-C. Nika, R. Aalizadeh, N.S. Thomaidis, Ozonation of ranitidine: effect of experimental parameters and identification of transformation products *Science of the Total Environment*, 557–558 ( 2016).
- [70] S. Kern, K. Fenner, H.P. Singer, R.P. Schwarzenbach, J. Hollender, Identification of Transformation Products of Organic Contaminants in Natural Waters by Computer-Aided Prediction and High-Resolution Mass Spectrometry, *Environmental science & technology*, 43 (2009) 7039-7046.
- [71] R. Aalizadeh, N.S. Thomaidis, A.A. Bletsou, P.G. Ferrero, QSRR models to support non-target high resolution mass spectrometric screening of emerging contaminants in environmental samples, *Journal of Chemical Information and Modeling*, 56 (2016).
- [72] V.S. Thomaidi, A.S. Stasinakis, V.L. Borova, N.S. Thomaidis, Is there a risk for the aquatic environment due to the existence of emerging organic contaminants in treated domestic wastewater? Greece as a case-study, *Journal of hazardous materials*, 283 (2015) 740-747.
- [73] R. Gulde, U. Meier, E.L. Schymanski, H.E. Kohler, D.E. Helbling, S. Derrer, D. Rentsch, K. Fenner, Systematic Exploration of Biotransformation Reactions of Amine-containing Micropollutants in Activated Sludge, *Environmental science & technology*, (2016).
- [74] K.S. Jewell, S. Castronovo, A. Wick, P. Falas, A. Joss, T.A. Ternes, New insights into the transformation of trimethoprim during biological wastewater treatment, *Water research*, 88 (2016) 550-557.
- [75] M.E. Dasenaki, N.S. Thomaidis, Multianalyte method for the determination of pharmaceuticals in wastewater samples using solid-phase extraction and liquid chromatography-tandem mass spectrometry, *Analytical and bioanalytical chemistry*, 407 (2015) 4229-4245.
- [76] V.L. Borova, N.C. Maragou, P. Gago-Ferrero, C. Pistos, N.S. Thomaidis, Highly sensitive determination of 68 psychoactive pharmaceuticals, illicit drugs, and related human metabolites in wastewater by liquid



chromatography-tandem mass spectrometry, *Analytical and bioanalytical chemistry*, 406 (2014) 4273-4285.

[77] C. Trautwein, K. Kummerer, Incomplete aerobic degradation of the antidiabetic drug Metformin and identification of the bacterial dead-end transformation product Guanylurea, *Chemosphere*, 85 (2011) 765-773.

[78] C.I. Kosma, D.A. Lambropoulou, T.A. Albanis, Comprehensive study of the antidiabetic drug metformin and its transformation product guanylurea in Greek wastewaters, *Water research*, 70 (2015) 436-448.

[79] C. Trautwein, J.D. Berset, H. Wolschke, K. Kummerer, Occurrence of the antidiabetic drug Metformin and its ultimate transformation product Guanylurea in several compartments of the aquatic cycle, *Environment international*, 70 (2014) 203-212.

[80] A.A. Bletsou, D.E. Damalas, P.G. Ferrero, E.L. Schymanski, H.P. Singer, J. Hollender, N.S. Thomaidis, Wide-scope target screening of 2327 emerging pollutants during wastewater treatment by RP-LC-QTOF-HR-MS/MS with an accurate-mass database, in: 14th International Conference on Environmental Science and Technology (CEST) Rhodes, Greece, 2015.

[81] M. Bergheim, R. Giere, K. Kummerer, Biodegradability and ecotoxicity of tramadol, ranitidine, and their photoderivatives in the aquatic environment, *Environmental science and pollution research international*, 19 (2012) 72-85.

[82] P.C. Rua-Gomez, W. Puttmann, Occurrence and removal of lidocaine, tramadol, venlafaxine, and their metabolites in German wastewater treatment plants, *Environmental science and pollution research international*, 19 (2012) 689-699.

[83] M. Ibanez, V. Borova, C. Boix, R. Aalizadeh, R. Bade, N.S. Thomaidis, F. Hernandez, UHPLC-QTOF MS screening of pharmaceuticals and their metabolites in treated wastewater samples from Athens, *Journal of hazardous materials*, 323 (2017) 26-35.

[84] K.J. Ottmar, L.M. Colosi, J.A. Smith, Fate and transport of atorvastatin and simvastatin drugs during conventional wastewater treatment, *Chemosphere*, 88 (2012) 1184-1189.

[85] K.S. Jewell, P. Falas, A. Wick, A. Joss, T.A. Ternes, Transformation of diclofenac in hybrid biofilm-activated sludge processes, *Water research*, 105 (2016) 559-567.

[86] V.G. Beretsou, A.K. Psoma, P. Gago-Ferrero, R. Aalizadeh, K. Fenner, N.S. Thomaidis, Identification of biotransformation products of citalopram formed in activated sludge, *Water research*, 103 (2016) 205-214.

[87] S. Castronovo, A. Wick, M. Scheurer, K. Nodler, M. Schulz, T.A. Ternes, Biodegradation of the artificial sweetener acesulfame in biological wastewater treatment and sandfilters, *Water research*, 110 (2017) 342-353.

[88] T. Kosjek, N. Negreira, E. Heath, M.L. de Alda, D. Barcelo, Biodegradability of the anticancer drug etoposide and identification of the transformation products, *Environmental science and pollution research international*, 23 (2016) 14706-14717.

- [89] J. Funke, C. Prasse, T.A. Ternes, Identification of transformation products of antiviral drugs formed during biological wastewater treatment and their occurrence in the urban water cycle, *Water research*, 98 (2016) 75-83.
- [90] R. Aalizadeh, N.S. Thomaidis, Wide-scope QSRR models to support suspect and non-target screening of polar compounds in HILIC-ESI(+)-LC-HRMS, in: *9th International Conference on Instrumental Methods of Analysis: Modern Trends and Applications*, 2015, pp. 189.
- [91] R. Aalizadeh, P.C. von der Ohe, N.S. Thomaidis, Prediction of acute toxicity of emerging contaminants on the water flea *Daphnia magna* by Ant Colony Optimization-Support Vector Machine QSTR models, *Environmental science. Processes & impacts*, 19 (2017) 438-448.
- [92] R. Aalizadeh, P.C.v.d. Ohe, N.S. Thomaidis, ToxTrAMS: a platform with wide scope models to do chemical risk assessment, In preparation, (2017, In preparation, (2018).
- [93] D.B. James A. Platts, Michael H. Abraham, and Anne Hersey, Estimation of Molecular Linear Free Energy Relation Descriptors Using a Group Contribution Approach, *J. Chem. Inf. Comput. Sci.*, 39 (1999) 835–845.
- [94] R. Todeschini, V. Consonni, *Molecular Descriptors for Chemoinformatics*, Wiley-VCH Verlag GmbH & Co. KGaA., 2010.
- [95] Y. Men, P. Han, D.E. Helbling, N. Jehmlich, C. Herbold, R. Gulde, A. Onnis-Hayden, A.Z. Gu, D.R. Johnson, M. Wagner, K. Fenner, Biotransformation of Two Pharmaceuticals by the Ammonia-Oxidizing Archaeon *Nitrososphaera gargensis*, *Environmental science & technology*, 50 (2016) 4682-4692.
- [96] S.S. Johansen, A.C. Hansen, I.B. Müller, J.B. Lundemose, M.-B. Franzmann, Three Fatal Cases of PMA and PMMA Poisoning in Denmark, *Journal of Analytical Toxicology*, 27 (2003) 253-256.
- [97] M.R. Meyer, J. Wilhelm, F.T. Peters, H.H. Maurer, Beta-keto amphetamines: studies on the metabolism of the designer drug mephedrone and toxicological detection of mephedrone, butylone, and methylone in urine using gas chromatography-mass spectrometry, *Analytical and bioanalytical chemistry*, 397 (2010) 1225-1233.
- [98] A.J. Pedersen, L.A. Reitzel, S.S. Johansen, K. Linnet, In vitro metabolism studies on mephedrone and analysis of forensic cases, *Drug testing and analysis*, 5 (2013) 430-438.
- [99] I. Linhart, M. Himl, M. Zidkova, M. Balikova, E. Lhotkova, T. Palenicek, Metabolic profile of mephedrone: Identification of nor-mephedrone conjugates with dicarboxylic acids as a new type of xenobiotic phase II metabolites, *Toxicology letters*, 240 (2016) 114-121.
- [100] M. Vevelstad, E.L. Øiestad, G. Middelkoop, I. Hasvold, P. Lilleng, G.J.M. Delaveris, T. Eggen, J. Mørland, M. Arnestad, The PMMA epidemic in Norway: Comparison of fatal and non-fatal intoxications, *Forensic Science International*, 219 (2012) 151-157.

- [101] P.D. Maskell, G.D. Paoli, C. Seneviratne, D.J. Pounder, Mephedrone (4-Methylmethcathinone)-Related Deaths, *Journal of Analytical Toxicology*, 35 (2011) 188-191.
- [102] M.J. Reid, L. Derry, K.V. Thomas, Analysis of new classes of recreational drugs in sewage: Synthetic cannabinoids and amphetamine-like substances, *Drug testing and analysis*, 6 (2014) 72-79.
- [103] J. Kinyua, A. Covaci, W. Maho, A.K. McCall, H. Neels, A.L. van Nuijs, Sewage-based epidemiology in monitoring the use of new psychoactive substances: Validation and application of an analytical method using LC-MS/MS, *Drug testing and analysis*, 7 (2015) 812-818.
- [104] J. Kinyua, N. Negreira, A.K. McCall, T. Boogaerts, C. Ort, A. Covaci, A.L.N. van Nuijs, Investigating in-sewer transformation products formed from synthetic cathinones and phenethylamines using liquid chromatography coupled to quadrupole time-of-flight mass spectrometry, *The Science of the total environment*, 634 (2018) 331-340.
- [105] A.K. McCall, R. Bade, J. Kinyua, F.Y. Lai, P.K. Thai, A. Covaci, L. Bijlsma, A.L.N. van Nuijs, C. Ort, Critical review on the stability of illicit drugs in sewers and wastewater samples, *Water research*, 88 (2016) 933-947.
- [106] R. Bade, L. Bijlsma, J.V. Sancho, J.A. Baz-Lomba, S. Castiglioni, E. Castrignanò, A. Causanilles, E. Gracia-Lor, B. Kasprzyk-Hordern, J. Kinyua, Liquid chromatography-tandem mass spectrometry determination of synthetic cathinones and phenethylamines in influent wastewater of eight European cities, *Chemosphere*, 168 (2017) 1032-1041.
- [107] T. Gao, P. Du, Z. Xu, X. Li, Occurrence of new psychoactive substances in wastewater of major Chinese cities, *Science of The Total Environment*, 575 (2017) 963-969.
- [108] S. Castiglioni, A. Borsotti, I. Senta, E. Zuccato, Wastewater Analysis to Monitor Spatial and Temporal Patterns of Use of Two Synthetic Recreational Drugs, Ketamine and Mephedrone, in Italy, *Environmental science & technology*, 49 (2015) 5563-5570.
- [109] A.L.N.v. Nuijs, A. Gheorghe, P.G. Jorens, K. Maudens, H. Neels, A. Covaci, Optimization, validation, and the application of liquid chromatography-tandem mass spectrometry for the analysis of new drugs of abuse in wastewater, *Drug testing and analysis*, 6 (2014) 861-867.
- [110] E.M. Mwenesongole, L. Gautam, S.W. Hall, J.W. Waterhouse, M.D. Cole, Simultaneous detection of controlled substances in waste water, *Analytical Methods*, 5 (2013) 3248-3254.
- [111] P.K. Thai, F.Y. Lai, M. Edirisinghe, W. Hall, R. Bruno, J.W. O'Brien, J. Prichard, K.P. Kirkbride, J.F. Mueller, Monitoring temporal changes in use of two cathinones in a large urban catchment in Queensland, Australia, *Science of the Total Environment*, 545 (2016) 250-255.
- [112] V.L. Borova, P. Gago-Ferrero, C. Pistos, N.S. Thomaidis, Multi-residue determination of 10 selected new psychoactive substances in wastewater samples by liquid chromatography-tandem mass spectrometry, *Talanta*, 144 (2015) 592-603.

- [113] P. Ramin, A.L. Brock, F. Polesel, A. Causanilles, E. Emke, P.d. Voogt, B.G. Plósz, Transformation and sorption of illicit drug biomarkers in sewer systems: understanding the role of suspended solids in raw wastewater, *Environmental science & technology*, 50 (2016) 13397-13408.
- [114] A.-K. McCall, A. Scheidegger, A.E.S. M.M. Madry, D.G. Weissbrodt, P.A. Vanrolleghem, T. Kraemer, E. Morgenroth, C. Ort, Influence of different sewer biofilms on transformation rates of drugs, *Environmental science & technology*, 50 (2016) 13351-13360.
- [115] J. Kinyua, N. Negreira, B. Miserez, A. Causanilles, E. Emke, L. Gremeaux, P.d. Voogt, J. Ramsey, A. Covaci, A.L.N.v. Nuijs, Qualitative screening of new psychoactive substances in pooled urine samples from Belgium and United Kingdom, *Science of the Total Environment*, 573 (2016) 1527-1535.
- [116] F.Y. Lai, C. Erratico, J. Kinyua, J.F. Mueller, A. Covaci, A.L.N.v. Nuijs, Liquid chromatography-quadrupole time-of-flight mass spectrometry for screening in vitro drug metabolites in humans: investigation on seven phenethylamine-based designer drugs, *Journal of pharmaceutical and biomedical analysis*, 114 (2015) 355-375.
- [117] R.C. Baselt, *Disposition of Toxic Drugs and Chemicals in Man*, Biomedical Publications, 2014.
- [118] A.J. Pedersen, L.A. Reitzel, S.S. Johansen, K. Linnet, In vitro metabolism studies on mephedrone and analysis of forensic cases, *Drug testing and analysis*, 5 (2013) 430-438.
- [119] C.W. Randal, D.Sen, Full-scale evaluation of an integrated fixed-film activated sludge (IFAS) process for enhanced nitrogen removal *Water science and technology : a journal of the International Association on Water Pollution Research*, 33 (1996) 155-162.
- [120] D. Di Trapani, M. Christensson, M. Torregrossa, G. Viviani, H. Ødegaard, Performance of a hybrid activated sludge/biofilm process for wastewater treatment in a cold climate region: Influence of operating conditions, *Biochemical Engineering Journal*, 77 (2013) 214-219.
- [121] G. Mannina, G. Viviani, Hybrid moving bed biofilm reactors: an effective solution for upgrading a large wastewater treatment plant, *Water science and technology : a journal of the International Association on Water Pollution Research*, 60 (2009) 1103-1116.
- [122] D. Di Trapani, M. Christensson, H. Ødegaard, Hybrid activated sludge/biofilm process for the treatment of municipal wastewater in a cold climate region: a case study, *Water science and technology : a journal of the International Association on Water Pollution Research*, 63 (2011) 1121-1129.
- [123] T. Reemtsma, U. Miehle, U. Duennbier, M. Jekel, Polar pollutants in municipal wastewater and the water cycle: occurrence and removal of benzotriazoles, *Water research*, 44 (2010) 596-604.
- [124] P. Herrero, F. Borrull, E. Pocurull, R.M. Marcé, An overview of analytical methods and occurrence of benzotriazoles, benzothiazoles

and benzenesulfonamides in the environment, *TrAC Trends in Analytical Chemistry*, 62 (2014) 46-55.

[125] Thorsten Reemtsma, Stefan Weiss, Jutta Mueller, Mira Petrovic, Susana Gonzalez, Damia Barcelo, Francesc Ventura, T.P. Knepper, Polar Pollutants Entry into the Water Cycle by Municipal Wastewater: A European Perspective, *Environmental Science and Technology*, 40 (2006) 5451-5458.

[126] A.G. Asimakopoulos, A. Ajibola, K. Kannan, N.S. Thomaidis, Occurrence and removal efficiencies of benzotriazoles and benzothiazoles in a wastewater treatment plant in Greece, *The Science of the total environment*, 452-453 (2013) 163-171.

[127] A.S. Stasinakis, N.S. Thomaidis, O.S. Arvaniti, A.G. Asimakopoulos, V.G. Samaras, A. Ajibola, D. Mamais, T.D. Lekkas, Contribution of primary and secondary treatment on the removal of benzothiazoles, benzotriazoles, endocrine disruptors, pharmaceuticals and perfluorinated compounds in a sewage treatment plant, *The Science of the total environment*, 463-464 (2013) 1067-1075.

[128] D. Molins-Delgado, M.S. Diaz-Cruz, D. Barcelo, Removal of polar UV stabilizers in biological wastewater treatments and ecotoxicological implications, *Chemosphere*, 119 Suppl (2015) S51-57.

[129] Y.S. Liu, G.G. Ying, A. Shareef, R.S. Kookana, Biodegradation of three selected benzotriazoles under aerobic and anaerobic conditions, *Water research*, 45 (2011) 5005-5014.

[130] A.A. Mazioti, A.S. Stasinakis, Y. Pantazi, H.R. Andersen, Biodegradation of benzotriazoles and hydroxy-benzothiazole in wastewater by activated sludge and moving bed biofilm reactor systems, *Bioresource technology*, 192 (2015) 627-635.

[131] A.A. Mazioti, A.S. Stasinakis, G. Gatidou, N.S. Thomaidis, H.R. Andersen, Sorption and biodegradation of selected benzotriazoles and hydroxybenzothiazole in activated sludge and estimation of their fate during wastewater treatment, *Chemosphere*, 131 (2015) 117-123.

[132] M. Farre, L. Kantiani, M. Petrovic, S. Perez, D. Barcelo, Achievements and future trends in the analysis of emerging organic contaminants in environmental samples by mass spectrometry and bioanalytical techniques, *Journal of chromatography. A*, 1259 (2012) 86-99.

[133] A.K. Ghattas, F. Fischer, A. Wick, T.A. Ternes, Anaerobic biodegradation of (emerging) organic contaminants in the aquatic environment, *Water research*, 116 (2017) 268-295.

[134] B.D. Blair, J.P. Crago, C.J. Hedman, R.D. Klaper, Pharmaceuticals and personal care products found in the Great Lakes above concentrations of environmental concern, *Chemosphere*, 93 (2013) 2116-2123.

[135] B.O. Clarke, S.R. Smith, Review of 'emerging' organic contaminants in biosolids and assessment of international research priorities for the agricultural use of biosolids, *Environment international*, 37 (2011) 226-247.

[136] P. Gago-Ferrero, V. Borova, M.E. Dasenaki, S. Tauhomaidis Nu, Simultaneous determination of 148 pharmaceuticals and illicit drugs in

sewage sludge based on ultrasound-assisted extraction and liquid chromatography-tandem mass spectrometry, *Analytical and bioanalytical chemistry*, 407 (2015) 4287-4297.

[137] N.A. Alygizakis, P. Gago-Ferrero, V.L. Borova, A. Pavlidou, I. Hatzianestis, N.S. Thomaidis, Occurrence and spatial distribution of 158 pharmaceuticals, drugs of abuse and related metabolites in offshore seawater, *The Science of the total environment*, 541 (2016) 1097-1105.

[138] W. Zheng, Y. Zou, X. Li, M.L. Machesky, Fate of estrogen conjugate 17 $\alpha$ -estradiol-3-sulfate in dairy wastewater: comparison of aerobic and anaerobic degradation and metabolite formation, *Journal of hazardous materials*, 258-259 (2013) 109-115.

[139] E. Koumaki, D. Mamais, C. Noutsopoulos, Environmental fate of non-steroidal anti-inflammatory drugs in river water/sediment systems, *Journal of hazardous materials*, 323 (2017) 233-241.

[140] P. Falas, A. Wick, S. Castronovo, J. Habermacher, T.A. Ternes, A. Joss, Tracing the limits of organic micropollutant removal in biological wastewater treatment, *Water research*, 95 (2016) 240-249.

[141] A. Gobel, C.S. McArdell, A. Joss, H. Siegrist, W. Giger, Fate of sulfonamides, macrolides, and trimethoprim in different wastewater treatment technologies, *The Science of the total environment*, 372 (2007) 361-371.

[142] O.A. Jones, N. Voulvoulis, J.N. Lester, The occurrence and removal of selected pharmaceutical compounds in a sewage treatment works utilising activated sludge treatment, *Environmental pollution*, 145 (2007) 738-744.

[143] A. Goel, M.B. Müller, M. Sharma, F.H. Frimmel, Biodegradation of Nonylphenol Ethoxylate Surfactants in Biofilm Reactors, *Acta hydrochimica et hydrobiologica*, 31 (2003) 108-119.

[144] J. Greskowiak, H. Prommer, G. Massmann, G. Nutzmann, Modeling Seasonal Redox Dynamics and the Corresponding Fate of the Pharmaceutical Residue Phenazone During Artificial Recharge of Groundwater, *Environmental Science and Technology*, 40 (2006) 6615-6621.

[145] A. Carucci, G. Cappai, M. Piredda, Biodegradability and toxicity of pharmaceuticals in biological wastewater treatment plants, *Journal of environmental science and health. Part A, Toxic/hazardous substances & environmental engineering*, 41 (2006) 1831-1842.

[146] R. Gulde, S. Anliker, H.E. Kohler, K. Fenner, Ion Trapping of Amines in Protozoa: A Novel Removal Mechanism for Micropollutants in Activated Sludge, *Environmental science & technology*, 52 (2018) 52-60.

[147] S. Rühmland, A. Wick, T.A. Ternes, M. Barjenbruch, Fate of pharmaceuticals in a subsurface flow constructed wetland and two ponds, *Ecological Engineering*, 80 (2015) 125-139.